DISSERTATIONS IN
FORESTRY AND
NATURAL SCIENCES

Katja Myllymaa

Novel Carbon Coatings and Surface Texturing for Improving Biological Response of Orthopedic Implant Materials

Publications of the University of Eastern Finland
Dissertations in Forestry and Natural Sciences

UNIVERSITY OF
EASTERN FINLAND

KATJA MYLLYMAA

Novel Carbon Coatings and Surface Texturing for Improving Biological Response of Orthopedic Implant Materials

Publications of the University of Eastern Finland
Dissertations in Forestry and Natural Sciences
Number 15

Academic Dissertation
To be presented by permission of the Faculty on Sciences and Forestry for public examination in the Auditorium, Mediteknia Building at the University of Eastern Finland, Kuopio, on Friday 19th November 2010, at 10 a.m.

Department of Physics and Mathematics

Kopijyvä Oy
Kuopio, 2010
Editors: Prof. Pertti Pasanen,
Prof. Tarja Lehto, Prof. Kai Peiponen

Distribution:
Eastern Finland University Library/Sales of publications
P.O. Box 107, FI-80101 Joensuu, Finland
tel. +358-50-3058396
http://www.uef.fi/kirjasto

ISBN 978-952-61-0218-4
ISSN 1798-5668
ISSNL 1798-5668
ISBN 978-952-61-0219-1 (PDF)
ISSN 1798-5676 (PDF)

Author's address: Department of Clinical Neurophysiology
Kuopio University Hospital
P.O. Box 1777
FI-70211 KUOPIO
FINLAND
E-mail: katja.myllymaa@kuh.fi

Supervisors: Prof. Reijo Lappalainen, Ph.D.
Department of Physics and Mathematics
University of Eastern Finland

Prof. Yrjö T. Konttinen, M.D., Ph.D.
Department of Medicine
Helsinki University Central Hospital, University of Helsinki

Virpi Tiitu, Ph.D.
Institute of Biomedicine, Anatomy
University of Eastern Finland

Reviewers: Prof. Jari Koskinen, Ph.D.
Department of Material Science and Engineering
Aalto University School of Science and Technology

Prof. Juha Tuukkanen, Ph.D., D.D.S.
Department of Anatomy and Cell Biology
University of Oulu

Opponent: Prof. Heimo Ylänen, Ph.D.
Department of Biomedical Engineering
Tampere University of Technology

ABSTRACT

The occurrence of musculoskeletal disorders, such as osteoporosis (weakening of the bones) and osteoarthritis (inflammation in the bone joints), is recognized as one of the most common human health problems. During the history of biomaterial engineering, a wide range of musculoskeletal implants has been evaluated for the treatment or even the prevention of these diseases. Nonetheless, the major problems concerning the success and survival of these implants under physiological conditions is their low degree of osseointegration at the implant–tissue interface, which not only delays the bone reconstruction process but also prolongs the healing time. Despite of good osseointegration, there is a need to devise an implant which inhibits biofilm formation and infection. Modifying the physicochemical properties of the material surface, such as surface chemistry, wettability, micro- and nano-texture and electric charge, may help to develop implants with the desired cellular responses.

In this thesis, lithographic and injection molding methods were successfully used to produce micro- and nanotexture in order to study the adhesion and contact guidance of osteoblastic cells and the behaviour of bacteria. Moreover, physical vapour deposition methods were utilized to prepare novel carbon coatings with different chemical composition and wettability properties in order to improve osteoblastic cells attachment and spreading as well as to inhibit biofilm formation.

As a result, micropatterning was able to regulate the contact guidance of osteoblastic cells and provided detailed knowledge about bacterial adhesion and colonization processes. In addition, the synergetic effect of surface micro- and nanotexturing with moderately wettable carbon-based coating enhanced osteoblast-like cells adhesion. Surface free energy determinations proved that the Lewis acid-base component (γ_S^{AB}) of surface free energy is a critical factor in osteoblast-like cells adhesion. An ultra-short pulsed laser deposition was demonstrated to be an effective

technique to produce novel carbon implant coatings with the desired physicochemical properties.

To conclude, the novel carbon-based materials and their surface modifications tested *in vitro* were found to be potential candidates for bone implant applications due to their capability to enhance osteoblastic cells adhesion and to prevent bacterial adhesion and biofilm formation.

National Library of Medicine Classification: QT 36, QT 37, QW 90, WE 172

INSPEC Thesaurus: biomedical materials; orthopaedics; prosthetics; vapour deposited coatings; diamond-like carbon; surface texture; surface topography; microfabrication; ultraviolet lithography; bone; nanopatterning; nanotechnology; adhesion; injection moulding; pulsed laser deposition; metals; polymers; surface phenomena; surface energy; contact angle; wetting

Yleinen suomalainen asiasanasto: biomateriaalit; ortopedia; implantit; kiinnitys; luu; bakteerit; pintailmiöt; adheesio; pinnoitus; pinnoitteet; pintarakenteet; kuviot; timantti; mikrotekniikka; nanotekniikka

Preface

The studies described in this thesis were carried out in the Department of Physics, University of Kuopio (currently University of Eastern Finland) during the years 2006-2010. The part of sample fabrication and characterization was performed in the Department of Chemistry, University of Joensuu (currently University of Eastern Finland), in the BioMater Centre, University of Kuopio (currently University of Eastern Finland) and in the Microsensor laboratory, School of Engineering, Savonia University of Applied Sciences. Biological experiments were conducted in the Department of Anatomy, University of Kuopio (currently Institute of Biomedicine, Anatomy, University of Eastern Finland) and in the Department of Anatomy, Institute of Biomedicine, University of Helsinki.

There are many people to thank, and I hereby wish to sincerely acknowledge everybody who has contributed to this work in one way or another. Especially, I would like to thank the following persons: My principal supervisor, Professor Reijo Lappalainen is most warmly acknowledged for providing me the opportunity to work in his research group and for showing me his scientific and humorous way of guidance throughout this work. I am also grateful to my other supervisor, Professor Yrjö T. Konttinen for his professional guidance and never-ending ability for giving valuable advice and encouragement during this work. Pasi Kivinen, PhD, who acted as my third supervisor at the beginning of this study, is acknowledged for encouraging me to start this project and believing in my capabilities. Later on, Virpi Tiitu, PhD, acted as my supervisor and she is thanked for providing academic and cell biology related guidance.

I want to express my sincere gratitude to the reviewers Professor Jari Koskinen and Professor Juha Tuukkanen for their important and constructive criticism. Ewen MacDonald is

warmly acknowledged for his valuable revision of the language of the thesis.

This thesis would not have been possible without the expert guidance and precious help of my all colleagues involved in this study. I owe my sincere thanks to Professor Mikko Lammi, Professor Tapani Pakkanen, Mika Suvanto, Jaakko Levon, Hanna Saarenpää, Vesa-Petteri Kouri, Riina Rautemaa-Richardson, Teemu Kinnari, Veli-Matti Tiainen, Antti Soininen, Emilia Kaivosoja, Professor Maria-Pau Ginebra and Montserrat Español Pons. Picodeon Ltd. Oy is acknowledged for providing thin film depositions.

I would like to thank all current and former members of the Biomaterial Technology Research Group and BioMater Centre for their friendly and helpful attitude. Especially, Hannu Korhonen, Sanna Miettinen, Virpi Miettinen, Ritva Sormunen and Juhani Hakala are sincerely acknowledged.

I express my gratitude to all of the personnel of the Information Technology R&D Unit, Savonia University of Applied Sciences, Kuopio. Matti Sipilä is acknowledged for helping me to do this research in co-operation with the Information Technology R&D Unit. My special thanks belong to my colleagues, Mikko Laasanen and Ari Halvari for their invaluable help in microfabrication and surface analysis methods.

My parents, Anneli and Jukka: Thanks for supporting me in whatever I do in my life and taking care and loving of our little daughters when I have been carrying out this project. My brothers and their families are also acknowledged for their support. I also owe my warm thanks to my parents-in-law, Seija and Heimo for their invaluable help and support. Similarly, my dear friends are remembered for their irreplaceable support, actions and enlightening discussions during my life. And finally, I want to express my dearest thanks with all respects to my family: Sami, Lumia and Neelia. Lumia and Neelia- you are the best and the dearest. You have given so much power and happiness to your mom during this process. Nothing is more important than you. Sami: During the years we have spent

together, besides you have given me our little daughters, you have given me so much love and support and taught me to be more patient. Without you, I would not be here. But now, we are here -only we know how many weeks, months and years we have worked on this project, sometimes crying but usually loving and laughing. Now it is time to move forward to face new projects and new challenges –together.

This work was financially supported by Finnish funding Agency for Technology and Innovation (TEKES), the National Graduate School of Musculoskeletal Diseases and Biomaterials, Finnish Cultural Foundation of Northern Savo, Otto A. Malm Foundation, Foundation for Advanced Technology of Eastern Finland, European Science and Foundation and COST, European Cooperation in Science and Technology.

Kuopio, October 2010

Katja Myllymaa

Abbreviations

AB	Lewis acid base
a-C:H	hydrogenated amorphous carbon
AD	amorphous diamond
AD-PDMS-h	amorphous diamond-polydimethylsiloxane- hybrid
AD-Ti-h	amorphous diamond-titanium- hybrid
AFM	atomic force microscopy
Ag	silver
Al	aluminium
Al_2O_3	alumina
ALP	alkaline phosphatase
Alb	albumin
ANOVA	analysis of variance
ATCC	American type culture collection
C	carbon
CFU	colony forming unit
CLSM	confocal laser scanning microscopy
CN	carbon nitride
C_3N_4-Si	silicon-doped carbon nitride
Co	cobalt
Cr	chromium
DC	direct current
DLC	diamond-like carbon
DLC-PDMS-h	diamond-like carbon-polydimethylsiloxane –hybrid
DLC-PTFE-h	diamond-like carbon-polytetrafluoroethylene –hybrid
DLVO	Derjaguin, Landau, Verwey, Overbeck (the theory describes the force between charged surfaces interacting through a liquid medium)
DNA	deoxyribonucleic acid
EL	electrostatic double layer
ECM	extracellular matrix
F	fluorine

FAR	Finnish Arthroplasty Register
FCS	fetal calf serum
Fe	iron
Fn	fibronectin
FPAD	filtered pulsed arc discharge
HA	hydroxyapatite
LW	Lifshitz-Van der Waals
Mo	molybdenum
MNST	micro- and nanostructured
MSC	mesenchymal stem cell
MST	microstructured
MTT	cell proliferation assay based on (3-[4,5-dimethylthiazol-2-yl]-2,5-diphenyltetrasodium bromide)-salt
N	nitrogen
NaCl	sodium chloride
Nb	niobium
Ni	nickel
O	oxygen
OW	Owens-Wendt
PBS	phosphate buffered saline
PDMS	polydimethylsiloxane
PP	polypropylene
Pt	platinum
PTFE	polytetrafluoroethylene
PVD	physical vapour deposition
QS	quorum sensing
RGD	arginine-glycine-aspartic acid
RNA	ribonucleic acid
S. aureus	*Staphylococcus aureus*
S. epidermidis	*Staphylococcus epidermidis*
SD	standard deviation of the mean
SEM	scanning electron microscopy
SFE	surface free energy
Si	silicon
SS	stainless steel
Ta	tantalum

ta-C	tetrahedral amorphous carbon
Ti	titanium
TiO_2	titanium dioxide
TSB	Tryptic Soy Broth
UHMWPE	ultra-high-molecular-weight-polyethylene
USPLD	ultra-short pulsed laser deposition
UV	ultraviolet
V	vanadium
Vn	vitronectin
VO	van Oss
Zr	zirconium
ZrO_2	zirconia

Symbols

R_a	arithmetic mean deviation of surface (average roughness)
γ_S	total surface free energy
γ_S^D	dispersive component of total surface free energy
γ_S^P	polar component of total surface free energy
γ_S^{LW}	Lifshitz-van der Waals component of total surface free energy
γ_S^{AB}	Lewis acid-base component of total surface free energy
γ_S^+	electron-acceptor component
γ_S^-	electron-donor component
ζ	zeta potential

LIST OF ORIGINAL PUBLICATIONS

This thesis is based on the following original articles referred to in the text by their Roman numerals (I-IV).

I Myllymaa, K., Myllymaa, S., Korhonen, H., Lammi, M.J., Tiitu, V. and Lappalainen, R. (2009) Interactions between Saos-2 cells and microtextured amorphous diamond or amorphous diamond hybrid coated surfaces with different wettability properties.
Diamond and Related Materials 18 (10), 1294-300.

II Myllymaa, K., Myllymaa, S., Korhonen, H., Lammi, M.J., Saarenpää, H., Suvanto, M., Pakkanen, T.A., Tiitu, V. and Lappalainen, R. (2009) Improved adherence and spreading of Saos-2 cells on polypropylene surfaces achieved by surface texturing and carbon nitride coating.
Journal of Material Science: Materials in Medicine 20 (11), 2337-47.

III Myllymaa, K*., Levon, J*., Tiainen, V-M., Myllymaa, S., Soininen, A., Korhonen, H., Kaivosoja, E., Lappalainen, R. and Konttinen, Y.T. Resistance of DLC and its hybrids to *Staphylococcus epidermidis* biofilm formation compared to metals used in biomaterials. (* Equal contribution)
Submitted to *Colloids and Surfaces B: Biointerfaces*.

IV Levon, J*., Myllymaa, K*., Kouri, V-P., Rautemaa, R., Kinnari, T., Myllymaa, S., Konttinen, Y.T. and Lappalainen, R. (2010) Patterned macroarray plates in comparison of bacterial adhesion inhibition of tantalum, titanium and chromium compared with diamond-like carbon. (* Equal contribution)
Journal of Biomedical Materials Research 92A (4), 1606-13.

 This thesis also contains unpublished data which demonstrate the effect of zeta potential (**unpublished data I**) and surface roughness (**unpublished data II)** on osteoblast-like cells behaviour.

AUTHOR'S CONTRIBUTION

Publication I: Apart from thin film depositions which were carried out by R. Lappalainen, the author of this thesis performed all the sample design and fabrication steps in collaboration with S. Myllymaa. The author performed surface characterizations with a contribution from H. Korhonen. The author designed the cell experiments together with M.J. Lammi and V. Tiitu who performed the cell experiments. The author was mainly responsible for preparing the results and wrote the article, after receiving comments from the co-authors. R. Lappalainen, V. Tiitu and M.J. Lammi supervised the work.

Publication II: The design and fabrication of polypropylene test samples was performed by H. Saarenpää, M. Suvanto and T.A. Pakkanen. The coating of these samples was conducted by R. Lappalainen. The surface characterization was performed by the author with a contribution from H. Korhonen. The author designed the cell experiments together with M.J. Lammi and V. Tiitu who performed the cell experiments. The author analyzed the most of the data as well as prepared the results with a contribution from S. Myllymaa. The author also wrote the paper while receiving some contributions from other authors. The study was mainly supervised by R. Lappalainen and V. Tiitu.

Publications III and IV: Y.T. Konttinen and R. Lappalainen originally presented the idea of studying the effect of surface micropatterning on bacterial attachment and colonization. Except for thin film depositions, carried out by H. Korhonen, R. Lappalainen, A. Soininen and V.-M. Tiainen, the author (K. Myllymaa) practically performed all sample design and sample fabrication steps in collaboration with S. Myllymaa. The surface characterization was mainly performed by the author with some contributions by H. Korhonen and S. Myllymaa. J. Levon performed most of the work design, experimental work and data analysis related to bacterial studies, in co-operation with the team members. The author and J. Levon mainly wrote the papers III and IV while receiving comments from the co-authors. Y.T. Konttinen and R. Lappalainen supervised these studies.

Contents

1 Introduction and objectives

An orthopedic implant is intended for use in the human body to repair a fractured bone or to replace a part or all of a damaged, defunct joint. Each orthopedic implant is designed to withstand the natural movement and stress associated with individual joint: hip, knee, elbow or shoulder. The primary needs for bone implants are diseases like osteoporosis and osteoarthritis as well as fall-related fractures. In Finland, according to Finnish Arthroplasty Register (FAR 2007), there was a total of 63 873 primary total hip arthroplasty operations performed during the years 1998-2007. In the USA, the annual demand for primary total hip arthroplasties is projected to increase from the present 209 000 units up to 572 000 units between 2005 and 2030 (Kurtz et al. 2007a). Many different material types, such as metals, ceramics and polymers used as implants are known to be biocompatible, *i.e.* they should not cause any undesirable local or systematic host responses. However, the number of total hip revision operations was 13 447 during the years 1998-2007 in Finland (FAR 2007). Moreover, the number of hip revisions is estimated to grow by about 137 % between the years 2005 and 2030 (Kurtz et al. 2007a). There are major economical costs related to every revision and the pain to the individual patient should not be overlooked. These statistics and the fact that the average implant lasts only about a decade, reveal that perfect bone implant has not yet been developed. There are many different reasons for bone implant revisions like fractures, dislocations and changes in the biomechanics of the implant due to wear or corrosion of implant material (Geetha et al. 2009). However, a significant part of the revisions can be traced to poor biocompatibility in which the signs are osteolysis, necrosis and formation of a thick fibrotic capsule between the implant

and bone (Burke & Goodman 2008) as well as infection (Revell 2008). A comprehensive understanding of tissue–implant interactions is important if one wishes to avoid this poor biocompatibility. The details of the optimal implant surface properties: surface chemistry, -wettability, -charge and –topography (roughness, micro- and nanotexture) affecting the "race for the surface" (Gristina 1987) and antimicrobial action are still largely unknown.

Main aim and the common thread running through in every sub-project of this thesis was to evaluate the interactions between the novel carbon coatings produced by ultra-short pulsed laser deposition (USPLD) or filtered pulsed arc discharge (FPAD) method and osteoblast-like cells or bacteria. The other aims were: 1) to investigate the effect of a textured surface with thin film coatings on the adhesion and the contact guidance of osteoblast-like cells and the behaviour of bacteria, 2) to study the possibilities to produce novel carbon-based hybrid materials with modified physicochemical properties (surface chemistry, surface wettability, surface topography and surface charge) and 3) to understand the role of these surface parameters on the adhesion of osteoblast-like cells and biofilm formation. All these issues are important in the development of new generation implants allowing biocompatible and functional integration to bone tissue.

2 Composition and structure of bone

Bones are relatively rigid, calcified, living organs that constitute most of the skeleton of higher vertebrates. Bones are intended by nature to fulfill a variety of mechanical, synthetic and metabolic tasks. Bones are the main storage of minerals and growth factors. Bone marrow contains some fat and is an important hematopoietic tissue responsible for the production of red and white blood cells. Bone marrow is also rich in mesenchymal stem cells (MSCs).The main functions from a mechanical point of view are the protection of internal organs like brain, heart and lungs, supporting the framework of the body and acting together with skeletal muscles, tendons, ligaments and joints to permit body movements possible. Bone can be divided into three sections: the cellular components, the inorganic bone matrix, which mainly consists of crystalline mineral salts and calcium and the organic bone matrix which is mainly composed of Type I collagen. (Steele & Bramblett 1988)

There are three types of cells present in bone: osteoblasts, osteocytes and osteoclasts (Steele & Bramblett 1988). These cells participate in following functions: production of proteins found in bone; stimulation of the mineralization of the matrix; maintenance of bone tissue; resorption of bone *i.e.* the cells play a major role in mineral physiology (Ortner & Putschar 1981). Osteoblasts participate in bone formation. They produce a protein matrix, osteoid, which is primarily composed of Type I collagen. Osteoblasts also synthesize membrane-associated alkaline phosphatase (ALP) and produce hormones. Osteoblasts are considered as osteocytes, the bone-maintaining cells, as soon as they are surrounded by and incorporated into the protein matrix. Osteoclasts are giant cells responsible for remodeling of bone during growth and repair. They have also an active role in

the destructive processes of bone where bone is removed. In addition to these cells, inactive osteoblasts, bone-lining cells, cover the bone surface that is not undergoing bone formation or resorption. These cells also function as a barrier for particular ions. (Steele & Bramblett 1988, An & Martin 2003)

Bone tissue can be morphologically divided into two types: compact and cancellous bone (Fig. 1b). Compact bone is much denser than cancellous bone and it has protective and mechanical functions. Compact bone is composed of cylindrical structures, osteons (Fig. 1c), that are typically several millimeters long and around 0.2 mm in diameter (Steele & Bramblett 1988). Each osteon consists of an anisotropic matrix composed of mineral crystals and collagen fibers, called lamellae. Lamellae contain uniformly spaced cavities, lacunae, which encompass osteocytes and surround a Haversian canal which contains the bone's nerves and blood supplies. Thin cylindrical spaces, called canaliculi, perforate the calcified bone matrix and facilitate the exchange of nutrients and metabolic waste. Osteons are connected to each other by channels called Volkmann's canals. Compared to hard compact bone, cancellous bone is softer and less stiff and is mainly responsible for the metabolic functions of bone tissue. The primary anatomical and functional unit of cancellous bone is the trabeculae (Fig. 1b), the structure where the calcified tissue is arranged in the form of plates or struts. (An & Martin 2003) Trabeculae are typically 200 μm thick (Martin et al. 1998), generating several interconnected cavities which are filled with bone marrow. Trabeculae consist of lamellae but very infrequently can contain osteons. For instance, long bones *e.g.* femur have a hard outer surface of compact bone filled with cancellous bone containing bone marrow. The epiphysis at either end of long bones is covered by hyaline cartilage forming an articular surface (Fig. 1a).

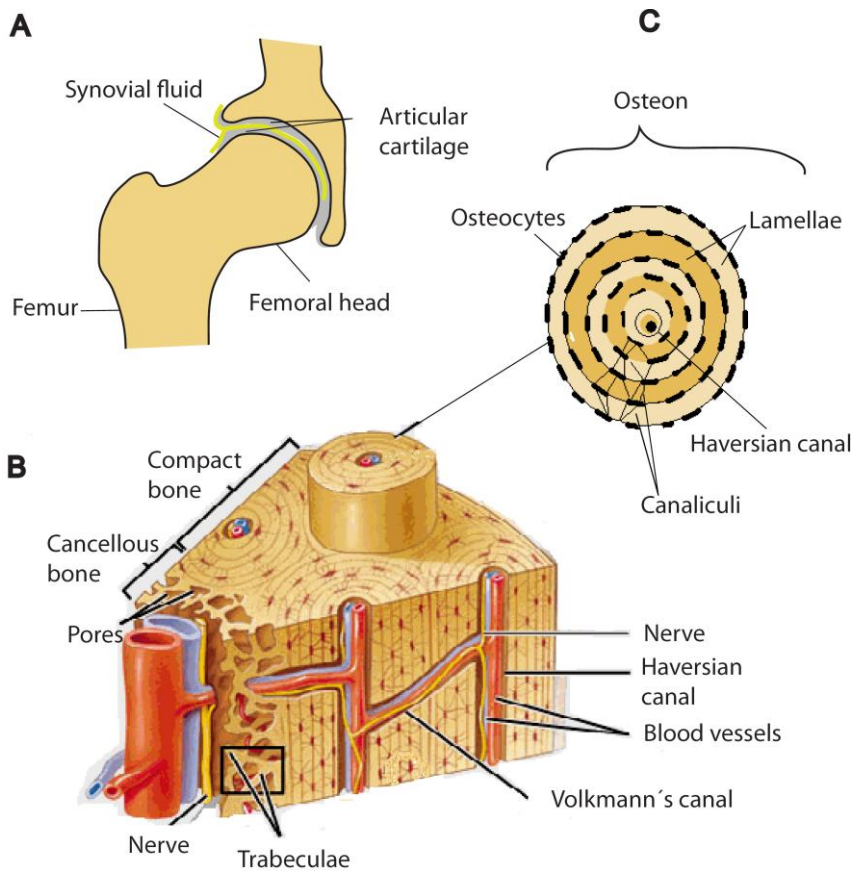

Figure 1: *(a) Schematic representation of a hip joint. (b) The hard outer layer of bones is composed of compact bone. The porous interior of the bone is called cancellous bone. The primary unit of cancellous bone is the trabeculae, which consists of parallel layers of lamellae. Cancellous bone is also highly vascular and frequently contains red bone marrow. (b,c) Compact bone consists of osteons which are composed of lamellae surrounding the Haversian canal. The Haversian canal contains the bone's nerves and blood vessels. Osteocytes make contact with the cytoplasmic processes of their counterparts via the canaculi. Osteons are connected to each other by Volkmann's canals. Fig. 1b was modified from the original figure (Shier et al. 2009) with kind permission of The McGraw-Hill Companies.*

The formation of bone in embryonic development and in adult bone renovation occurs by two processes: intramembraneous ossification and endochondral ossification. Intramembraneous ossification is the process used to make flat bones of the skull; the bone is formed when mesenchymal cells differentiate directly into osteoblasts. The replacement of cartilage by bone is called endochondral ossification and it occurs in long bones. (Steele & Bramblett 1988)

3 Bone implants

Implants are medical devices which have been developed to replace and act as a missing biological structure. Implants need to be made from a biocompatible material because they are in contact with tissue. According to Williams: "Biocompatibility is the ability of a material to perform with an appropriate host response in a specific application" (Williams 1987). Today, medical biomaterials/implants have a huge number of different applications and uses in different parts of the human body including orthopedic applications: joint replacements (hip, knee), bone cements, defect fillers and plates for fracture fixation and artificial tendons and ligaments; cardiovascular applications: heart valves, catheters, vascular grafts and blood substitutes; ophthalmic applications: intraocular- and contact lenses and cochlear replacements. There are also other applications including dental implants, artificial hearts, skin repair templates, tissue screws and tacks and drug-delivery systems. (Ratner et al. 1996) However, the number of implants used for hip, spinal and knee replacements is extremely high. The main reason behind the increasing need for bone implants in the western population is the increased number of elderly people. Typically reduced bone density and bone loss are linked with weaker motoric skills in the old which act together to predispose these people to fall-related fractures. The other reason for joint replacements is associated with diseases such as osteoporosis, osteoarthritis and trauma.

According to the National Agency for Medicines, the number of annual primary total hip arthoplasty operations in Finland has increased from 4835 to 7698 in the years between 1998 and 2007 (Fig. 2a) (FAR 2007). In addition, in the USA, Norway and Sweden the increases in hip arthoplasty operations were at least about 20 % during the years 1997-2004 (Kurtz et al. 2007b). It is also projected that in the USA, the number of total hip

replacements will rise by 174 % to 572 000 procedures during the years 2005-2030 (Kurtz et al. 2007a).

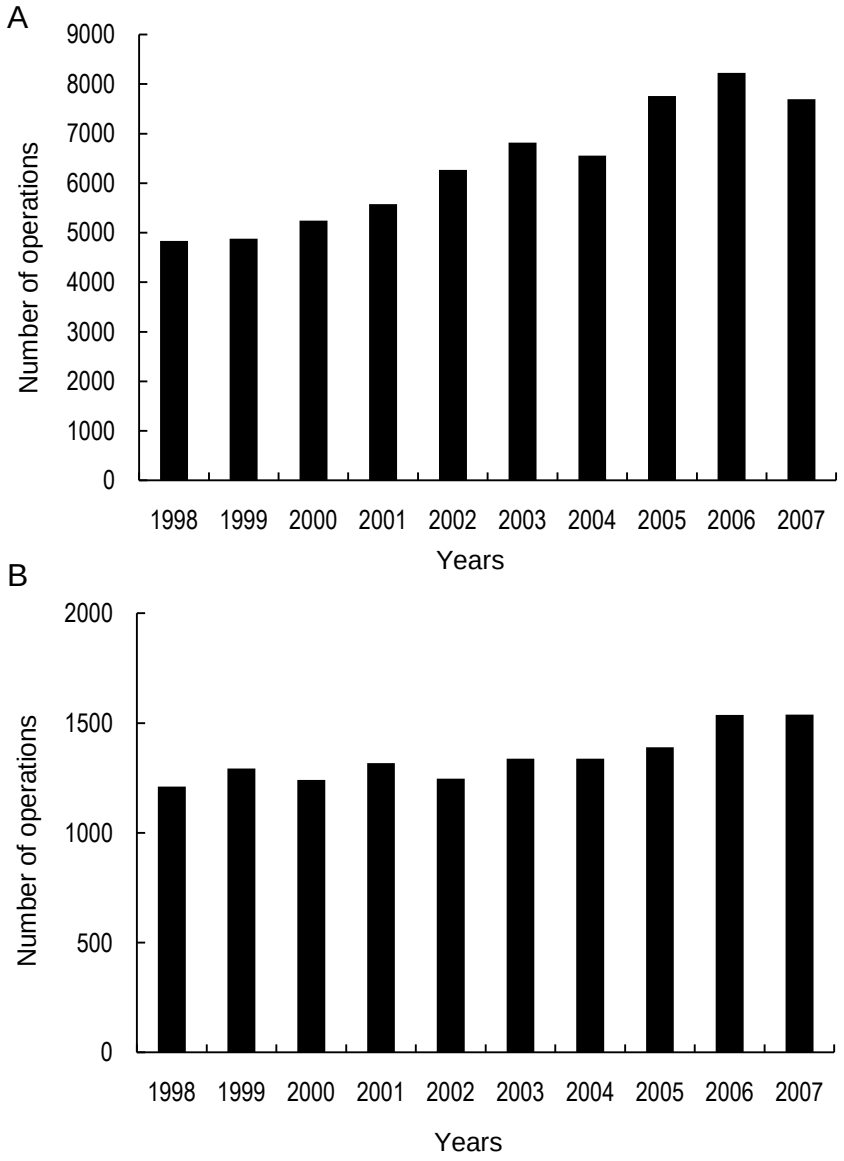

Figure 2: *Number of primary total hip arthroplasty operations (a) and total hip revision operations (b) in Finland during the years 1998 – 2007. Modified from FAR (2007).*

Although implants (such as hip replacements) have been in use for about 50 years, their durability does not meet the requirements of higher life expectancy. The average implant lasts only about a decade which is not long enough because the estimated life expectancy has increased due to advances in medical technology. In Finland, the rate of total hip revision operations was in the range of 1210-1538 per year during the years 1998-2007 (Fig. 2b) (FAR 2007). From data collected on total joint replacements one can estimate that the total hip revision surgery can be expected to increase by 137 % between the years 2005-2030 (Kurtz et al. 2007a). Every individual revision surgery is associated with pain for the patient and is very expensive. In addition, the success rate is rather small. All these facts stress that there is a crying need for long lasting implants made of appropriate materials with excellent biocompatibility.

3.1 BIOMATERIALS USED

Typically biomaterials are classified as follows: 1) metals, 2) polymers, 3) ceramics, 4) composites and 5) biological materials (Ratner et al. 1996). They can also be classified according to their interactions with their surrounding tissue: 1) biotolerant materials, 2) bioactive materials and 3) bioreabsorbable materials (Geetha et al. 2009). In biotolerant materials with almost inert, smooth or porous surfaces, the tissue response is a foreign body reaction, where a fibrous scar-like tissue forms around the implant, isolating the implant from the tissue. On the other hand, bioactive materials with chemically reactive surfaces are able to form bony tissue around the implant material and integrate strongly with the implant surface. Bioreabsorbable materials can be degraded and replaced by regenerating tissues either fully or partially (Geetha et al. 2009, Konttinen et al. 2008).

The typical metallic biomaterials used for orthopedic applications include stainless steel (SS), cobalt (Co) based alloys,

titanium (Ti) and its alloys and tantalum (Ta) (Konttinen et al. 2008). In implant applications generally used alloying elements are aluminium (Al), niobium (Nb), vanadium (V), molybdenum (Mo), zirconium (Zr), nickel (Ni) and chromium (Cr). Metallic materials have many desirable properties like high strength and fracture toughness, hardness and biocompatibility which make them a practical choice for bone implant applications. Still the disadvantages, such as their high elastic modulus compared to bone and the release of ions are notable concerns. Stainless steel alloys with favourable combination of mechanical properties, corrosion resistance, non-magnetic response, ease of manufacturing as well as low production costs have the longest history among the metallic biomaterials (Disegi & Eschbach 2000, Alvarez et al. 2009). Components such as Ni, Co and Cr improve the mechanical properties of SS by alteration of its microstructure (Katti et al. 2008a). Still, these components are the most common metal sensitizers in the human body (Hallab et al. 2001a, Basketter et al. 1993), and are known to be released from SS in the body environment (Okazaki et al. 2005). When these metal ions are released from the implant, they behave like haptens and may trigger a type-IV hypersensitivity reaction (Hallab et al. 2001a) which can be a significant factor in a process promoting the loosening of the prosthetic device (Granchi et al. 2006, 2008). At present, new Ni-free SS have been developed, primarily to address the issue of Ni sensitivity and to improve the corrosion resistance and mechanical stability (Disegi & Eschbach 2000, Alvarez et al. 2009, Sumita et al. 2004). NiTi is a superelastic shape memory alloy with good corrosion resistance and therefore has attained numerous biomedical applications *e.g.* orthodontics, cardiovascular and orthopedics. However, NiTi materials are still controversial biomaterials because of the risks of allergy and toxic effects that can be triggered by Ni release. Different surface treatments like oxidation have been thought to offer a protecting film against the adverse reactions of Ni (Michiardi et al. 2007, Muhonen et al. 2007). For implant applications (*i.e.* dental implants, joint replacements and bone fixation), commercially pure Ti and

$TiAl_6V_4$ are the most commonly used. Their lower elastic modulus (100-112 GPa) compared to SS (210 GPa) and Co-Cr alloys (240 GPa) (Geetha et al. 2009) in addition to their beneficial osteoconductive properties makes them a better choice for bone applications and uncemented joint replacements. Titanium and Ti alloys have also good biocompatibility, low toxicity, low corrosion rates and beneficial mechanical properties which are partly due to the spontaneously formed covering oxide layer (Long & Rack 1998). However, the release of Al ions from Ti alloys might cause long-term health problems, such as Alzheimer's disease (Landsberg et al. 1992, Frisardi et al. 2010). In addition, the difference compared to bone elastic modulus (10-40 GPa) may lead to stress shielding. Ti alloys are also relatively softer than SS and Co based alloys (Katti et al. 2008a). Therefore, they can not be used on articulating surfaces without a coating. Recently new Ti alloys containing Nb, Zr and Ni have been developed to solve the existing problems (Konttinen et al. 2008). Cobalt-based alloys may be ordinarily described as non- magnetic, wear-, corrosion- and heat-resistant (Marti 2000). Typically 20-30 % Cr is added to the alloy to improve the corrosion resistance. Molybdenum may be used to enhance strength properties (Marti 2000, Konttinen et al. 2008). Other elements used in cobalt alloys are nickel, silicon, iron, manganese and wolfram (Konttinen et al. 2008). Co alloys have also good rigidity, abrasion and fretting properties for example compared to Ti alloys (Breme & Biehl 1998). Today, the use of Co alloys for surgical applications is largely related to orthopedic prostheses for the knee, shoulder and hip (Fig. 3) such as to fracture fixation devices (Marti 2000). The weaknesses behind these alloys are the same as encountered with SS; high elastic modulus compared to bone and release of ions which may cause many adverse effects, such as chronic inflammation, carcinogenesis, mutagenesis and cellular death (Uo et al. 2001, Au et al. 2006). Tantalum and its principle oxide are known to be biocompatible materials with low solubility and toxicity (Black 1994). It is mainly used in the porous form because bone and soft tissues can rapidly infiltrate into porous Ta, enhancing

mechanical stability (Hacking et al. 2000, Bobyn et al. 1999, Welldon et al. 2007). These properties have increased the interest in the use of Ta at the bone-implant interface of cementless implants (Konttinen et al. 2008).

Figure 3: *A CoCrMo surface replacement hip prosthesis photographed by R. Lappalainen.*

In orthopedic implant applications, ceramic materials possess many useful properties like high stiffness, inert behaviour under physiological conditions and excellent wear resistance (Katti et al. 2008a). Therefore, ceramic-on-ceramic, mainly alumina (Al_2O_3)-on-alumina, bearing surfaces have been commonly used in total hip arthroplasty (Mehmood et al. 2008, Keurentjes et al. 2008). However, their brittleness and low tensile strength may cause the fractures of femoral head component and breakage of ceramic cup (Kluess et al. 2008). In addition, insufficient osseointegration may be a problem (Ignatius et al. 2005), though this might be inhibited by nanostructuring (Mendonca et al. 2009a). Zirconia (ZrO_2) ceramics are well known as having better fracture toughness and flexural strength compared to Al_2O_3 ceramics (Tanaka et al. 2003). Zirconia ceramics have been demonstrated to possess potential as dental implants (Wenz et al. 2008) and hip replacement applications (Lewis et al. 2008, Cohn et al. 2008, Kohal et al. 2009). Because of its tetragonal

phase, pure zirconia exists in an unstable state, and thus it is typically stabilized with yttrium. However, yttrium-stabilized tetragonal zirconia polycrystals undergoes low-temperature aging degradation caused by phase transformation. Lately, ZrO_2/Al_2O_3 composites have been examined to avoid of the disadvantages of ageing of ZrO_2, for instance in the bearing surfaces of total joint replacements (Tanaka et al. 2003).

Ultra-high-molecular-weight-polyethylene (UHMWPE) is one of the most preferred polymers as an orthopedic implant material because of its ability to combine superior wear resistance along with high fracture toughness and biocompatibility compared to other polymers (Brach del Prever et al. 2009). Bone resorption surrounding the implant, osteolysis, caused by the wear debris of UHMWPE is however a major concern. Highly cross-linked polyethylene compared to conventional UHMWPE has been demonstrated to significantly decrease wear in hip simulators and early prospective randomized clinical studies (Ries 2005, Santavirta et al. 2003, Atienza & Maloney 2008). However, one disadvantage is that cross-linking reduces the mechanical properties of UHMWPE (Ries 2005, Brach del Prever et al. 2009). Recent studies have demonstrated that a modified manufacturing processes like sterilization with gas plasma or ethylene oxide or the use of the antioxidant vitamin E (alpha-tocopherol) might be able to enhance the properties of UHMWPE in joint replacement applications (Brach del Prever et al. 2009). In addition, polyurethanes with a lower coefficient of friction than UHMWPE bearings have been evaluated as joint replacement materials (Quigley et al. 2002, Scholes et al. 2006).

Composite materials have been used in medical device fabrication, because seldom only one material can possess all the physical requirements for successful implantation and function. For instance, ceramic-polymer composites have shown to have potential properties when used as total hip replacement materials (Katti et al. 2008a). In particular, hydroxyapatite (HA) and carbon (C) fiber based composites have attracted significant research interest (Bougherara et al. 2010, Katti et al. 2008a).

Materials of biological origin can be categorized into tissue transplants, blood products, processed human or animal originating products, such as demineralized bone matrix and hybrid products. In the case of bone implants, it is logical to handle natural materials – a new class of materials with an identical structure or composition to bone or which are synthesized by using the basic principles of biomineralization (Katti et al. 2008a). The key step in this synthesis method is the growth of minerals on an organic matrix in aqueous media. The use of biomimetic methods has already been successfully demonstrated, for instance the production of an HA coating on materials such as Ti (Majewski & Allidi 2006) and glass (Giavaresi et al. 2004) for use with orthopaedic implants and with chitosan-based composites for potential use in load-bearing applications (Katti et al. 2008b, Zhang et al. 2008a). Biodegradable chitosan is a biocompatible polysaccharide and exhibits an excellent film-forming and antigenic properties and it is also known to improve initial cell attachment (Carlson et al. 2008, Chua et al. 2008). In addition, collagen and calcium phosphate have been tested for these composites (Katti et al. 2008a).

3.2 FAILURE MECHANISMS OF IMPLANTS

There are a number of causes for implant failure (Fig. 4) which may be traced to the mechanical properties of implant: wear/corrosion, low fracture toughness/low fatigue strength and mismatch in elastic modulus compared to bone (Geetha et al. 2009) or biological causes, where the main reason is infection (Revell 2008). Some other reasons for failures are dislocation and failure due to poor surgical technique.

When implant materials are in contact with each other during relative motion, small particles become detached from the implant as a result of abrasion, adhesion or fatigue. For instance, in joint replacements this material wear may change the biomechanics, function and range of motion of the joint as well

as enter into dislocation and alter the physicochemical properties of the bearings, surface coatings and other treatments. The basis of periprosthetic tissue destruction, the so-called biologic response to implant debris, is challenging, since this may lead to chronic synovitis, foreign body and chronic inflammatory reaction, pathologic fracture and most concerning of all, periprosthetic osteolysis (Burke & Goodman 2008), which is a devastating long-term complication in total joint arthroplasty (Archibeck et al. 2001, Arora et al. 2001, Abu-Amer et al. 2007). Although cement particles were once simply blamed for osteolysis, it has become clear that any type of particle debris can result in bone resorption. However, it is still unclear how the cellular response to particles varies with size, shape, composition, charge, and the number of particles (Gonzălez et al. 1996, Sabokbar et al. 2003).The pathogenesis of implant-associated osteolysis involves inflammatory and osteolytic processes (Abu-Amer et al. 2007). Wear particles increase secretion by macrophages of different proinflammatory cytokines. These cytokines synergistically stimulate differentiation of osteoclast precursors into mature, multinucleated osteoclasts that are capable of efficiently resorbing bone. In addition to these cells, the osteolytic response includes other cell types *e.g.* phagocytes, giant cells, fibroblasts, neutrophils and lymphocytes. (Abu-Amer et al. 2007, Greenfield et al. 2005)

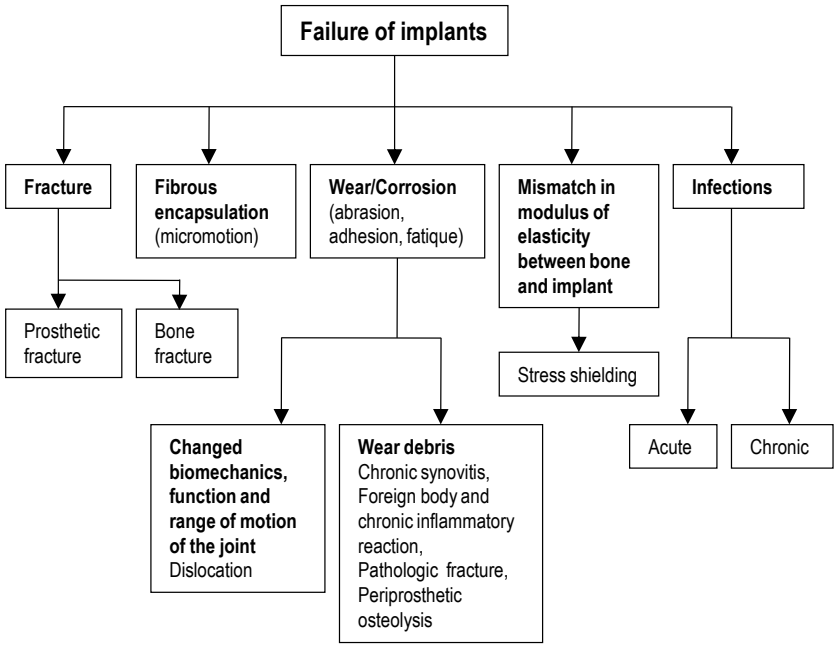

Figure 4: *Some causes for failure of bone implants. Modified from Geetha et al. (2009).*

Today, implant fracture is rarely a problem with the advent of the use of advanced materials and better prosthetic designs. Still, prosthetic fractures occur, for instance in ceramic total hip components due to their brittleness and low tensile strength. Instead, bone fractures around total joint replacements are increasing as reflected in the numbers of revision surgery. In addition, osteoporosis and osteomalacia expose the individual to this kind of fracture. (Burke & Goodman 2008) Wolff's law (Wolff 1892) describes the bone–stress relationship. According to this law, bone develops or adapts its structure so that it is best suited to resist the forces acting upon it (Wolff 1892). The refinement of Wolff's law, Frost's Mechanostat theory (Frost 1986) explains more extensively how the bone growth and bone loss can be stimulated in response to physical stresses, and on the other hand, to their lack. Mechanical loading is a particularly potent stimulus for bone cells, which improves bone strength and inhibits bone loss with age. However, also other stimuli *e.g.* hormones and cytokines affect the bone remodeling (Robling et

al. 2006). The distribution of mechanical stresses change when an implant is inserted into the bone. The implant supports the bone and enhances the bone resorption by shielding the bone from stress. Thus process, called stress shielding, can be seen for example around acetabular, femoral and total knee implants. For example, cemented or rigidly fixed femoral components constructed of stiff material release stress on the proximal femur and may enhance the resorption of proximal femoral bone. (Burke & Goodman 2008) By using implant materials with an elastic modulus near to bone, the problems associated with stress shielding maybe decreased. In joint arthroplasty operations, new surface replacement implants can be used to avoid this problem.

The success of implantation relies on the initial fixation and the retention of sufficient fixation over time. Primary stability is recognised as an important element in the aseptic loosening failure process of cementless implants. The inability of an implant surface to integrate with the adjacent bone due to micromotions can lead to fibrous encapsulation between the implant and bone with the resulting increased risk of implant loosening. (Viceconti 2000)

Infection related to implants is a very serious and clinically challenging problem and also responsible for major economical costs. According to the Finnish National Agency for Medicines, the rate of infection has been in a range of 10-30 % of all primary complications of primary total hip arthroplasty operations in 1998 – 2007 (FAR 2007). It has also been speculated that the revisions of total hip and total knee arthroplasties needing to be conducted because of deep infection may increase from 8.4% in 2005 to 47.5% in 2030 and from 16.8% to 65.5%, respectively (Kurtz et al. 2007b). Clinical implants may become infected and contaminated with microorganisms prior to placement of the implant, or may become colonized either from the spread of bacteria from a contiguous site, or from a distant site through the bloodstream or through a natural barrier to infection that has been disrupted by the implant (Millar 2000). Infections may be acute, usually occurring within a month of operation, or

chronic, becoming evident only after many months. If the typical signs of infection (pain, fever, chills or a draining sinus onto the skin) are present, the recognition is quite straightforward. However, if the symptoms are non-specific, the diagnoses are very challenging. Different blood tests, imaging with radio-isotopes, examination of joint fluid and the histological as well as microbiological examinations of tissue samples may reveal the presence of infection. (Revell 2008) The bacteria associated with implant infections include Gram positive staphylococci, enterococci, corynebacteria and Gram negative bacteria such as *Pseudomonas*, *Acinetobacter* and *Candida* species (Millar 2000). In prosthetic infections, *Staphylococcus aureus (S. aureus)*, *Staphylococcus epidermidis (S. epidermidis)* and *Pseudomonas* species are the most common bacteria types (Revell 2008). The ability of these bacteria to cause serious implant infection is due to their capability to form biofilms. Infecting bacteria grow predominantly within a confluent biofilm on the surface of the prosthesis. This protects bacteria against parenteral antibiotic therapy as well as the host response treatment and it often necessitates removal of the implant (Neut et al. 2007, Darouiche 2001). It has been also speculated that bacterial endotoxin may inhibit initial osseointegration of the implants and have a significant role in the induction of aseptic loosening. The classical endotoxin is lipopolysaccharide produced by Gram-negative bacteria. However, both Gram-negative and Gram-positive bacteria also produce other molecules, such as peptidoglycan, lipoteichoic acid and teichoic acid that exert endotoxin-like biological activities. (Greenfield et al. 2005)

4 Host tissue–bone implant interaction

The interaction between the material and the living system, also called biological performance, involves two components, the local and systemic response of host tissue to the material and the response of the material to host tissue (Black 1999). The material variables influencing the host response and the characterization of the generic host response to biomaterials are described in Table 1.

Table 1: *Material variables that influence the host response and the characterization of the generic host response to biomaterials. Material variables and host responses studied in this thesis are in bold font. Modified from Williams (2008).*

Material variable	**Host response**
Surface topography (roughness and texture)	**Tissue specific cell responses**
Surface energy	**Bacteria behaviour and biofilm formation**
Surface charge	Protein adsorption and desorption
Surface chemical composition, chemical gradients, surface molecular mobility	Cytotoxic effects
Elastic constants (Young`s modulus, Poisson`s ratio)	Neutrophil activation
Hydrophobic-hydrophilic properties	Macrophage activation, foreign body giant cell production, granulation tissue formation
Crystallinity and crystallography	Fibroblast behaviour
Porosity	Microvascular changes
Corrosion (metal ion toxicity)	Platelet adhesion, activation and aggregation
Degradation/Dissolution (product toxicity)	Complement activation
Wear debris	Antibody production, immune cell responses
Additives, catalysts, contaminants and leachables and their toxicity	Acute or delayed hypersensitivity
	Genotoxicity and reproductive toxicity
	Tumour formation

When an implant is placed in bone, the host response involves a series of complex protein and cell reactions, ideally leading to the intimate integration of adjacent bone with the biomaterial (Fig. 5). In osseointegration phenomena, gaps between bone and implant must be filled as well as repairing the bone damaged during preparation of the implant site (Puleo & Nanci 1999). One example of an immediate material response is the oxidation of the metallic implant in the physiological environment, and after that, the possible release of metal ions, *i.e.* corrosion (Puleo & Nanci 1999).

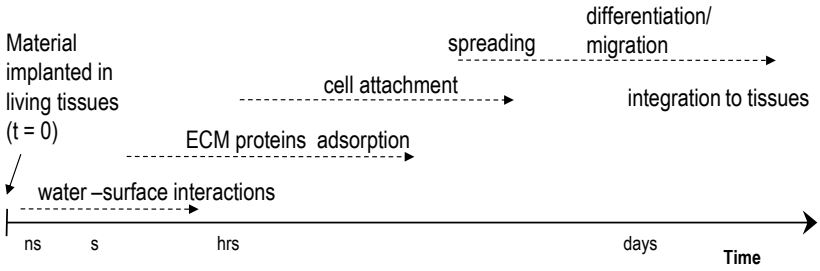

Figure 5: *A time scale picture of host tissue-bone implant interaction. Modified from Roach et al. (2007).*

Within nanoseconds, implanted materials placed in a biological milieu are coated with water molecules which create a water shell around the material (Roach et al. 2007). After that, in a period of seconds to hours after implantation, the material becomes covered in an adsorbed layer of proteins. These proteins originate from blood, tissue fluids and the extracellular matrix (ECM). Some of these proteins undergo rearrangement and desorption before cells reach the implant surface through the protein covered layer. Cell attachment, spreading, differentiation and mineralization takes from minutes up to several days after implantation and is influenced by biological molecules like ECM, cell membrane and cytoskeleton proteins. (Puleo & Nanci 1999, Roach et al. 2007) In bone implants, the final stage can last from a few months (*e.g.* various fracture fixation devices, such as plates and screws) up to several decades (total hip replacement). During this stage, also adverse

responses (*e.g.* clots, fibrous capsule formation and infection) and implant failure may occur.

4.1 PROTEIN ADSORPTION

In a physiological environment, cell adhesion always follows protein adsorption, and thereby the composition of the adsorbed layer of specific proteins is a key mediator of cell behaviour. For this reason, proteins favourable to specific cells can stimulate a constructive cell response, favouring wound repair and tissue integration, whereas proteins which are detrimental to cells may indicate an impossible healing and a foreign material to be removed or isolated. (Wilson et al. 2005) For example, the adhesion of bone cells is mediated by proteins of bone ECM synthesized by bone cells (Anselme 2000). In addition, osseointegration requires that the proteins encountered by the cells must support or actively promote bone cell functions at later stages.

As stated before, the implant is first covered by water molecules when it comes into contact with living tissue. The extent and pattern of interaction of the water molecules with the surface of the implant depends on the surface properties of the material, such as its surface hydrophilicity or hydrophobicity (Kasemo 1998). These properties have also an influence on which proteins will adhere following the formation of the hydration shell.

Adsorption of blood proteins occurs rapidly after the initial hydration layer surrounds the material. Since many hundreds of different proteins are present, there is a competition for the surfaces which takes place between proteins. Typically the more abundant small proteins win this competition because of their rapid transport to the surface. Subsequently, larger proteins from ECM of bone have higher affinities towards the surface and these replace the small proteins. (Roach et al. 2007) ECM of bone is composed of 90% collagenic proteins such as type I collagen and type V collagen and 10% non-collagenic proteins

like osteocalcin, osteonectin, bone sialoproteins, proteoglycans, osteopontin and fibronectin. (Anselme 2000) This phenomenon where the faster diffusing molecules are displaced by proteins with higher affinity towards the surface is generally termed the Vroman effect (Vroman & Adams 1969). After all of these complex processes of protein adsorption, desorption and rearrangement, this residual protein layer reaches equilibrium at the surface.

One of the most important properties of the surface influencing the protein adsorption is its wettability (Wilson et al. 2005). Proteins will be adsorbed to a greater amount to the hydrophobic surfaces than hydrophilic ones as has been reported in many studies (Kennedy et al. 2006, Sethuraman et al. 2004, Arima & Iwata 2007, Gessner et al. 2000, Wilson et al. 2005, Choi et al. 2008). However, this is not a universal result, because some studies have demonstrated that increased wettability causes increased amounts of fibronectin (Fn) (Hao & Lawrence 2007, Michiardi et al. 2007, Wei et al. 2009) and albumin (Alb) (Michiardi et al. 2007) adsorbed. Electrostatic effects may also be a driving force in protein adsorption. However, typically these effects are much weaker than hydrophobic effects because of the complexity attributable to the aqueous media where surface charges are shielded by hydrating water modified by pH and small ions (Wilson et al. 2005, Roach et al. 2007). Nonetheless it has been reported that charged proteins are rather adsorbed to oppositely charged surfaces or at least to surfaces where the charge repulsion with the protein is at its smallest (Xie et al. 2010, El-Ghannam et al. 2001, Cai et al. 2006). Surfaces that hinder protein adsorption because of their hydrophilic nature or because of their opposite charge cause the protein to be adsorbed with the help of a conformational change. Structural changes within the protein molecules may also increase the entropy of the system despite the dehydration and permit increasing contact between the protein and surface. These rearrangements are also related to the reversibility of adsorption and protein elutability. (Wilson et al. 2005)

4.2 BONE CELL ADHESION

Cell adhesion to the surface of the implant is one of the most critical factors when determining its biocompatibility. Surface properties of biomaterials like topography, chemistry, wettability and surface charge play a crucial role in osteoblast adhesion to the implant surface and are thus some of the main interests of this study. The previous studies of these interactions will be summarized later in this chapter. However, when optimizing the bone/biomaterial interface, it is essential to understand the role of biological molecules involved in bone cell adhesion since the surface of an implant is always covered by these molecules with which the bone cells interact. For a bone implant, complete fusion between the implant surface and the adjacent bone with no fibrous tissue is essential for good osseointegration (Anselme 2000).

When cells are faced with a surface, they firstly attach, adhere and spread. These events are mediated by the proteins adsorbed to the surface. Thereafter, the quality of this adhesion will influence the cell's morphology and the capacity to proliferate and differentiate. As described in the previous section, the proteins affecting the bone cell adhesion at the biomaterial interface originate from ECM. Added to this, human osteoblasts have been shown to adhere preferentially to fibronectin when compared with type I, type IV and type V collagen as well as vitronectin and laminin (Gronthos et al. 1997). The primary interaction between cells and ECM proteins occurs via integrins. The importance of these integrins has been demonstrated in a study where the cell adhesion decreased when antibodies were used to prevent these interactions (Degasne et al. 1999). Integrins belong to the family of adhesion molecules, which can be characterized by their capacity to interact with a specific ligand. These ligands may be located on the membrane of neighbouring cells or these may also be ECM proteins. Integrins are a large family of heterodimeric structures that consist of two types of sub-units, α and β. Each sub-unit is composed of a large extracellular domain, a transmembrane domain and a short

cytoplasmic domain. (Hynes 1992, Anselme 2000) For most cell types, including osteoblasts, adhesion to ECM is essential to build a multicellular organism and survive. Not only integrins, but also many cytoplasmic proteins on the internal face like talin, vinculin, paxillin and tensin participate in cell attachment, by forming focal adhesions (Fig. 6). In fact, these focal adhesions are large protein complexes containing a vast array of different proteins. (Zamir & Geiger 2001) Focal adhesions play a central role in cell migration since they connect the cytoskeleton of a cell to the ECM. Furthermore the architecture of the actin cytoskeleton is an integral part of the perpetuation of cell shape and cell adhesion since cells sense their surroundings by using finger-like protrusions known as filopodia or sheet-like protrusions known as lamellipodia (Roach et al. 2007, Anselme 2000). Another main function of integrins in addition to helping cell attachment to ECM is to promote signal transduction from the ECM to the cell. This "inside-out mode" consequently regulates cell growth, division and differentiation. Different cell types have their own blends of integrins; *e.g.* osteoblast and osteoclast have been demonstrated to possess different integrin subunits (Clover et al. 1992, Hughes et al. 1993). All human bone cell types have been shown to express β_1 and α_5 sub-units with uniformly expression of α_v which was heterogeneously expressed by osteocytes. Osteoclasts expressed α_2, α_v and $\alpha_v\beta_3$ sub-units. (Hughes et al. 1993)

All this information which is available about the mechanisms by which cells adhere to substrates has created increasing interest towards biochemical surface modification. This technique includes the immobilizing of proteins, enzymes or peptides on biomaterial surface with a view to induce specific cell and tissue responses. (Puleo & Nanci 1999) However, the use of proteins like fibronectin, collagen, or laminin may cause some problems when used in medical applications. They may evoke undesirable immune responses and increase infection risks and even accelerate protein degradation, since they are isolated from other organisms (Hersel et al. 2003). Another way for orthopedic materials to function is to immobilize cell

adhesion molecules like arginine-glycine-aspartic acid (RGD) adhesive sequence (Fig. 6) which is known to mediate cell attachment, for instance fibronectin, vitronectin, type I collagen, osteopontin and bone sialoprotein (Lebaron & Athanasiou 2000, Hersel et al. 2003). In addition, immobilized $\alpha_v\beta_3$ -integrin-specific FN fragment $FNIII_{7\text{-}10}$ (Petrie et al. 2008) and glycine–phenylalanine–hydroxyproline–glycine–glutamate–arginine (GFOGER) collagen-mimetic peptide (Reyes 2007) has been demonstrated to enhance osteoblastic responses.

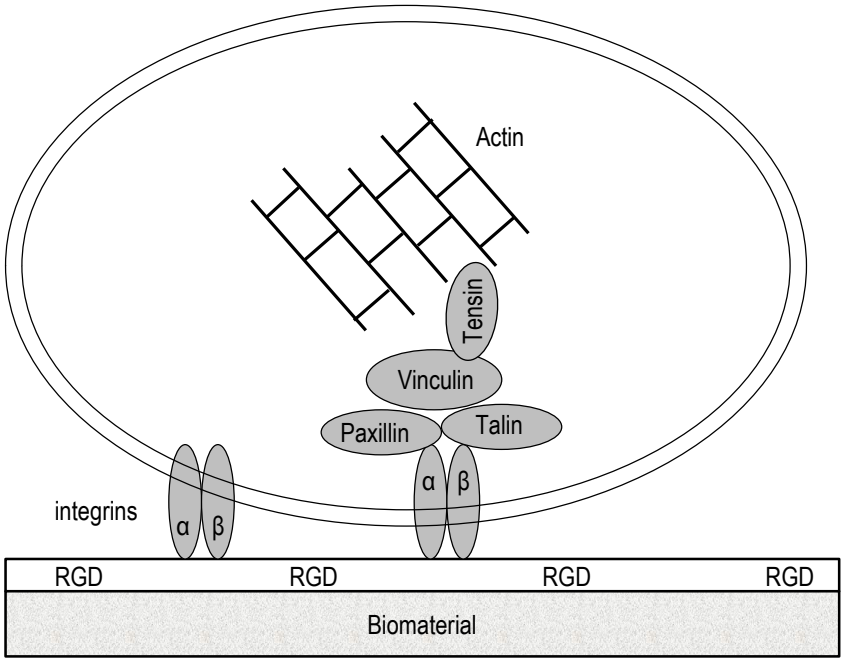

Figure 6: *Representation of the cell proteins involved in osteoblast adhesion on biomaterial. Modified from Anselme (2000).*

4.2.1 *In vitro* models

When one is developing a new implant material with an optimal interface between bone and implant surface, it must undergo rigorous testing both *in vitro* and *in vivo*. *In vitro* testing is popular for the characterization of bone-contacting materials, so that the need for animal models can be reduced. It is typical to use *in vitro* models as a first stage test for acute toxicity and

cytocompatibility to avoid the unnecessary use of animals in the testing of cytologically unknown materials. (Pearce et al. 2007) It is conventional to use the term biocompatibility when testing materials *in vitro* even though the correct term should be cytocompatibility. Biocompatibility is a better term when testing materials *in vivo* with animals or humans. (Richards et al. 2001) *In vitro* tests are very feasible in studies where the adhesion, proliferation, differentiation, contact guidance and mineralization of cells at the surface of the implant material are being evaluated. This is a more readily standardized and quantifiable method compared to *in vivo* tests. It is also cheaper and faster way to clarify how the different surface properties like wettability, charge and topography individually affect cellular functions. Of course one need to keep in mind that *in vitro* tests may also overrate the level of material toxicity and are limited to rather acute studies because of the limited lifespan of cultured cells. (Pearce et al. 2007, Pizzoferrato et al. 1994) Since the cells originate from the different microenvironments, such as bone marrow or calvaria, one cannot be sure that all osteoblastic cells will behave in the same way at the substrate (Puleo & Nanci 1999). *E.g.* MG-63 cells (human osteosarcoma cell line) have been shown to display similar responses to surface free energy (SFE) of treated quartz surfaces than hFOB (human fetal osteoblast progenitor) cells, whereas MC3T3-E1 (murine osteoblastic cell line) and Saos-2 cells (human osteocarcoma cell line) responded to SFE to a lesser degree than hFOB cells (Lim et al. 2008).

However, well-characterized osteoblasts or osteoblast-like cells do represents a successful *in vitro* model for the study of bone-biomaterial interactions. Most of the cell culture work has been conducted with osteoblastic cells (Cooper et al. 1998) and primary and passaged cells from several species and anatomical locations have been used, as well as several osteosarcoma, clonal, and immortalized cell lines (Puleo & Nanci 1999). For instance, the Saos-2 cells are derived from a primary osteosarcoma in a 11-year-old Caucasian girl by Fogh et al. in 1973 (Fogh et al. 1977). This non-transformed cell line is quite well characterized

and known to possess several osteoblastic features (Rodan et al. 1987, Dass et al. 2007). Thus it is widely used in studies on bone cell adhesion, proliferation, differentiation and metabolism (Lim et al. 2008, Okumura et al. 2001, Osathanon et al. 2006, Ku et al. 2002). Overall, the interactions of osteoblasts or osteoblastic cells with potential orthopedic implant material can be measured in terms of viability, attachment, proliferation, differentiation and synthesis of matrix. This offers unique insights into the process and phenomenon of osseointegration (Cooper et al. 1998, Davies 1996) which can be tested later *in vivo* when also the mechanical loading of the bone implant in the natural environment is being conducted.

4.3 BACTERIAL ADHESION ON IMPLANT SURFACES

Infection related to implanted medical devices is a very challenging and partly unclear process since it includes complex mechanisms of bacterial adhesion and biofilm formation. The risk of clinical implant affiliated infections is dependent on many factors related to the patient (*e.g.* age, general health and immune status), implant (design and material composition), insertion site, procedure, operating environment and the management of implant after insertion (McCann et al. 2008, Millar et al. 2005). The dangers related to the adherence of pathogenic bacteria are their capability to establish multilayered, highly structured biofilms on implant surfaces. Colonized biofilms are extremely difficult to eradicate since antimicrobial treatment has little or no effect against biofilm populations even though the same drugs may be effective against their planktonic (free-floating) counterparts (Gilbert et al. 1997). Surgical removal and replacement of the implant is often necessary after biofilm formation (McCann et al. 2008, Neut et al. 2007, Darouiche 2001) and in cases where the implant or device cannot be removed, patients need to take intermittent antibiotic therapy for the remainder of their lives (Costerton et al. 2003). In addition to arthroprostheses the typical implants that can be

compromised by biofilm related infections are: dental implants, central venous catheters, heart valves, ventricular assist devices, coronary stents, neurosurgical ventricular shunts, implantable neurological stimulators, fracture-fixation devices, inflatable penile implants, breast implants, and intra-ocular lenses (Costerton et al. 2005).

4.3.1 Biofilm formation

Biofilm formation is a multistep process which can be categorized into four distinct phases; attachment (adhesion), accumulation, maturation and detachment (McCann et al. 2008). Since coagulase-negative *S. epidermidis* and coagulase-positive *S. aureus* are the most frequent causes of nosocomial infections and infections on indwelling medical devices involving biofilms (Otto 2008, O´Gara & Humphreys 2001, Fitzpatrick et al. 2005) more emphasis will be devoted to investigate their abilities to form biofilms. Clinical manifestations of infections due to *S. epidermidis* differ from those of *S. aureus* infections. Bacteremia caused by coagulase-negative staphylococci is rarely life-threatening, especially if treated rapidly and appropriately. The clinical prospect is typically non-specific, and the clinical course more often subacute or even chronic. (von Eiff et al. 2002) *Staphylococcus epidermidis* is much less toxigenic than *S. aureus. Staphylococcus aureus* produces many toxins and tissue damaging exoenzymes in a strain-dependent manner and cause infections which are much more likely to result in serious adverse consequences for the patient (von Eiff et al. 2002, Katsikogianni & Missirlis 2004, Millar 2005).

In general, bacteria prefer to grow attached to surfaces in contact with liquids (Davies 2000). Surfaces are thought to provide a higher concentration of nutrients and to promote genetic exchange as well as conferring protection from the host`s immune system to destroy the pathogenic strain (Donlan 2001). Initial bacterial attachment is the first critical step in the development of implant-associated infection. There are a multitude factors involved in this first phase *e.g.* surface conditioning, mass transport, surface charge, hydrophobicity

and roughness as well as surface micro- or nanotexture (Palmer et al. 2007). Before bacterial attachment, proteinaceous, macromolecular components present in the body fluids immediately are adsorbed onto the implant forming a conditioning film (Gristina 1987) which plays an important role in bacterial adhesion (Wadström 1989) and these host proteins may even serve as receptors for bacterial attachment (Fitzpatrick et al. 2005).

The physicochemical properties of the implant surface listed above also influence proteins adhesion. Many proteins in serum or tissue such as albumin, fibronectin, fibrinogen, laminin, denatured collagen and others promote or inhibit bacterial adhesion binding to substrata or bacterial surface (Katsikogianni & Missirlis 2004, An & Friedman 1998). Most of the binding between proteins and bacteria is specific ligand- and receptor-mediated interactions (An & Friedman 1998). This protein adsorption is important to be taken into consideration also *in vitro* models, for instance by precoating the surfaces with serum proteins before bacterial culturing. Patel et al. (2007) demonstrated that the initial adhesion of *S. epidermidis* was suppressed in the presence of adsorbed serum proteins even though inter-bacterial adhesion, possibly aided by slime production, led to the formation of a robust biofilm. Physical forces such as van der Waals attraction and gravitational forces as well as the effect of surface electrostatic charge and hydrophobic interactions are involved in this initial attachment of bacteria to the surface. These physical interactions can be divided into weak long-range interactions of low specificity (electrostatic and or van der Waals forces) existing during reversible attachment and highly specific short-range interactions (dipole, ionic and hydrogen bonding) during irreversible attachment (An & Friedman 1998). During this initial contact, bacteria display Brownian motion and can be readily removed by fluid shear forces *e.g.* rinsing (Marshall et al. 1971). In addition, the involvement of specific protein factors including the staphylococcal surface proteins, SSP-1 and SSP-2, has been observed in the initial attachment of *S. epidermidis* to

abiotic surfaces (Veenstra et al. 1996). Moreover teichoic acids, highly charged cell wall polymers, play a key role in the primary attachment phase of biofilm development (O`Gara et al. 2007). In *S. epidermidis* adherence, the cell wall lytic enzyme AtlE, which affects the hydrophobicity of the cell surface, is thought to play an important role (Heillman et al. 1997, Rohde et al. 2006). This initial attachment of bacteria forms the base for the second phase of adhesion where the molecular- and protein-specific reactions between bacterial surface structures and implant surfaces become predominant. This phase is indicative of a stronger adhesion of bacteria to a surface by the bridging function of bacterial surface polymeric structures such as capsules, fimbriae, pili and slime (An & Friedman 1998). With *S. epidermidis* and *S. aureus,* the best-known adhesins during the accumulation are the extracellular polysaccharide adhesin, termed polysaccharide intercellular adhesin and polymeric N-acetyl-glucosamine (O`Gara et al. 2007). In addition, the role of surface proteins like accumulation associated protein, biofilm-associated protein and biofilm-associated homologue protein are associated in biofilm development in staphylococci (McCann et al. 2008, O`Gara et al. 2007,Katsikogianni & Missirlis 2004).

When bacteria have irreversibly attached to a surface, the process of biofilm maturation begins where the density and complexity of the biofilm increase, since surface-bound organisms begin to actively replicate or die and extracellular components generated by attached bacteria interact with organic and inorganic molecules in the immediate environment to create the glycocalyx. For example, with implants this may include a host-derived inflammatory response proteins or matrix proteins like fibrinogen, fibronectin and glycosaminoglycans attached to the implant surface. (Dunne 2002) The regulation of gene expression in response to increasing cell density and thereby enabling the bacteria to adapt to changing environmental conditions like a change in the nutrient supply, altered oxygen levels and the switch from plancktonic to biofilm growth is called cell-cell communication or a quorum sensing (QS) system (Otto 2004). Two QS systems,

the *luxS* QS system and the accessory gene regulator system have been identified to regulate several of the biofilm associated factors of *S. epidermidis* and *S. aureus* at various stages of biofilm formation (McCann et al. 2008, Xu et al. 2006, Vuong et al. 2004). Accessory gene regulator has been demonstrated to play a key role in the detachment process of biofilm bacteria (Vuong et al. 2004). Also the delta-toxin has been shown to be involved in detachment process (McCann et al. 2008). The detached cells of biofilm may contribute to the toxemia associated with acute staphylococcal infections (Yarwood & Schlievert 2003).

Biofilm resistance is typically multifactorial and may vary from one organism to the next. The complexity of factors makes biofilm eradication very complicated and often requires prompt removal of the implant (Aslam 2008, Neut et al. 2007, Darouiche 2001). First of all, bacteria in biofilms are enclosed within a protective matrix composed of exopolysaccharide, proteins and nucleic acids which act as a barrier against penetration of antimicrobial agents (Arciola et al. 2005, McCann et al. 2008). In addition, the growth rate of the bacteria in biofilms plays a role in antibiotic resistance, since antimicrobials are more effective in killing rapidly growing cells and the bacteria in biofilm are in a slow-growing or stationary phase (Lewis 2005, Ashby et al. 1994, Fux et al. 2005, McCann et al. 2008). It has also been suggested that some bacterial cells in the biofilm develop a distinct phenotype including expression of genes which renders them resistant to antibiotics (McCann et al. 2008). Biofilm bacteria may also produce so-called persister cells which are a unique class of inactive but highly protected cells having tolerance to antibiotics (Cogan 2006, Lewis 2005). In addition, the altered chemical microenvironment present within a biofilm including pH, pO_2, pCO_2, the divalent cation concentration, the hydration level and the pyrimidine concentration can influence the activity of certain antimicrobials (Dunne 2002).

4.3.2 *In vitro* tests

Evaluating bacteria-material interaction *in vitro* is challenging and complicated process and these simplified measurements

might be misleading since the whole system is very complex and dynamic. *In vivo*, an implanted material is typically under a mechanical stress state and the surface of the implant may change the composition with time. The biological fluid flow also interacts with surface and the number, specificity and activity of adhesive receptors may vary as a function of time (Katsikogianni & Missirlis 2004). Furthermore, there is always the race for the surface between bacteria and tissue cells (Gristina 1987). However, well sophisticated *in vitro* techniques provide useful means for investigating the adhesion process and biofilm formation of infected bacteria. There are many important environmental factors that should be taken into account when performing *in vitro* tests. These include general culturing circumstances such as temperature, pH, time period of exposure, bacterial concentration and the possible sterilization or chemical treatments of substrate before culturing or the presence of antibiotics (An & Friedman 1998).

Serum proteins have also a significant role, either promoting or inhibiting bacterial adhesion. These proteins may bind to the surface of the material or bacteria or may influence the bacterial adhesion just by being present in the culture medium. By changing these environmental factors, one can better control the whole adhesion process. The adhesion process for a specific material depends to a great extent on the bacterial species and strains. This can be explained by different physicochemical characteristics of separate species and strains (An & Friedman 1998). One of the most important physical factors of bacteria is its hydrophobicity. Another parameter is the bacterial surface charge which is almost always negative in an aqueous suspension even though the degree from species to species may vary. The surface charge of bacteria varies in different bacterial species and is affected by the growth medium, the pH and the ionic strength of the suspending buffer, bacterial age, and bacterial surface structure. (Katsikogianni & Missirlis 2004)

One commonly used *in vitro* technique is the static assay. In this assay, the surface is overlaid with a suspension of bacteria for a predetermined period of time. Subsequently non-adherent

bacteria are removed by rinsing or centrifugation and the adhered bacteria are counted and visualized. (Katsikogianni & Missirlis 2004) The remaining bacteria and biofilm can be investigated by many methods : 1) microscopy for counting and morphological visualization of adherent bacteria (light-, image-analyzed epifluorescence-, scanning electron-, confocal laser scanning- and atomic force microscopy), 2) viable bacteria counting methods ("Colony forming unit" (CFU) plate counting, radiolabelling and "Circulating tumor cell" staining) and 3) direct and indirect methods like spectrophotometry, coulter counter and biochemical markers (*e.g.* adenosine-5'-triphosphate). Methods of evaluating slime or biofilm include visualizing the biofilm by different staining and microscopy methods. Biofilm thickness, density, morphology and content measurements are essential for biofilm study and could be recognized using different microscopical (such as light-, confocal-, epifluorescence- and scanning electron microscopy) and immunochemical methods. (An & Friedman 1997, Katsikogianni & Missirlis 2004) Different flow chamber techniques in which the parallel-plate and radial techniques are the most widely used to study microbial surface interactions under conditions of flow. Rotating a disc in liquid is one way to achieve a flow effect. *In vitro* techniques also enable the measurement of the interaction forces between the bacteria and the surfaces. Nowadays, the atomic force microscope (AFM) has become a powerful tool for this kind of study (Katsikogianni & Missirlis 2004). In addition, there is a great need for an *in vitro* system which would allow the race between bacteria and tissue cells to be investigated and the first experimental set-up has now been tested. According to this setup, both the absence and presence of flow, as well as the number of adhering bacteria, appear to determine whether tissue cells are able to grow on a biomaterial surface (Subbiahdos et al. 2009).

4.3.3 Effects of material properties on bacterial adhesion and biofilm formation

The decisive material properties influencing the bacterial adhesion are as follows: topography (roughness, micro- or nanotexture), wettability, charge and chemical composition. These material properties may be utilized in creating novel surface coatings to prevent bacterial adhesion but one needs to remember that these influences are not so straightforward since the first adhering proteins may change these properties. It has been reported that rough surfaces promote bacterial adhesion and colonization in general (Tang et al. 2009, Harris et al. 2007, Amarante et al. 2008, Chin et al. 2007, Taylor et al. 1998). Recent studies have also suggested that nanostructured materials may be used for inhibition of bacterial adhesion and biofilm formation in orthopedic implants not only do they have a better efficacy as bone implants but they also promote osseointegration as compared to conventional orthopedic implant materials (Montanaro et al. 2008, Weir et al. 2008).

Several studies have reported a strong positive relationship between surface hydrophobicity and the rate of bacterial adhesion (MacKintosh et al. 2006, Cerca et al. 2005, Patel et al. 2007, Bayoudh et al. 2009, Kodjikian et al. 2003, Sousa et al. 2009). However, Tang et al. (2009) demonstrated that there was a decreasing order of *S. epidermidis* adhesion with increasing surface hydrophobicity on polymeric surfaces. Furthermore, a hydrophobic diamond-like carbon-polytetrafluoroethylene-hybrid (DLC-PTFE-h) has been demonstrated to resist bacterial adhesion (Kinnari et al. 2007). An important factor when investigating the effects of these wettability properties on bacterial adhesion is also the presence of serum proteins (Patel et al. 2007, MacKintosh et al. 2006) and the ionic strength of the culture medium (Bayoudh et al. 2009). Some investigators have found that more hydrophobic bacteria strains have higher adhesion rates than their less hydrophobic counterparts and usually adhere better to hydrophobic than onto hydrophilic surfaces (Bruinsma et al. 2001, Bayoudh et al. 2006, 2009). It has been also demonstrated that hydrophilic surfaces are subjected

to lower adhesion rates as compared with hydrophobic control surfaces regardless of the bacterial strain's surface hydrophobicity (Cerca et al. 2005, Bayoudh et al. 2009). Thus, the results in the literature are still in controversial.

The classical DLVO (Derjaguin, Landau, Verwey, Overbeck) theory of colloid stability has been used to explain the adhesion of microorganisms towards a substratum. According to this theory, particle adhesion is driven by the sum of the attractive Lifshitz-Van der Waals (LW) interactions and the electrostatic double layer (EL) interactions, which can be either attractive or repulsive, depending on the surface charge. (Derjaguin & Landau 1941, Verwey 1947) However, this theory is not valid for the bacterium and substratum surfaces, where hydrogen and chemical bonds are involved in the adhesion mechanisms. The extended XDLVO theory takes into account how these bonds affect the close approach of bacteria and substrate surface by incorporating an additional term called the short-range Lewis acid base (AB) interactions in addition to LW and EL interactions (van Oss et al. 1986, van Oss 1995). The AB interactions are based on electron donor/electron acceptor interactions between polar moieties in polar media and can be attractive or repulsive and may be up to 10-100 orders of magnitude greater than these non-specific LW and EL interactions (van Oss et al. 1989). Some researchers have evaluated the relationship between different modes of the adhesion and adhesion dynamics of staphylococci to a hydrophilic and hydrophobic substrate. According to that study, more adsorption and desorption events were found on hydrophilic surfaces compared to hydrophobic counterparts. This difference was concluded to be attributable to repulsive AB interactions between the staphylococci and the hydrophilic surface, as opposed to the hydrophobic surface exerting attraction. (Boks et al. 2009) Baier (Baier 1980) determined a relationship between bacterial adhesion and SFE, known as Baier's curve, demonstrating that the lowest bacterial adhesion is obtained with a SFE level around 25 mN/m. Other studies have also obtained the same correlation between bacterial

adhesion and SFE (Pereni et al. 2006, Litzler et al. 2007). However, one has to remember that both DLVO and XDLVO theories are limited to the first stages of attachment and they do not account for the biological specific interactions and specific experimental conditions these have a major influence on the adhesion process between adhesive proteins and bacteria (Vitte et al. 2004, Pereni et al. 2006, Litzler et al. 2007). As mentioned above, bacteria typically have a net negative charge on their cell wall at neutral pH. Thus one can conclude that material surface charge has an influence on bacterial adhesion and that greater repulsive forces exist between negatively charged bacterial cells and negatively charged surfaces. In addition to all of the above mentioned material surface properties which have been demonstrated to have an influence on bacterial adhesion, there is a study which suggests that mechanical stiffness of substrate material represents an additional parameter that can regulate adhesion and subsequent colonization by viable bacteria (Lichter et al. 2008).

4.3.4 Preventing of bacterial adhesion

Optimizing the surface properties of implant material may be one effective way to prevent bacterial adhesion. In addition, coatings that release metals with antibacterial properties have been used to prevent implant infections. The commonly used are the biomaterials coated or impregnated with silver oxide (Ag_2O), Ag alloy or Ag nanoparticles (Furno et al. 2004, Verne et al. 2009, Zhang et al. 2008b, Secinti et al. 2008, Stobie et al. 2008, Chen et al. 2006). However, there exists a risk that the wide use of Ag products may result in the growth of Ag resistant bacteria (Silver 2003). The usefulness of Co as an antibacterial agent has also been known for a long time (Kim et al. 2006, Zhang et al. 2007). The enhancement of antibacterial properties of diamond-like-carbon (DLC) has been extensively studied and many dopants have been found to increase this property *e.g.* Ag and platinum (Pt) (Morrison et al. 2006), silicon (Si) (Shao et al. 2010, Liu et al. 2008, Zhao et al. 2007a, Zhao et al. 2009), fluorine (F)

(Ishihara et al. 2006), nitrogen (N) (Liu et al. 2008, Zhao et al. 2009) and polytetrafluoroethylene (PTFE) (Kinnari et al. 2007).

Some other examples of studies where the bacterial resistance towards typical implant materials have been tested are gas nitriding of $TiAl_6V_4$ alloy (Sarrò et al. 2006) and ion-implantation (N^+, O^+ and SiF_3) of SS (Zhao et al. 2008). The anti-biofilm properties of chitosan-coated surfaces have been recently tested (Carlson et al. 2008, Shi et al. 2008, Chua et al. 2008) and by utilizing surface-grafted chitosan in conjunction with the cell adhesive RGD peptide, it has been possible to increase osteoblast cell attachment, proliferation and ALP activity (Shi et al. 2008, Chua et al. 2008). Loading of antimicrobial agents into the medical devices has been used to produce bacteria-inhibitory and bactericidal surfaces. In total joint arthroplasty, this means that the bone cement has been loaded with antibiotic (Block & Stubbs 2005, Jiranek et al. 2006). However, several investigators have demonstrated that biofilm can be easily formed on antibiotic-loaded bone cement: biofilm production may be reduced but not totally eliminated in the presence of locally delivered antibiotics (van de Belt et al. 2000, 2001, Dunne et al. 2008, Oga et al. 1992). There is also the possibility that the coating of medical devices with antibiotic may lead to the proliferation of antibiotic-resistant bacteria. Furthermore, recent advances in the knowledge of the molecular mechanisms of biofilm formation have opened the way to the development of a number of strategies which concentrate on the functional molecules, gene systems and regulatory circuits and which can be used to inhibit biofilm infections. For *S. epidermidis*, surface-expressed components such as polysaccharide intercellular adhesin, techoid acid, proteinaceous adhesins and cell-wall anchored proteins have been identified as promising targets for vaccine development (Götz 2004). However, the occurrence of allelic variations in staphylococci makes the production of an effective vaccine very challenging (Marra 2004).

All in all, the need for prevention of bacterial adhesion and biofilm formation is as acute as ever and also in this matter "prevention is better than cure".

4.4 SURFACE PROPERTIES OF IMPLANT MATERIAL

An evident factor that differentiates a biomaterial from any other material is its ability to be in contact with tissues of the human body without causing unacceptable adverse effects in the body. Within biomaterials science, the term biocompatibility is extensively used, but still it is not fully understood what it actually means and especially unraveling all the mechanisms behind these phenomena. (Williams 2008) The definition of biocompatibility which refers to the ability of a material to perform with an appropriate host response in a specific situation (Williams 1987) is based on the three principles: 1) a material has to perform, not only exist in the tissues, 2) the response which it creates has to be appropriate for the application and 3) the nature of the response to a specific material and its suitability may vary from one situation to another (Williams 1999). These parameters relate to an important feature of novel implant materials: the material should specifically react with the tissues rather than be ignored by them. For bone implants, one of the single most important characteristic is the support of osseointegration. There is a huge number of chemical, biochemical, physiological, physical and other mechanisms which are involved in the contact between biomaterials and the tissues and which affect the biocompatibility (Williams 2008). The development of medical implants is now concerned not only with the bulk characteristics of the material used, but also those of surface. Surface wettability, energy, charge, chemistry and composition are among the characteristics that could influence the host response. In addition, alterations in the surface topography have been used to influence cell, protein and bacteria responses to implants.

4.4.1 Topography

The determination of surface topography can be based on either texture which refers to configurations with defined dimensions or roughness which refers to changes in surface topography with random size and distribution. Surface roughness is

quantified by the vertical deviations of a real surface from its ideal form. There are many different roughness parameters in use, but arithmetic mean deviation of the surface, R_a, is by far the most common:

$$R_a = \frac{1}{lr}\int_0^{lr} |z(x)| dx. \quad (1)$$

Z(x) is the profile from a midline and *lr* is the sampling length over which the surface profile has been measured (Tomlins et al. 2005).

A number of techniques are available for measuring surface roughness. Contact methods involve stretching a measurement needle across the surface. Profilometers are the best known instruments for contact measurements. Non-contact methods include interferometry, atomic force microscopy and scanning tunneling microscopy (Tomlins et al. 2005). *E.g.* the resolution of the 3D AFM images is typically below 0.1 nm in the vertical direction and several nanometers at the horizontal level. This kind of detailed information from the surface topography is particularly relevant for studies into protein adsorption onto substrates and cell-biomaterial interactions (Tomlins et al. 2005). The surface roughness of a sample for studying cell, protein or bacteria interactions has been modified via sandblasting (Lampin et al. 1997, Iwaya et al. 2008, Orsini et al. 2000, Anselme & Bigerelle 2005), plasma spraying (Nebe et al. 2007, Saldańa et al. 2006), mechanical polishing (Ponsonnet et al. 2003, Iwaya et al. 2008, Anselme & Bigerelle 2005, Harris et al. 2007) and acid-etching (Iwaya et al. 2008, Orsini et al. 2000, Anselme & Bigerelle 2005) of the surface. Specifically, surface roughness of materials in the nanometer range plays an important role in the adsorption of osteoblast friendly proteins *e.g.* vitronectin (Vn) and Fn and consequently the adhesion, spreading, and proliferation of osteoblasts (Degasne 1999). *In vitro* studies on osteoblastic cells grown on the surfaces with varying roughnesses have also reported changes in cell morphology (Puckett et al. 2008, Kim et al. 2005), adhesion (Puckett et al.

2008, Pareta et al. 2009, Khang et al. 2008), proliferation (Das et al. 2009, Reising et al. 2008), differentiation (Lincks et al. 1998, Kieswetter et al. 1996), and gene expression (Das et al. 2009, Brett et al. 2004, Harle et al. 2004). A summary of surface topography effects on the cell behaviour is presented in Appendix table. There are many of studies which have shown that implant surfaces of different roughness have marked effects on bone growth, and osseointegration *in vivo* (Abe et al. 2008, Schwartz et al. 2008, Feighan et al. 1995, Jinno et al. 1998, Cochran et al. 1996). However, it has to be noted that a change in the surface roughness is also related to changes in wettability and SFE properties of surface and it may be difficult to conclude which mechanism is modulating cell behaviour (Khang et al. 2008, Das et al. 2009, Ponsonnet et al. 2003). Furthermore, the surface roughness effects depend on the substrate material (Hallab et al. 2001b, Jinno et al. 1998) and cell line. For example, fibroblasts prefer smoother surfaces (Kunzler et al. 2007, Ponsonnet et al. 2003, Wirth et al. 2005), in contrast to osteoblasts which adhered better on rougher surfaces.

Control of the cellular micro- and nanoenvironment is of great importance in the development of novel medical devices such as biosensors, tissue engineering constructs, high throughput drug screening systems and implants. Although material surface properties have been studied intensively, for instance the superordinate principles of cellular responses to surfaces with a defined texture are still poorly understood. This is due to the fact that many variables influence cellular interactions to surface structures and general trends in cell behaviour are difficult to establish because of differences in cell type and line, substrate material, feature aspect-ratio and geometry as well as the parameters being measured (Jäger et al. 2007, Martinez et al. 2009). However, it is generally accepted that the three-dimensional surface topography is one of the most important parameters that influences cellular reactions (Jäger et al. 2007, Martinez et al. 2009, Flemming et al. 1999, Curtis & Wilkinson 1997). Modern implants for bone application have been designed with a smooth surface at the nanometer level

since they are composed of constituent micron grain sizes. (Kaplan et al. 1994) When studying the effects of surface topography on cell behaviour, various etching and laser micromachining techniques (Curtis & Wilkinson 1997, Flemming et al. 1999, Mwenifumbo et al. 2007) are typically used to texture different substrate materials such as Si (den Braber et al. 1996, Ismail et al. 2007, Mwenifumbo et al. 2007). However, the creation of complex three dimensional shapes with traditional Si microfabrication techniques would be extremely difficult. Polymeric substrate materials are more suitable for this purpose and previous studies have focused on certain polymers *i.e.* polystyrene, polymethylmethacrylate, polydimethylsiloxane and polycarbonate (Flemming et al. 1999), mainly textured using electron beam lithography, photolithography (Bentacourt & Brannon-Peppas 2007) and soft lithographic (Xia & Whitesides 1998) techniques. There are a large number of studies which have examined the micro- and nano-sized patterning effects on various properties of *e.g.* osteoblastic cells alignment (Mwenifumbo et al. 2007, Ismail et al. 2007, Lu & Leng 2003, Charest et al. 2004), morphology (Flemming et al. 1999, Puckett et al. 2008), proliferation (Rea et al. 2004, Teixeira et al. 2007) as well as osteoprogenitor cell differentiation towards an osteoblastic phenotype (Dalby et al. 2006, Kantawong et al. 2009). It is well-known that bone cells align along defined substrate morphologies (Charest et al. 2004, Rea et al. 2004, Hamilton et al. 2006). This "contact guidance" was first observed in the early 1900's (Harrison 1912). There are some review articles which have summarized the substrate topographical effects on cell behaviour. These studies have mainly concentrated on the cell alignment through microgrooves, and revealed them to align along the long axis of the grooves, while actin and other cytoskeletal elements organize in an orientation parallel to the grooves. (Curtis & Wilkinson 1997, Flemming et al. 1999, Martinez et al. 2009).

Microscale pillars and wells can influence both osteoblastic cells alignment (Rea et al. 2004, Hamilton et al. 2006) and the cellular microenvironment and thus be of potential importance

in the field of bone regeneration (Hamilton et al. 2006). The comparison of pillar and wells revealed that pillar formations increased cell proliferation and density in comparison to surfaces patterned with wells (Rea et al. 2004, Green et al. 1994). Pillar structures have also been demonstrated to exhibit a greater number of human connective tissue progenitor cells compared to smooth surfaces (Mata et al. 2002) and to influence astroglial cell attachment, growth and morphology (Turner et al. 2000). Previously it was thought that a continuous edge of the surface feature is a prerequisite for guided cell migration, however it is known that microfabricated discontinuous-edge surfaces can also guide cell migration in fibroblasts and epithelial cells (Hamilton et al. 2005) as well as in osteoblastic cells (Hamilton et al. 2006). More results of previous studies are presented in Appendix table.

4.4.2 Wettability and surface energy

The investigation of surface wettability by means of contact angle determination is of special interest in the characterization of the biomaterial surface. Wetting is the ability of a liquid to maintain contact with a solid surface and the degree of wetting (wettability) is defined by a force balance between adhesive and cohesive forces. Adhesive forces between a liquid and solid allow a liquid drop to spread across the surface whereas cohesive forces cause the drop to ball up, avoiding contact between the liquid and surface. Conversely, the disposition of a drop to spread out over a flat, solid surface increases as the contact angle decreases. Therefore, the contact angle may be determined as an inverse measure of wettability. The contact angle may be defined as the angle which forms when a liquid/vapor interface meets the solid surface. The energy of the surface, which is directly related to its wettability properties, is a feasible parameter that has often connected closely with biological interaction. These interfacial energies (solid-vapor interfacial energy $\gamma_{sv,}$ solid-liquid interfacial energy γ_{sl} and the liquid-vapor energy γ_{lv}) are given by Young`s equation (Young 1805), where θ is the equilibrium contact angle:

$$\gamma_{sv} = \gamma_{sl} + \gamma_{lv}\cos\theta. \quad (2)$$

It is notable that at thermodynamic equilibrium, the chemical potential of three phases (the liquid phase of the droplet, the solid phase of the substrate and the vapor phase of the ambient) should be equal and that possible surface roughness or impurities cause a deviation in the equilibrium. A non-wettable surface may be termed as being hydrophobic (Fig. 7a) when water forms droplet on the surface and a wettable surface may be also called hydrophilic (Fig. 7b) when water spreads on the surface. Usually a contact angle less than 90° indicates that the wetting of surface is favourable whereas angles greater than 90° generally proves wetting of the surface being unfavourable. (Hasirci & Hasirci 2005, Ratner et al. 1996, Neumann & Godd 1979, Young 1805) It has also been suggested that water contact angles smaller than 65° are hydrophilic, while those larger than 65° are hydrophobic (Vogler 1998).

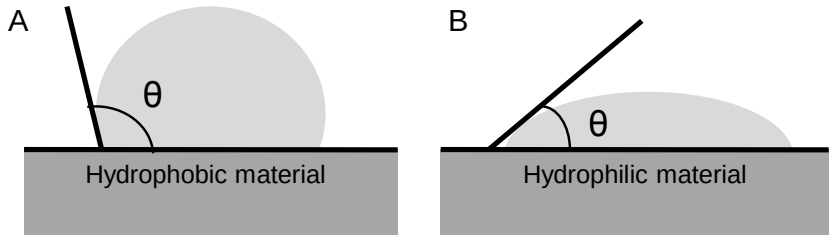

Figure 7: *Presentation of how the droplet behaves on hydrophobic (a) and on hydrophilic (b) surfaces.*

There are many various methods with different sensitivity to measure contact angles. Typically they are conducted with a goniometer using an optical subsystem to capture the profile of a pure liquid on a solid substrate and a syringe with a needle that is used to apply the solvent droplet onto the surface. The static sessile drop method is an optical contact angle method used to estimate wetting properties of a localized region on a solid surface. The static contact angle is formed when all participating phases have reached their natural equilibrium

positions. The dynamic sessile drop method determines the advancing angle (maximum angle) and receding angle (smallest angle) when fluid is added or removed to the drop already on the surface respectively. (Hasirci & Hasirci 2005, Neumann & Godd 1979) The material's SFE and its components may be calculated using different approaches when contact angles are measured using different polar and unpolar liquids whose surface tensions are known. The dispersive component of the material SFE refers to van der Waals and other non-site specific interactions between solid surface and an applied liquid whereas hydrogen bonding, dipole-dipole, dipole-induced dipole and other site-specific interactions are related to the polar component of the material SFE.

When culturing cells on biomaterial surfaces, the contact angle is an important parameter that guides surface property modification attempts. The wettability of a solid surface depends on two factors - the surface structure and the surface chemistry. As discussed before, by modifying surface roughness, it also affects the wettability properties of material. In hydrophobic materials, patterning increases the hydrophobic nature of material as well as in hydrophilic materials, patterning increases the hydrophilicity. The synergistic effect of favourable wettability and topography properties has been observed to promote osteoblast-like cells adhesion (Khang et al. 2008, Feng et al. 2003, Misra et al. 2009) and osteocalcin production (Zhao et al. 2007b) on the Ti surfaces. One of the most widely used techniques to enhance the hydrophilicity of a biomaterial is plasma treatment (Lim et al. 2008, Liao et al. 2003). Laser treatments (Wang et al. 2006, Hao & Lawrence 2007), self-assembled monolayers (Kennedy et al. 2006), and different chemical treatments have also been used to modify the wettability properties. Another approach to modify the contact angle of material is to use different dopants. For example, the wettability properties of carbon films have been modified with Si (Liu et al. 2008, Zhao et al. 2007a, Wan et al. 2006), F (Schulz et al. 2005, Ishihara et al. 2006), iron (Fe) (Chen et al. 2001), Al (Chen et al. 2001), Ag (Choi et al. 2008) and Ni (Chen et al. 2001)

dopants. Increased wettability with higher SFE has been shown to enhance the osteoblastic cells spatial growth and mineralization (Lim et al. 2008), adhesion (Khang et al. 2008, Feng et al. 2003) and differentiation (Lim et al. 2008, Liao et al. 2003, Zhao et al. 2005, Zhao et al. 2007b). An *in vivo* study in which hydrophilic and hydrophobic Ti discs were implanted in rat tibia for three weeks demonstrated that the rate and extent of bone formation was increased around hydrophilic disc, supporting the hypothesis that SFE does promote bone cell maturation and differentiation (Eriksson et al. 2004). However, also intermediate SFE has been shown to be favourable in cell functions (van Wachem et al. 1985, Lee et al. 1998), and Fn-mediated proliferation of osteoblastic cells has been demonstrated to be enhanced on hydrophobic surfaces (Kennedy et al. 2006). If compared polar and dispersive component of SFE, polar component of the surface has been found to have a dominant role in the functions of osteoblastic cells (Feng et al. 2003, Redey et al. 2000).

4.4.3 Surface charge

The electric charge of a biomaterial surface is considered to be one of the main physical factors affecting cell/protein-biomaterial interactions (Khorasani et al. 2006, Cai et al. 2006). When a solid surface is in contact with a liquid, surface charges accumulate and an EL is established. The zeta potential (ζ) is widely used for quantification of the magnitude of the electrical charge at the double layer (Fig. 8). In the vicinity of a solid-liquid interface, the charge carriers are fixed (stationary layer), whereas they are mobile in the liquid phase (mobile layer) at a greater distance. A plane of shear separates these layers from each other and the potential at this interface between the immobile and mobile layers is known as the zeta potential. Thus, the zeta potential is not equal to electric surface potential in the double layer but is often the only available path for characterization of its properties. (Lyklema 1995)

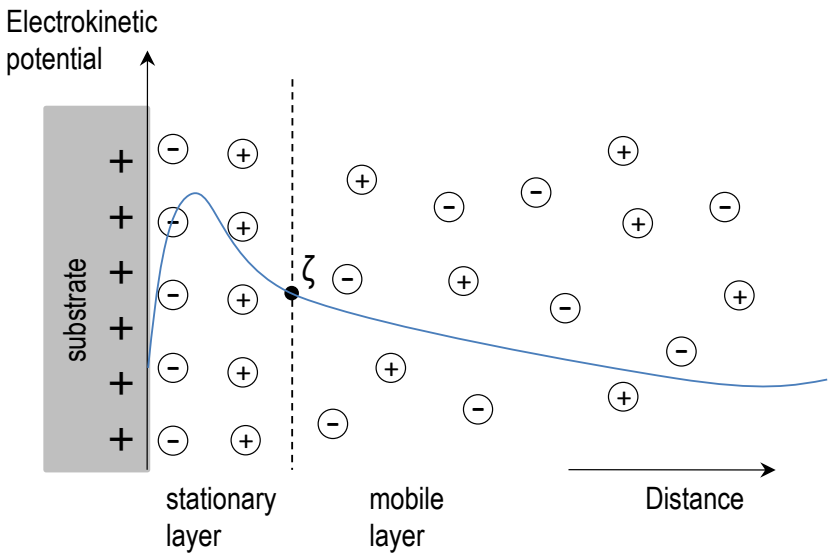

***Figure 8**: Schematic diagram of the electrostatic double layer in zeta potential measurements. The charge distribution is divided into a stationary and a mobile layer which are separated by a plane of shear. The zeta potential (ζ) is assigned to the potential decay at this shear plane.*

The zeta potential is measured by electrophoresis for particles or alternatively by streaming potential/current methods for solid surfaces. From the instrumental viewpoint, electrophoretic light scattering is the mostly used electrophoretic method to determine the velocity of the particles suspended in a liquid medium under an applied electric field. In this technique, the particles are irradiated with a laser light and the scattered light emitted from the particles is detected. The electrophoretic mobility of the particles can be measured from the frequency shift of the scattered light. In the streaming potential/current method, an electrolyte is circulated through the measuring cell and is forced under pressure to flow directly through a small gap formed by two geometrically identical sample surfaces. Streaming current/potential is measured with two electrodes placed at both end of the samples, and the zeta potential can be then determined using mathematical models. When determining the effects of biomaterial surface charge in

implant applications, several factors such as the chemical composition of the material surface in contact with the tissues, the inflammatory situation, the composition of the surrounding body fluid and the environmental pH value need to be taken into account (Krajewski et al. 1998).

Zeta potential is one of the properties which is believed to have profound effects on the biological response of cells to materials and it is stated that the zeta potential might be a critical parameter for cellular interactions (Altankov et al. 2003). However, the effects of magnitude and polarity of surface charge on the behaviour of osteoblastic and other cells are not well understood. There are more published results of zeta potential effects on protein adsorption. It has been demonstrated that the lower the absolute value of zeta potential of the surface, the lower is the adsorption of albumin (Krajewski et al. 1996, 1998), fibrinogen (Cai et al. 2006) and other serum proteins (El-Ghannam et al. 2001). The zeta potential has been shown to correlate with cell biological activation (Veronesi et al. 2002), fibroblast attachment (Khorasani & Mirzadeh 2007, Khorasani et al. 2006, Hamdan et al. 2006) and osteoblast-like cells adhesion (Cheng et al. 2005, Tanimoto et al. 2008, Bodhak et al. 2010, Thian et al. 2010). *In vivo* tests with bone implants have demonstrated the importance of surface charge of implant material *e.g* HA ceramics (Itoh et al. 2006, Nakamura et al. 2009) and biphasic calcium composite (Smeets et al. 2009) on bone formation and osseointegration. However, in attempts to investigate the correlation between zeta potential and protein/cell/bacteria adsorption behaviour on implant materials, it has to been noted that many other factors like functional groups, surface treatments and dopants which have been used to modify the surface charge may have affects the behaviour of cells, proteins and bacteria.

5 Carbon coatings

Carbon is a unique element, which provides the basic framework for all tissues of plants and animals. Carbon is non-metallic and tetravalent where out of six electrons surrounding the C atom nuclei, four are able to create chemical bonds. It is able to form tetrahedral (sp^3), trigonal (sp^2) and linear (sp^1) bond coordinations. There are many allotropes of C of which the graphite, diamond and amorphous carbon forms are best known. In addition, fullerenes, nanotubes and carbines belong to this group. The physical, chemical and biocompatible properties of C vary widely according to the allotropic form but all of the mentioned forms in medical applications are worth being considered. (Narayan 2007, Mitura et al. 2006) Carbon biomaterials have been used for over 30 years. The first of these were low-temperature isotropic pyrolytic C, in which a pyrolytic C-coated aortic valve prosthesis was demonstrated to possess biocompatibility, inertness and immunity to fatigue. Pyrolytic C is still a common valve prosthesis biomaterial but the most widely used C allotrope coating in medical prostheses and surgical instruments is DLC, a metastable form of amorphous C. (Narayan 2007) The properties of the produced C coatings depend on the method of synthesis, parameters of being selected and of course the substrate on which the layer is deposited. The first DLC coatings were deposited using a beam of C ions produced in argon plasma at room temperature substrates at the beginning of the 1970s (Aisenberg & Chabot 1971). Nowadays, DLC films can be produced by a number of techniques such as ion beam deposition, ion plating, radio-frequency plasma enhanced chemical vapour deposition, filtered cathodic vacuum arc process, plasma immersion ion implantation and deposition, ion beam sputtering, magnetron sputtering, mass selected ion beam deposition and pulsed laser deposition (Roy & Lee 2007, Robertson 2002).

5.1 DIAMOND-LIKE CARBON/AMORPHOUS DIAMOND

In DLC film, C exists in an amorphous state that does not possess long-range order and consists of a mixture of sp^2 (graphite-like) and sp^3 (diamond-like) C bonds deposited using high energy carbon species. Diamond-like carbon shares properties of both graphite and diamond. Some extreme properties of diamond like hardness, elastic modulus and chemical inertness can be found in DLC but these are achieved in an isotropic disordered thin film with no grain boundaries. This makes DLC much cheaper to produce when compared to diamond itself. The high fraction of sp^3 bonds of DLC enhances its properties such as mechanical hardness and chemical and electrochemical inertness. (Narayan 2007, Robertson 2002) It is typically stated that DLC contains a significant fraction of sp^3 bonds (Robertson 2002), however the DLC coating is generally used for a large variety of coatings with some diamond-like bonding and it does not guarantee a high fraction of sp^3 bonds.

Different deposition methods have been developed to produce increasing degrees of sp^3 bonding and the term tetrahedral amorphous carbon (ta-C) has been proposed (McKenzie 1996, Narayan 2007) for DLC when the fraction of sp^3 bonding reaches a high degree ($sp^3 > 70\%$) to distinguish it from the sp^2 bonded amorphous carbon. Also the term amorphous diamond (AD) has been used to describe ta-C (Lappalainen et al. 1998, Santavirta et al. 1999). The properties of DLC films depend also on its hydrogen content and thus DLC can also be described with terms such as hydrogenated DLC which contains up to 30 atom.% hydrogen and up to 10 atom.% oxygen within an amorphous carbon matrix. Hydrogenated DLC may also be referred to as hydrogenated amorphous carbon (a-C:H). In the late 1980's, it was noted that hydrogen-free DLC possesses favourable mechanical, optical and tribological properties. Subsequently, both DLC film types have been produced with different deposition methods, but hydrogen-free DLC is considered to be a more appropriate material for medical coatings. (Narayan 2007) In the publications of this thesis both

terms DLC (studies **III** and **IV**) and AD (study **I**) have been used. But even though the deposition methods used to create DLC and AD coatings are different, both of these deposition methods have created diamond coatings with high fraction of sp^3 diamond bondings (80–85%) and containing no hydrogen as well as having similar mechanical properties.

5.1.1 Physical and chemical properties

Typically DLC is defined as a material with high hardness, wear and corrosion resistance, low friction coefficients and chemical inertness (Hauert 2003, Grill 2003). Other beneficial properties of DLC are high electrical resistivity, infrared transparency, high refractive index and excellent smoothness (Roy & Lee 2007). As mentioned before, the properties of DLC depend on its sp^3, sp^2 and hydrogen content. For instance, the elastic modulus, mechanical hardness and density of DLC films correlates with the sp^3/sp^2 ratio and hydrogen content (Table 2). High quality DLC coatings can rival crystalline diamond in terms of mechanical performance - the hardness of crystalline diamond is approximately 100 GPa with the Young's modulus being approximately 1000 GPa (Voevodin & Donley 1996). The excellent mechanical and tribological properties of DLC confirm its feasibility for orthopedic implant applications (Lappalainen et al. 2003, Santavirta et al. 1999, Sheeja et al. 2004, Affatato et al. 2000). However, the evident factor which limits the use of DLC coatings is the lack of adhesion between the substrate and the coating. The poor adhesion poses some demands for substrate material. It has been noticed that the substrate material has to be soft enough (Vickers hardness, $H_v < 3$ GPa) (Anttila et al. 1997), since there is a risk that DLC coating will peel off from a hard substrate material because of the high internal stress. Furthermore, the substrate material needs to be carbide forming material or it is recommended to use carbide forming materials like Ta as a thick intermediate layer (Anttila et al. 1997). Some other ways to relieve this internal stress are to use post deposition thermal annealing (Friedmann et al. 1997), substrate

biasing (Sheeja et al. 2002) or to incorporate certain impurities in the coating during deposition (Tay et al. 2001).

Table 2: *Comparison of major properties of natural diamond compared to tetrahedral amorphous carbon (ta-C), also called diamond-like carbon or amorphous diamond, and hydrogenated amorphous carbon (a-C:H). Modified from Voevodin & Donley (1996) and Robertson (2002).*

Material	Sp^3 (%)	H (at %)	Density (g/cm^3)	Hardness (GPa)	Young's modulus (GPa)
Natural diamond	100	0	3.52	100	1050
ta-C	80-88	< 1	3.1	80	100 - 500
a-C:H	40 - 60	30 - 50	1.2 – 2.2	10 - 20	100 - 200

5.1.2 Biocompatibility

The biocompatible properties of DLC have been the focus of extensive research in recent years due to its potential use in many biomedical applications (Roy & Lee 2007, Hauert 2003, Grill 2003, Dearnaley & Arps 2005). A review article (Roy & Lee 2007) of biomedical applications of DLC coatings indicated that these coatings are rather biocompatible and they do not induce any inflammatory reaction when placed inside animals. DLC coatings may also be used to reduce thrombogenicity by minimizing the platelet adhesion and activation. Due to these properties, DLC coated medical devices are finding use in orthopedic, cardiovascular and dental applications as well as being incorporated into soft contact lenses. (Roy & Lee 2007, Dearnaley & Arps 2005) There are many *in vitro* and *in vivo* studies confirming the biocompatibility of DLC coatings. However, due to different deposition techniques and dopants which affect the surface chemistry, atomic bond structure and hydrogen content of films, all the mechanisms behind the biocompatibility are not fully understood. The cytocompatibility of DLC has been most widely investigated by using a-C:H films in cell experiments. (Roy & Lee 2007) *In vitro* interactions between DLC and osteoblast-like cells (Du et al. 1998, Allen et al.

1994, Chai et al. 2008, Allen et al. 2001, Popov et al. 2007, Yang et al. 2009, Bendavid et al. 2007, Calzado-Martin et al. 2010), red blood cells (Kwok et al. 2004), endothelial cells (Jing et al. 2007, Okpalugo et al. 2006), neuronal cells (Kelly et al. 2008), mouse peritoneal macrophages and fibroblasts (Evans et al. 1991), bone marrow cells (Schroeder et al. 2000) as well as human monocytes and macrophages (Linder et al. 2002), 3T3 fibroblasts and T98-G glial cells (Singh et al. 2003) and human MSCs (Calzado-Martin et al. 2010) have demonstrated promising results in terms of DLC cytocompatibility.

In vivo tests, where a DLC coated implant has been placed inside laboratory animals have also shown good results. The lack of harmful reaction to DLC coated CoCr cylinders, implanted for 90 days in the lateral femoral cortex of sheep demonstrated that the DLC coated surfaces were well tolerated by the body (Allen et al. 2001). Another study confirmed the biocompatibility of DLC coated Ti samples which stayed in the skeletal muscle of rabbits for up to 1 year (Mohanty et al. 2002). Furthermore, *in vivo* tests by implanting DLC-coated orthopedic pins and screws into guinea pig for 52 weeks (Mitura et al. 1994) and implanting DLC coated Zr in the tibiae of Wistar rats for 30 days (Guglielmotti et al. 1999) have demonstrated the potential of DLC coating in implant applications. Consistent results have been reported in studies where DLC coated cylinders were implanted into both muscular tissue and femoral condyles of rats for intervals of 4 and 12 weeks (Uzumaki et al. 2006) and when ta-C coated Si wafers were implanted in subcutaneous tissue of SV129 mice for six months (LaVan et al. 2005). One report where DLC coated steel rods were implanted in a human body for 7 months to fixate a fractured bone demonstrated that these rods do not provoke inflammation and thus enabled the healing of a complicated bone fracture (Zolynski et al. 1996).

DLC coatings have also been tested with *in vitro* bacterial adhesion studies. The results of interactions with *Escherichia coli* (Jones et al. 2006), *Pseudomonas aeruginosa* (Liu et al. 2008) and *S. epidermidis* (Katsigogianni et al. 2006) have been promising. In a comparative study of DLC and SS testing the adhesion of seven

bacterial strains, including six clinical isolates and one American type culture collection (ATCC) strain demonstrated that bacterial adhesion to DLC was similar to the adhesion to commonly used SS (Soininen et al. 2009). Furthermore Smith et al. (2006) evaluated soft tissue reactions and biofilm formation on percutaneous external SS pins coated with DLC and HA. The pins were inserted into the cortex of the right tibia of each 32 skeletally mature Friesland ewes. They demonstrated that DLC coated pins have the potential to prevent biofilm formation and bacterial colonization (Smith et al. 2006). In addition, a total of 26 DLC coated urethral stents were tested *in vivo* with no crystalline biofilm formation being observed (Laube et al. 2007).

5.1.3 Hybrid materials

The properties of DLC can be modified by incorporating other elements into the films to tailor them for specific applications. In the literature, many dopants have been used to maintain or improve cell adhesion or anti-bacterial performance of pure DLC in addition to enhancing its physicochemical properties (Fig. 9). In order to evaluate the influence of Si and F content, short term mouse fibroblasts (cell line 3T3) culture tests have been performed. The morphology of the cells on the surfaces was examined using a scanning electron microscope (SEM) and a good surface biocompatibility was seen by means of morphological behaviour and spreading, but no dependence could be seen on the Si or F content in the a-C:H films (Hauert et al. 1997). Addition of Ti into DLC films enhanced differentiation of osteoblast- and reduced osteoclast-like cell activity (Schroeder et al. 2000, Francz et al. 1999). This was demonstrated with bone marrow cells which were cultured for 14 days. Alkaline phosphatase activity was used as a marker for osteoblast differentiation and tartrate-resistant acid phosphatase activity was used as a marker for osteoclast activity. (Schroeder et al. 2000, Francz et al. 1999) The cytocompatibility of DLC-Si surfaces was evaluated using MG-63 osteoblast-like cell cultures that were left to grow for 3 days and the proliferation was assessed by SEM. The results indicated good cell adhesion and

proliferation for both the DLC and the DLC-Si surfaces. (Bendavid et al. 2007) The addition of V to DLC films reduced lysosomal activity as well as prevented cell attachment, thus being a possible coating for short-term implants where reduced cell attachment is required (Francz et al. 1999). Okpalugo *et al*. (2006) demonstrated that the number of attached endothelial cells was highest on Si-DLC, followed by the N-DLC and undoped DLC. Fluorine corporated DLC films have also been claimed to have enhanced hemocompatibility properties. An *in vitro* whole blood model confirmed the decreased adhesion of platelets to F-DLC coated materials and experiments with the *in vivo* rat implant model studies revealed no excessive local and systemic inflammatory responses in the F-DLC group. (Hasebe et al. 2006) In another study, the hemocompatibility of DLC film was investigated with N doping and the results indicated that the blood compatibility of DLC could be improved by the addition of an appropriate amount of N (Kwok et al. 2004). Also Ag (Kwok et al. 2007, Choi et al. 2008) and Si (Roy et al. 2009) doped DLC films have been demonstrated to have good blood compatibility properties. In an attempt to reduce bacterial adhesion to DLC films various "antibacterial dopants" such as Ag (Katsikogianni et al. 2006, Morrison et al. 2006, Kwok et al. 2007), Pt (Morrison et al. 2006), Si (Shao et al. 2010, Liu et al. 2008, Zhao et al. 2007a, Zhao et al. 2009), F (Ishihara et al. 2006), N (Liu et al. 2008, Zhao et al. 2009) and PTFE (Kinnari et al. 2007) have been tested.

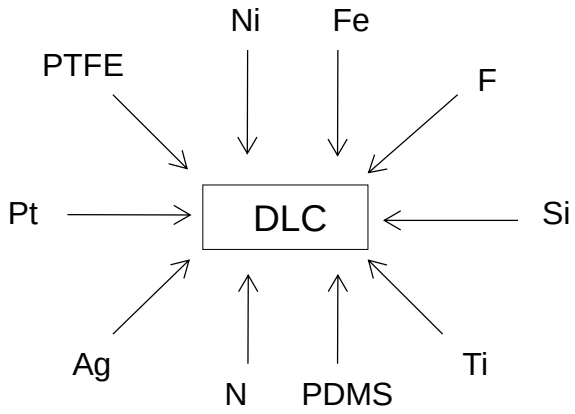

Figure 9: *Typically used doping elements or compounds with DLC.*

5.2 CARBON NITRIDE

Not only DLC, but also carbon nitride (CN) is an excellent candidate as a coating material for biomedical applications. Its superb mechanical and tribological properties, chemical inertness and biocompatibility are similar to DLC, and thus one of the most promising applications of CN coatings is in surface modification of artificial hip joint replacements. (Cui & Li 2000) CN or actually beta carbon nitride (β-C_3N_4) was theoretically predicted by Liu and Cohen in the late 1980's to have a bulk modulus comparable to or even greater than that of diamond (Liu & Cohen 1989). They theorized that C and N atoms could form a particularly short and strong bond in a stable crystal lattice in a ratio of 1:1.3 (Liu & Cohen 1989). Nowadays, it is agreed that CN films consist of amorphous CN matrix embedded with nanocrystalline structures of C_3N_4. Furthermore, the CN matrix can be described as a sp^2-hybridized C network in which N atoms are incorporated either into aromatic rings or connected to these sp^2 microdomains depending on the deposition conditions. (Cui et al. 2005) The abbreviation "CN" is widely used in the literature to describe all carbon nitride coatings with different stoichiometry. The incorporation of N atoms leads to a higher degree of sp^3 bondings and enhances the

hardness as well as making the properties closer to ta-C (Cui et al. 2005). Depending on the deposition process of CN films, also the hydrogen content and not only the N content and sp^3 / sp^2 fraction of C atoms may be varied influencing the biocompatibility and other properties of these films (Cui et al. 2005).

The material has been considered difficult to produce and could not be synthesized for many years. Even today, the fabrication of CN coatings represents a major challenge. CN films have been prepared by ion beam deposition (Boyd et al. 1995), reactive magnetron sputtering (Lopez et al. 1997), dual ion beam sputtering (Baker & Hammer 1997), plasma enhanced chemical vapour deposition (Dawei et al. 1997), ion implantation (Gouzman et al. 1995) and pulsed laser deposition (Franco et al. 2008). Even though there are many more reports of the mechanical and biocompatible properties of DLC there are also some papers which have verified the bio- and hemocompatible nature, (Du et al. 1998, Cui & Li 2000, Cui et al. 2005, Rodil et al. 2003, 2005) or hardness and wear resistance (Quiros et al. 1999, Fujimoto & Ogata 1993) of CN films. Osteoblasts have been demonstrated to attach, spread and proliferate on CN films when this has been investigated by SEM (Du et al. 1998). Complementary cytocompatibility of CN film have been demonstrated with favourable proliferation of osteoblast-like cells (MC3T3-E1) (Tessier et al. 2003) and human alveolar bone derived cells (Olivares et al. 2004) to these films. In addition, the normal attachment and proliferation of endothelial cells (Cui et al. 2005, Li & Niu 2003), fibroblasts (Li et al. 2001, Li & Niu 2003) and macrophages (Li et al. 2001) have been verified and furthermore their hemocompatibility has been confirmed (Cui et al. 2005, Kwok et al. 2004).

6 Aims of the present study

The interface phenomena occurring between human bone tissue and the surface of artificial implant material play an important role in implant survival and tissue response. The surface properties of implant material such as surface chemistry, surface wettability, charge, roughness and texture will all affect the behaviour of the biological response, *i.e.* integration with the bone. However, it is well known that the major problem concerning the lifetime of these implants is their low degree of osseointegration at the implant–tissue interface. The general hypothesis of this thesis was that the novel carbon coating with optimal physicochemical properties would improve osteoblastic cell attachment and spreading as well as inhibiting biofilm formation. The specific aims of this thesis work were:

1. to investigate the effect of surface microtexturing, designed using photolithographic techniques and carbon-based thin films on the contact guidance of osteoblast-like cells and behaviour of bacteria,
2. to study the possibilities to modify the physicochemical properties of polymers and novel ceramics using injection molding and USPLD methods in order to enhance their suitability to implantable biomaterials,
3. to understand the role of the surface free energy components, surface topography and zeta potential to the attachment, adhesion and proliferation of osteoblast-like cells,
4. to examine the effect of surface properties (surface chemistry, surface free energy, zeta potential and topography) of novel carbon-based hybrid materials on the bacterial attachment and biofilm formation in comparison to typically used implant materials, and

5. to provide new knowledge for on-going biomaterial research to help in the development of new generation intelligent orthopedic implants which would be more bioactive than current implant materials.

7 Materials and methods

This thesis consists of four studies, two (**I** and **II**) of which focus on the evaluation of techniques to produce novel implant coatings and to modify the surface properties of these materials in order to study the attachment, adhesion, proliferation and contact guidance of osteoblast-like cells, while two studies (**III** and **IV**) concentrate on the evaluation the bacterial attachment and biofilm formation of novel hybrid materials in comparison to typically used metallic implant materials. This thesis also includes some unpublished data related to surface roughness and zeta potential effects on osteoblast-like cells behaviour. The study design is summarized in Table 3.

7.1 SAMPLE FABRICATION

The tested samples were prepared upon Si wafers using ultraviolet (UV)-lithography (studies **I** and **IV**) and thin films were deposited using USPLD (study **I** and **unpublished data I**) or direct current (DC) sputtering and FPAD methods (studies **III** and **IV**). In study **II,** the polypropylene (PP) samples were fabricated using injection molding and USPLD methods. Matt and rough Si wafers (**unpublished data II)** were roughened with SiC papers and diamond pastes into two different roughness values.

7.1.1 Ultraviolet lithography

The UV-lithography or photolithography is a microfabrication technique widely employed to produce the desired patterns onto a material (Fig. 10).

Table 3: *Summary of Materials and Methods.*

Study	Materials	Sample fabrication	Sample characterization and pretreatments	Cell/bacteria line	Characterization of biological response
I	AD, AD-Ti-h, AD-PDMS-h (textured)	UV-lithography, USPLD	contact angle, SFE and its components, surface roughness	Saos-2	MTT assay, CLSM, SEM
II	PP, PP coated with C_3N_4-Si (textured)	injection molding, USPLD	contact angle, SFE and its components, surface roughness	Saos-2	MTT assay, SEM
III	DLC, DLC-PTFE-h, DLC-PDMS-h, Ti, Ta, Cr	FPAD, DC sputtering	contact angle, SFE and its components, surface roughness, zeta potential, pre-incubation in fetal calf serum [a]	*S. epidermidis* (ATCC 35984)	epifluorescence microscopy, quantification of biofilm formation
IV	DLC, Ta, Ti, Cr (textured)	UV-lithography, FPAD, DC sputtering	pre-incubation in fetal calf serum	*S. aureus* (S-15981)	epifluorescence microscopy, quantification of biofilm formation
Unpub. I	C_3N_4, Al_2O_3, TiO_2	USPLD	zeta potential	Saos-2	MTT assay, SEM
Unpub. II	Smooth, matt and rough Si wafers	roughening with SiC papers and diamond pastes	surface roughness	Saos-2	MTT assay, SEM

AD: amorphous diamond, Ti: titanium, PDMS: polydimethylsiloxane, UV: ultraviolet, USPLD: ultra-short pulsed laser deposition, SFE: surface free energy, CLSM: confocal laser scanning microscopy, SEM: scanning electron microscopy, PP: polypropylene, C_3N_4-Si: silicon-doped carbon nitride, DLC: diamond-like carbon, PTFE: polytetrafluoroethylene, FPAD: filtered pulsed arch discharge, DC: direct current, Ta: tantalum, Cr: chromium, Al_2O_3: alumina, TiO_2: titanium dioxide, SiC: silicon carbide

[a] pre-incubation in fetal calf serum was performed both before bacteria incubation and before contact angle measurements.

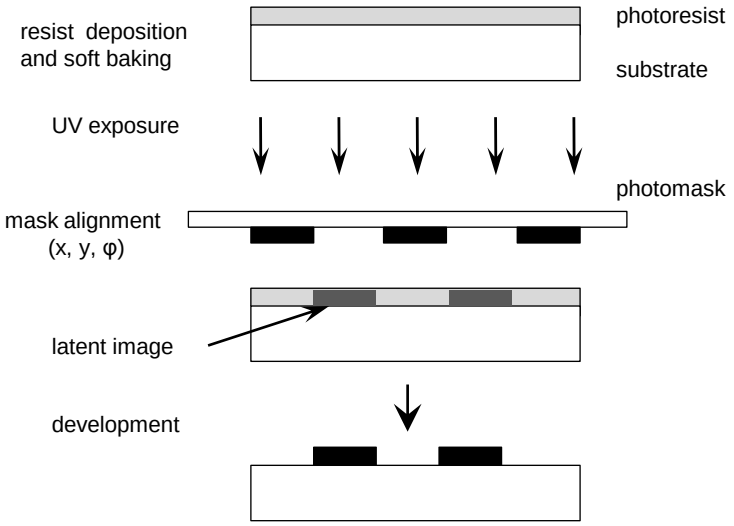

Figure 10: *Photolithographic patterning using negative-tone photoresist. A photomask with opaque regions in the desired pattern is used to expose the photoresist layer. The photoresist will become insoluble after UV light exposure, thus generating the desired pattern after developing in liquid chemicals.*

Firstly, patterns are designed using computer assisted design software and transferred onto a photomask, typically obtained using ion beam or laser machining of Cr layer on glass. After that, a viscous, liquid solution of photosensitive polymer, *i.e.* a photoresist is dispensed onto the substrate material, such as a Si wafer, and the wafer is spun rapidly to produce a uniformly thick layer of photoresist. The spin coating typically runs at 2000 to 5000 rpm for 10 to 60 seconds, and produces a layer between 1 and 2 μm thick. The resulting photoresist thickness, *t*, can also be estimated as a function of spinner rotational speed, solution concentration, and molecular weight (Madou 2002):

$$t = \frac{KC^{\beta}\eta^{\gamma}}{\omega^{\alpha}}. \qquad (3)$$

K is overall calibration constant, *C* is polymer concentration in g/100 ml solution, η is intrinsic viscosity and ω is spinner

rotational speed (rotations per minute, rpm). α, β and γ are exponential factors dependent on process. The photoresist coated wafer is then prebaked to drive off excess solvent, typically at 90 to 100 °C for 30 to 60 seconds on a hotplate. After prebaking, the photomask is placed on top of the photoresist coated wafer and UV light is used to illuminate the photoresist film through the photomask. In the case of a positive photoresist, it becomes soluble in the basic developer when exposed, whereas exposed negative photoresist becomes insoluble in the (organic) developer (Fig. 10). After developing, the resulting photoresist pattern can be used to pattern a metallization layer on the surface of the substrate in the case of thin film deposition, whereas in the etching step, it can be used to prevent the covered substrate from being removed. After the photoresist is no longer needed, it must be removed from the substrate, leaving the pattern design on the substrate. This usually requires sonication in an organic solvent, *e.g.* in acetone or photoresist may be removed by a plasma containing oxygen. The ability to project a clear image of a small feature onto the wafer is limited by the wavelength of the exposure tool that is used and the quality of mask. The shorter the wavelength of light used, the higher resolution, *i.e.* the smaller feature sizes are possible. Deep UV light with wavelengths of 248 and 193 nm allow minimum feature sizes down to 50 nm. (Madou 2002) The resists and parameters used in the studies **I** and **IV** have been summarized in Table 4.

In study **I,** the size of each sample was 10 mm x 10 mm including the features on an 8 mm x 8 mm area. The size of features was 25 μm for square patterns and 175 μm for cruciform patterns (Fig. 13 in Results section) and the distance between features was 50 μm. Thin film coatings; AD, amorphous diamond-polydimethylsiloxane-hybrid (AD-PDMS-h) and amorphous diamond-titanium-hybrid (AD-Ti-h) were in the features, while the background was Si. Samples for AFM, contact angle characterization and MTT (3-[4,5-dimethylthiazol-2-yl]-2,5-diphenyltetrasodium bromide) assay were fabricated

so that one sample included one coating (AD, AD-Ti-h or AD-PDMS-h) in 10 mm x 10 mm areas without any features.

Table 4: *Summary of fabrication steps, used chemicals and parameters of ultraviolet lithography process.*

Study	**I**	**IV**
Mask design	CleWin layout editor, version 4.0.2[a]	CleWin layout editor, version 4.0.2[a]
Mask fabrication	laser scanning technique[b] on 4-inch glass plates with a structured Cr layer	laser scanning technique[b] on 4-inch glass plates with a structured Cr layer
Substrate	Si wafers[c]	Si wafers[d]
Resist	A negative photoresist : ma-N 1420[e]	A negative photoresist: SU-8 2003[f]
Preparation of substrate	Clean Si wafers were baked for 20 min on a hot plate at 200 °C to remove any moisture. To achieve a sufficient adhesion between wafer and the photoresist, 20% hexamethyldisilazane[g] in xylene was spun at 3000 rpm for 30 s upon the dry wafer	Clean Si wafers were baked for 20 min on a hot plate at 200 °C to remove any moisture. To achieve a sufficient adhesion between wafer and the photoresist, 20% hexamethyldisilazane[g] in xylene was spun at 3000 rpm for 30 s upon the dry wafer
Spin coating	5000 rpm for 30 s	500 rpm for 5 s and 3000 rpm for 30 s
Prebaking	2 min on a hot plate at 100 °C	1 min on a hot plate at 65 °C and 2 min on a hot plate at 95 °C
Exposure	365 nm UV light[h] for 35 s	365 nm UV light[h] for 25 s
Postbaking	-	1 min on a hot plate at 65 °C and 2 min on a hot plate at 95 °C
Developing	ma-D 533s[e] for 2 min and rinsed several times with deionized water	propylene glycol methyl ether acetate[i] for 1 min and cleaned in isopropanol and deionized water in an ultrasonic bath
Hardbaking	30 min in oven at 100 °C	20 min in oven at 95 °C
Film thickness	approximately 2 µm	approximately 5 µm

Cr: chromium, Si: silicon, [a] WieWeb software, Hengelo, The Netherlands, [b] Mikcell Oy, Ii, Finland, [c] Okmetic Oyj, Vantaa, Finland, [d] Si-Mat, Landsberg am Lech, Germany, [e] Micro Resist Technology GmbH, Berlin, Germany, [f] MicroChem Corp., Newton, MA, USA, [g] HMDS, Riedel-de-Haen AG, Seelze, Germany, [h]Karl Suss MA45, Suss Microtec Inc., Waterbury Center, VT, USA, [i]PGMEA, Sigma-Aldrich Corp., St. Louis, MO, USA

In study **IV,** the size of each sample was 10 mm x 10 mm, which was divided into four 4 mm x 4 mm areas. One of them was an unpatterned reference and three were patterned with spots of different diameters (5, 25, or 125 µm) (Fig. 14 in Results

section). Regardless of the diameter of the spots, they coated 30.6% of the total sample surface area. Samples were fabricated with thin film (DLC, Ti, Ta and Cr) spots on Si background or Si spots on thin film background.

7.1.2 Injection molding

The creation of complex three dimensional shapes with traditional Si microfabrication techniques is extremely difficult whereas polymeric substrate materials permit the fabrication of these structures. In addition, the low cost and chemical availability of polymers are advantageous. Injection molding is a new method where the structural dimensions at the micro- and nano-scales can be simultaneously adjusted. In this technique, mould inserts with micro-, nano- or micro-nano dual structures are fabricated with the microsized working robot technique and electrochemical treatment of Al. After that, the molds are used to transfer the structures to plastic surfaces by injection molding. In study **II,** electropolished Al foils (0.25 mm thick, Puratronic, 99.997%, Alfa Aesar GmbH, Karlsruhe, Germany) were microstructured with a microsized working robot (RP-1AH) made by Mitsubishi Electric Corp. (Tokyo, Japan), having a feedback unit from Oy Delta Enterprise Ltd. (Espoo, Finland). Tungsten carbide based needles were made by Gritech Oy Ltd. (Joensuu, Finland). Nanopatternings on the Al foils were obtained using an anodization process. The injection molding of polypropylene homopolymer (HD 120MO, Borealis Polymers Oy, Porvoo, Finland) sample disks (diameter 25 mm) was done with a DSM (Geleen, The Netherlands) Midi 2000 extruder-microinjection molding machine. The extruder screw temperature was set at 255°C, the pressure of the injection piston was set at 4.5 bar, and the screw rotation speed was set at 80 rpm. Mold temperature is a major parameter affecting the filling of micro- and nano-features in injection molding. Therefore 50 °C mold temperature for PP injection molding of nanofeatures was selected based on previous studies (Puukilainen et al. 2006, 2007).

In the present samples, the size of the structured area was 10 mm x 10 mm as centered. Microstructured (MST) samples contained 20 μm high micropillars with diameter of 20 μm. The distance between pillars was also 20 μm. Micro- and nano-structured (MNST) samples had the same microstructure as the MST samples but there was also nanostructuring all over the structured area. Structured PP surfaces were characterized with a Hitachi S4800 FE-SEM instrument (Hitachi High-Technologies Europe GmbH, Krefeld, Germany). Figure 15 in Results section shows the SEM images of the structured PP surfaces. A more detailed description of injection molding procedures has been reported elsewhere (Puukilainen et al. 2006, 2007, Koponen et al. 2007, Miikkulainen et al. 2008).

7.1.3 Physical vapour deposition

Physical vapour deposition (PVD) is a general term used to describe any of a variety of methods to deposit thin films onto various surfaces. PVD reactors may use a solid, vapor or liquid raw material in a variety of source configurations. Examples of PVD methods include thermal evaporation, electron beam physical vapour deposition, cathodic arc deposition and sputtering. When one wishes to deposit complex compound materials, molecular beam epitaxy and laser ablation are very useful methods.

In studies **III** and **IV,** the FPAD method was used to deposit DLC, DLC-PTFE-h and diamond-like carbon-polydimethyl-siloxane-hybrid (DLC-PDMS-h) films on the Si wafers. This method utilizes high-energy carbon plasma beams with high deposition rates and the coatings prepared with FPAD are amorphous, ultra thick (up to 200 μm), high-quality (amount of sp^3 diamond bonds > 80%) and well-adherent. When depositing DLC and its hybrid thin films, the plasma pulse was created by igniting a vacuum arc at the cathode where ignition plasma short circuits the cathode and anode leading to a discharge of the main capacitor banks. The system was operated in pulses with a 1-7 Hz repetition frequency. An adhesion layer was produced by high energy plasma accelerated using a 5000-6000

V capacitor (C=16.0 μF) voltage. Plasma was steered towards the sample with a magnetic field generated by the arc discharge current in a 90° curved solenoid. The curved solenoid filters out neutral atoms and graphite particles emitted from the cathode. In order to produce DLC polymer hybrid coatings, a graphite cathode was used together with a PTFE tube (Irpola Oy, Lieto, Finland) or a polydimethylsiloxane (PDMS) tube (Irpola). After deposition of an extremely thin adhesion layer, the main portion of a 200 nm thick film was deposited with a low energy deposition unit run at 500 V average voltage for 15 min. A DC sputtering technique (Stiletto Serie ST20, AJA International Inc., North Scituate, MA, USA) was used to deposit thin films of Ta, Ti and Cr from high purity (99.6 % or better) target materials (Goodfellow Metals Ltd., Huntingdon, UK) onto a surface of Si wafers. Argon gas ions were created in plasma and accelerated onto a target material. A negative target potential up to 400 to 500 V was applied to accelerate the positively charged ions to the target. The impacting ions remove material from the target and sputter deposit it on the substrate in its vicinity. The gas pressure was typically maintained in the range of 3-4 x 10^{-4} mbar providing ignition of the plasma. Deposition of a 200 nm thick layer took about 5 min.

In studies **I** and **II,** the deposition of AD and AD-h coatings on Si wafers and C_3N_4-Si (silicon-doped carbon nitride) coatings on PP disc samples was carried out by using the USPLD technique. This method was also used to deposit ceramic coatings (C_3N_4, Al_2O_3, TiO_2) on Si wafers (**unpublished data I**). Laser ablation deposition utilizes intense laser radiation to erode a target and deposit the eroded material onto a substrate. Ultra-short pulsed laser deposition technique has several advantages for producing thin films, like high adhesion, smooth or nanostructured topography and the possibility to deposit films or particles on heat sensitive substrates like polymers. It is also a good technique for preparing thin films of any desired stoichiometry and producing single material films, composites or homogenous or graded composite films from different kinds of materials (polymers, metals or ceramics). (Myllymaa et al.

2009) The sample surfaces were gently cleaned using argon ion sputtering (SAM-7KV, Minsk, Belarus) just before deposition. For USPLD, a new type of mode-locked fiber laser (Corelase Oy, Tampere, Finland) and Coldab™ deposition technology developed by Picodeon Ltd. Oy (Helsinki, Finland) was used to achieve optimal laser parameters in USPLD (Amberla et al. 2006). The maximum average power was 20 W at 4 MHz which results in a 5 μJ pulse energy and the pulse length was 20 ps. In study **I,** high purity graphite was used as the target for AD deposition and high purity Ti (99.9 %) (Koch-Light Laboratories Ltd, Colnbrook, UK) and commercial grade PDMS (Etra Oy, Helsinki, Finland) were utilized for AD-h coatings. PDMS or Ti content in the AD films was analyzed by energy dispersive X-ray spectrometer (Röntec GmbH, Berlin, Germany) employing at 15 kV. The modified AD coatings contained about 55 at.% PDMS and 0.15 at.% Ti. In study **II,** a high purity sintered target of C_3N_4 and Si (10 wt %) was used for deposition. In every case, the deposition parameters were adjusted to obtain stable plasma in order to deposit about a 200 nm thick layer.

After deposition, in studies **I** and **IV**, the samples were immersed in resist remover, mr-Rem 660, (Micro Resist Technology GmbH, Berlin, Germany) in an ultrasonic bath for a few minutes and the biomaterial coatings deposited on the top of the resist were lifted off with the dissolving resist, and the final microtextures were revealed. In studies **I, III** and **IV** and **unpublished data I** and **II**, Si wafers were cut into individual samples using an apparatus with a diamond knife. After cutting, the samples were sonicated for a few minutes in mr-Rem 660 to remove the resist and Si dust. In study **II**, samples were cut using a custom-made device with parallel SS blades. Then the samples were sonicated in 7× detergent (OneMed Oy, Helsinki, Finland), and rinsed many times in deionized water. Finally, the samples were sonicated for a few minutes in ethanol, and rinsed many times in sterile water before sample characterization or cell seeding. In study **III**, before the bacteria culturing, samples were cleaned in 70 % ethanol for 45 minutes and rinsed with distilled water three times whereas in study **IV**, samples were

sterilized by cleaning with sterile wipes dipped in ethanol and rinsing with 70% ethanol and finally using gamma irradiation of 28 kGy at the VTT Technical Research Centre of Finland.

7.1.4 Roughening of silicon wafers

Roughening with SiC papers and diamond pastes was used to form Si wafer test samples with two different roughness values compared to untreated one (R_a < 10 nm) (**unpublished data II**). Si wafers, p-type, 4", <100> (Si-Mat, Landsberg am Lech, Germany), were roughened with diamond paste with a grade of 3/5 microns and with a grade of 28/40 microns to achieve the samples with R_a ~ 100 nm (matt) and R_a ~ 1000 nm (rough), respectively. Subsequently, the samples were ultrasonically cleaned in acetone, ethanol and deionized water.

7.2 SAMPLE CHARACTERIZATION

Prior biological tests, surfaces of the biomaterial samples produced in this thesis were systematically characterized by optical microscope or SEM, measuring their contact angles (**I-III**), estimating SFEs and their components (studies **I-III**) and determining the values of surface roughness (studies **I-III** and **unpublished data II**) and zeta potential (study **III** and **unpublished data I**).

7.2.1 Microscopy

In study **I**, SEM, JEOL JSM-840 (JEOL Ltd, Tokyo, Japan) with SemAfore 5.0 digitizer (Insinööritoimisto J. Rimppi Oy, Ojakkala, Finland), was utilized for examining the quality of photolithographically patterned AD surfaces. In study **II**, PP samples were studied by Hitachi S4800 FE-SEM, equipped with upper and lower (semi-in-lens) secondary electron detectors. An optical microscope, Zeiss Axioskop 2MAT (Carl Zeiss Inc., Thornwood, NY, USA), was used in this thesis in quality control monitoring and in characterization of produced samples (studies **I, III** and **IV** and **unpublished data I** and **II)**.

7.2.2 Contact angle measurement and surface free energy calculations

Contact angle measurements (studies **I-III**) were performed using the sessile drop (15 µl) method with a custom made apparatus based on an optical microscope SZ-PT (Olympus Corp., Tokyo, Japan) equipped with a digital camera, Olympus Camedia C-3030-ZOOM. Prior measurement, samples were cleaned by ultrasonication in ethanol and deionized water and then dried. To assess the total SFE and its polar/dispersive component, contact angles for two liquids, *i.e.* for water (polar) and diiodomethane (non-polar) (studies **II** and **III**) or even for three liquids (water, diiodomethane, glycerol) (study **I**) were measured within 5 s after placement of the drop at 22 °C and 45% relative humidity on a surface. The spreading pressure was not taken into account. The drop image was stored in a digital camera (Olympus Camedia C-3030-ZOOM), and Gnu Image Manipulation Program (GIMP, www.gimp.org) was used to determine the contact angle from the shape geometry of the drop.

In study **III**, contact angles of samples were also determined after incubating them in fetal calf serum (FCS, Perbio Science N.V., Erembodegem, Belgium) for 15 minutes at +37 °C and washed 3 x 5 minutes in 11 mM phosphate buffered, 140 mM saline (PBS, pH 7.4).

Two theoretical models for SFE calculations were utilized. The Owens-Wendt (OW) approach (Owens & Wendt 1969) was used in the studies **II** and **III,** whereas both OW and van Oss (VO) (van Oss et al. 1988) models were exploited in study **I**. These models are presented in respective studies **I-III**.

7.2.3 Surface roughness determinations

In studies **I-III,** the characterization of atomic level surface topography was performed using a PSIA XE-100 (Park Systems Corp., Suwon, Korea) AFM at ambient temperature and humidity. Aluminium coated Si cantilevers (Acta-10, ST Instruments B.V., LE Groot-Ammers, The Netherlands) were used in a non-contact mode (Fig. 11) to scan the surface across

an area of 2 x 2 μm with a scanning rate of 0.25 Hz. The parameters of R_a (studies **I-III**) and peak-to-valley roughness (R_{pv}) (study **II**) were determined from randomly taken AFM images using the instrument analysis software (XIA). Surface roughness of the roughened test samples (**unpublished data II**), was determined by using a Mitutoyo SJ-301 (Mitutoyo Corp., Kanagawa, Japan) profilometer. Measurement area, measuring speed and stylus tip radius of 0.75 mm x 3 mm, 0.25 mm/s and 2 μm, respectively, were used to determine the R_a values with Mitutoyo instrument.

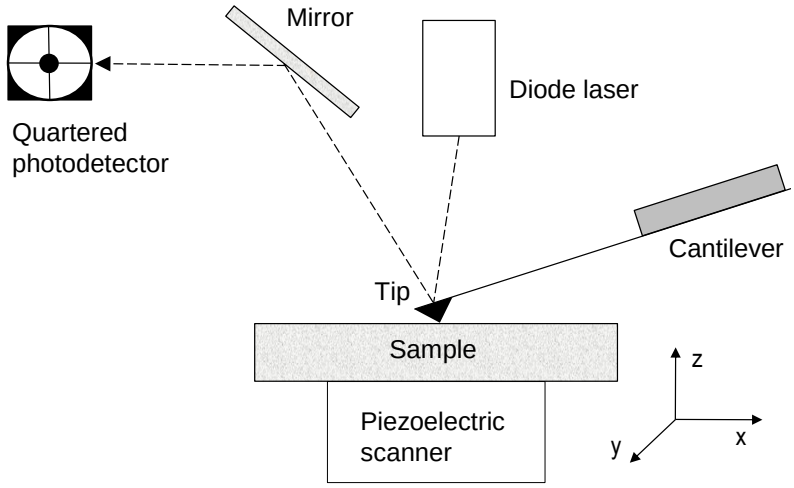

Figure 11: *The schematic drawing of the atomic force microscopic surface roughness determinations. A cantilever with a sharp tip is used to scan the sample surface. In the non-contact mode, the tip is brought into proximity of a sample surface, and forces between the tip and the sample lead to the response oscillation which is measured using a diode laser spot reflected from the top surface of the cantilever into a quartered photodetector.*

7.2.4 Zeta potential measurements

Zeta potential measurements were performed in order to estimate the existing interface charges of biomaterials in a liquid (study **III** and **unpublished data I**). An electrokinetic analyzer (SurPASS, Anton Paar GmbH, Graz, Austria) based on the streaming current measurement principle was used to evaluate

the electrical potential at the shear plane in the electric double layer, *i.e.* zeta-potential. In each measurement using an adjustable gap cell, two identical test samples, *i.e.* pieces of Si wafer coated with biocompatible thin film were fixed on the sample holders with a cross-section of 20 mm x 10 mm using double-sided adhesive tape. A gap of approximately 100 μm was adjusted between the surfaces of the samples during the measurement. An electrolyte was circulated through the adjustable gap cell and forced under pressure to flow through a narrow gap. The pressure difference was continuously increased and the resulting streaming current was measured (Fig. 12). Two Ag-AgCl electrodes placed at both ends of the gap channels were used to record the comparative movement of charges in the electrochemical double layer. The measurements were performed using 0.001 M potassium chloride as an electrolyte solution at a fixed pH of 7.4 ± 0.5.

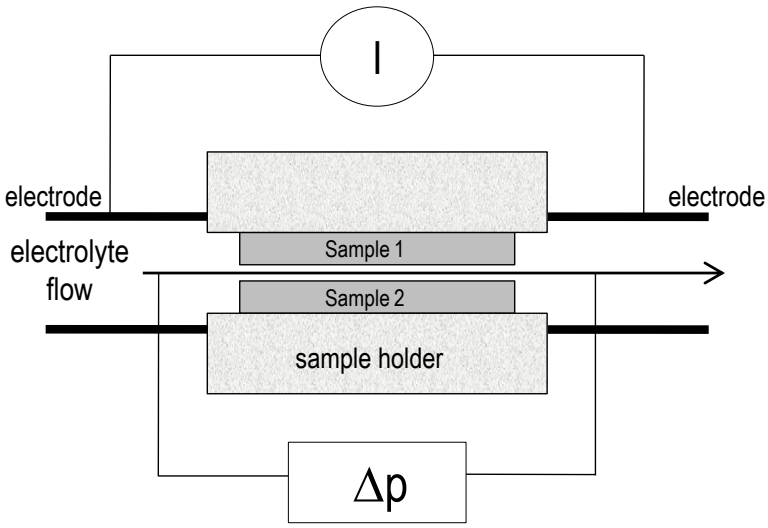

Figure 12: *The principle of streaming current (I) measurement. An electrolyte (1 mM potassium chloride) is forced under constantly changing pressure (Δp) to flow through a narrow gap (ca 100 μm) formed by the surfaces of two identical biomaterial samples. The electrolyte flow causes a comparative movement of charges in the electrochemical double layer which could be detected by two Ag-AgCl electrodes placed at both ends of the streaming channel.*

The zeta potential (ζ) was obtained from streaming current measurements according to the Helmholtz-Smoluchowski equation (Lyklema 1995):

$$\zeta = \frac{dI}{dp} \times \frac{\eta}{\varepsilon \times \varepsilon_0} \times \frac{L}{A}. \quad (4)$$

dI/*dp* is the slope of the streaming current versus pressure, η is the electrolyte viscosity, ε_0 is the vacuum permittivity, ε is the dielectric constant of the electrolyte and *L* and *A* are the length and the cross-section of the streaming channel, respectively.

7.3 SAOS-2 CELLS IN CULTURE

Saos-2 is a non-transformed cell line which possesses several osteoblastic features and thus is useful as a permanent line of human osteoblast-like cells (Rodan et al. 1987). Saos-2 cells were cultured in Dulbecco's Modified Eagle's medium (EuroClone S.p.A., Pero, Italy) containing 10% FCS (PAA Laboratories GmbH, Linz, Austria), 2 mM L-glutamine (Sigma-Aldrich Corp., St. Louis, MO, USA), 200 IU/ml of penicillin (EuroClone), 200 μg/ml of streptomycin (EuroClone), 2.5 μg/ml of fungizone (Sigma-Aldrich) and 50 μg/ml of ascorbic acid (Sigma-Aldrich). The cells were seeded on top of various Si wafer or PP samples by adding a medium which contained 1.0×10^5 cells/ml to each sample cultured in separate cell culture plates (Greiner Bio-One GmbH, Frickenhausen, Germany). The cells were cultured on the samples for 48 hours (study **II** and **unpublished data I** and **II**) and for 24 or 48 hours (study **I**) at 37 °C and in a 5% CO_2 atmosphere. After the incubations, the specimens were collected for further analyses.

7.4 MICROSCOPIC TECHNIQUES FOR CELL STUDIES

In studies **I** and **II**, SEM was used for qualitative analysis of cultured Saos-2 cells. In study **I**, also the confocal laser scanning microscopy (CLSM) was utilized.

7.4.1 Scanning electron microscopy

In study **II**, Saos-2 cells were cultivated for 48 h, and after that, the cells were fixed with 2.5% w/v glutaraldehyde (Sigma-Aldrich) in sodium cacodylate buffer (pH 7.4), and dehydrated in an ethanol gradient and hexamethyldisilazane (Sigma-Aldrich). The specimens were coated with gold by sputtering (Sputter Coater E 5100, Polaron Equipment Ltd., Hertfordshire, UK), and examined with a environmental scanning electron microscope (Philips XL30 ESEM TMP , FEI Company, Eindhofen, The Netherlands) at an accelerating voltage of 15–20 kV. In study **I**, also 24 h cultivation timepoint was used and another SEM, JEOL JSM-840 (Tokyo, Japan) with SemAfore 5.0 digitizer (Insinööritoimisto J. Rimppi) was utilized.

7.4.2 Confocal laser scanning microscopy

After 24 or 48 hour cultivation periods, the specimens were stained with fluorochrome-labeled probes to reveal cytoskeletal (actin) and focal adhesion (vinculin) proteins. Fluorochromes contain fluorophores which are the molecules with fluorescent properties and will absorb energy of a specific wavelength and re-emit energy at a different (but equally specific) wavelength. The use of direct labeling with fluorochromes decreases the number of steps in the staining procedure and generally avoids cross-reactivity and high background problems. After cultivation, the specimens were removed from the multi-well plates, and the cells were washed with phosphate buffered saline (PBS)/Hank's buffered salt solution for 2 min before fixing for 20 min with a 2% w/v paraformaldehyde solution. The cells were permeabilized by exposure to a 0.3% Triton X-100 (Sigma-Aldrich) solution for 30 min in 3% bovine serum albumin. To visualize the actin filaments, the cells were incubated with

Bodiby FL Phalloidin (594 nm, Molecular Probes Inc., Eugene, OR, USA) for 30 min. After washing, the cells were incubated for 2 h at room temperature with primary murine monoclonal antibody against vinculin (1:1000 dilution, Sigma-Aldrich), followed by PBS washings. Finally, the fluorescein labelled secondary anti-mouse antibody was added (1:1000 dilution, Vector Laboratories, Burlingame, CA, USA) for 1 h at room temperature followed by PBS washings. Double-stained cells were viewed in a CLSM system consisting of Nikon Eclipse TE300 (Nikon Corp., Tokyo, Japan) and PerkinElmer UltraVIEW (PerkinElmer, Fremont, CA, USA) with appropriate filter sets.

7.5 CELL PROLIFERATION – MTT ANALYSIS

The MTT (3-[4,5-dimethylthiazol-2-yl]-2,5-diphenyltetrasodium bromide) based cell proliferation assay is used as a colorimetric method to assess the numbers of viable cells. This assay is based on the cellular reduction of the yellow insoluble MTT salt to formazan, a blue precipitate, which happens only in actively functioning mitochondria with the reaction being catalyzed by the dehydrogenase enzymes.

At the end of the culture period, *i.e.* 24 hours (study **I**) or 48 hours (studies **I** and **II** and **unpublished data I** and **II**), the medium was changed to fresh medium, and 0.5 mg/ml of MTT (Sigma-Aldrich) was added. The following incubation lasted 2 h, after which the medium was removed and the wells were washed with PBS. Then, formazan salts were dissolved with with 1000 µl of dimethylsulphoxide/ethanol (1:1), and the absorbances were measured at 595 nm with an ELISA reader (Molecular Devices, Inc., Sunnyvale, CA, USA). The numbers of living cells were determined using a standard curve normalized to the number of osteoblast-like cells. Experiments were performed twice with six sample of each material group.

7.6 STAPHYLOCOCCAL CULTURES

Before bacteria culturing, biomaterial samples were preincubated in FCS (Perbio Science N.V.) for 15 minutes at +37 °C and after that, the materials were washed three times in 11 m*M* phosphate buffered, 140 m*M* saline, pH 7.4 for 5 min. Biomaterials were precoated with serum proteins to produce a biomaterial adhesion environment which resembles the environment in the human body. In study **IV**, the patterned samples of four different biomaterials (DLC, Ti, Ta and Cr) were manually fixed on the array plate with nail varnish.

In study **III**, a biofilm producing coagulase-negative strain, *S. epidermidis* ATCC 35984, was cultured in blood-agar plates. First, twenty CFUs were suspended into 10 ml Tryptic Soy Broth (TSB, Bacto Tryptic Soy Broth, Becton & Dickinson and Company, Sparks, NJ, USA) and cultured for 24 hours at +37°C. Refreshing the bacterial suspension was done by diluting 1 ml of the bacterial suspension with 9 ml of TSB, followed by a culture for 18 hours. McFarland standard (Chapin & Lauerdale 2007) was utilized when bacteria were suspended and diluted into TSB to 5 x 10^8 CFUs per ml and controlled by dilution plating on blood agar (Trypticase soy agar, BBL 211047, and Mueller Hinton agar, BBL 212257, Beckton & Dickincon and Company) supplemented with 5% horse blood. After, the bacterial suspension was pipetted on the biomaterial array plates, the incubation time was selected for 16 hours (at +37°C) based on the previous pilot experiments, to allow biofilm formation, followed by three washes in 0.9% sodium chloride (NaCl). Experiments were repeated three times and all samples were run as duplicates.

In study **IV**, coagulase-positive strain, *S. aureus* S-15981, kindly supplied by Dr. Lasa (Valle et al. 2003) was cultured in blood-agar plates for 24 hours at +37°C. Before culturing, twenty CFUs were suspended into 10 mL TSB (Becton & Dickinson and Company). The bacterial suspension was refreshed for the experiments by diluting 1 mL of the bacterial suspension with 9 mL of TSB and culturing for 18 hours. After that, bacteria were

suspended and diluted into PBS before the concentration was adjusted to 5 × 10^8 CFUs per ml utilizing McFarland standard (Chapin & Lauerdale 2007) and controlled by dilution plating on blood agar (Trypticase soy agar BBL 211047 and Mueller Hinton agar BBL 212257 supplemented with 5% horse blood). After pipetting the bacterial suspension on the biomaterial array plates, incubation was carried out at +37 °C for 90 min to allow adhesion of bacteria, followed by three washes in distilled water. All the samples were run in triplicate.

7.6.1 Acridine Orange staining

Acridine Orange 3R (Chroma-Gesellschaft Schmid GmbH & Co., Münster, Germany) is a nucleic acid selective fluorescent cationic dye, which penetrates the cell or bacterial membrane and binds to deoxyribonucleic acid (DNA) and ribonucleic acid (RNA) electrostatically through intercalating and therefore is useful for cell cycle determination (study **IV**). Patterned sample chips as such or on array plates containing adherent *S. aureus* cells were incubated for 2 min in 1:10,000 (w/v) Acridine Orange 3R stain in 0.2 M acetate buffer, pH 3.8. Acridine Orange staining solution was stored in the dark at room temperature.

7.6.2 Calcofluor White staining

In study **III**, the stain used was Calcofluor White. Calcofluor White is a fluorescent dye that binds to glycans and can be used to detect the component of biofilm, extracellular polysaccharide, in many bacteria. Fluka 18909 Calcofluor White stain (Sigma-Aldrich) was pipetted for two minutes on the sample chips containing biofilms produced by *S. epidermidis.* The biofilms on the surface of the biomaterial samples were washed with 0.9 % NaCl 3 x 5 minutes after Calcofluor White staining.

7.6.3 Epifluorescence microscopy

In study **III**, Calcofluor White stained biofilms were visualized under epifluorescence microscope (Olympus AX70) using Olympus U-MWU2 DAPI-filter (excitation: 330-385 nm; emission: 420 nm; dichroic: 400 nm) and photographed using an

Olympus digital camera coupled to analysis software program (Soft Imaging System GmbH, Münster, Germany). In study **IV**, Acridine Orange 3R stained bacteria were visualized in the same microscope as used in study **III** with Olympus U-MWIB3 FITC filters (excitation: 460-495 nm; emission 510 nm; dichroic: 505 nm) and photographed using PCO Sensicam (PCO AG, Kelheim, Germany) digital camera attached to a computer.

7.6.4 Quantification of bacterial adhesion

In both studies **III** and **IV**, Adobe Photoshop CS2 (Adobe Systems Inc., San Jose, CA, USA) was used for quantification of bacterial adhesion. In study **III**, all 19 images were analyzed with the help of a mask layer that revealed 25 identical rectangular areas of each image. If less than 50 % of the area of interest was covered by biofilm, its value was set to 0, but if more than 50% was covered, it was set to 1. Finally, the sum of these values (mean ± standard deviation of the mean, SD) was calculated as the measure of the biofilm covered area. Also in study **IV**, the mask layer of four circles of approximately 91μm diameter that showed the image below was used. After that, these images were processed so that the background was set as the black point in each image. Finally, individual images were opened in ImageJ 1.37c (National Institute of Health, Bethesda, MD, USA), and the area covered by the bacteria in each image was calculated using the nucleus-counter function of the WCIF plug-in. (Abramoff et al. 2004)

7.7 STATISTICAL ANALYSES

The results of the test quantities are reported as mean and standard deviation or standard error of the mean. Results from tests (surface roughness, contact angle, SFE, MTT assay and biofilm quantification) were considered to be independent and thus, one-way ANOVA (SPSS software, versions 14.0 and 16.0, SPSS Inc., Chicago, IL., USA) variance analysis followed by Tukey Post-Hoc Tests were applied to determine the statistical

significance of the differences observed between groups. A *p*-value less than 0.05 was considered as statistically significant.

8 Results

The main results of this thesis are summarized in Table 5 and presented in more detail in the following chapters.

Table 5: *Summary of the main results of the studies of this thesis.*

Study	**Conclusions**
I: Interactions between Saos-2 cells and microtextured AD or AD hybrid coated surfaces with different wettability properties	AD and its Ti and PDMS hybrids are noteworthy coating material candidates with respect to their interactions with osteoblast-like cells. The Lewis acid-base (γ_S^{AB}) polar component calculated by the van Oss method correlates best with Saos-2 cells adhesion Microtexturing together with osteocompatible surface coating is effective method to enhance contact guidance of Saos-2 cells
II: Improved adherence and spreading of Saos-2 cells on PP surfaces achieved by surface texturing and C_3N_4-Si coating	Combining surface micro- and nanotexturing and deposition of C_3N_4-Si coating upon PP surfaces remarkably improves adhesion, spreading and contact guidance of Saos-2 cells
III: Resistance of DLC and its hydrids to *S. epidermidis* biofilm formation compared to metals used in biomaterials	DLC-PTFE-h and DLC are superior in their ability to resist adhesion and colonization by *S. epidermidis* compared to DLC-PDMS-h, Ti, Ta and Cr
IV: Patterned macroarray plates in comparison of bacterial adhesion inhibition of Ta, Ti and Cr compared with DLC	Micropatterned surfaces are useful for quantitative comparison of bacterial adherence on different biomaterials and textures DLC is superior in its ability to resist adhesion and colonization by *S. aureus* compared to Ti, Ta and Cr
Unpublished data I: The effect of zeta potential of ceramic materials on Saos-2 cells adhesion	Ceramics (TiO_2, C_3N_4, Al_2O_3) with the negative zeta potential values in a same range evokes the same proliferation rates of osteoblast-like cells
Unpublished data II: The effect of surface roughness of silicon samples on Saos-2 cells adhesion	Silicon samples with greater surface roughness evokes the higher Saos-2 adhesion

AD: amorphous diamond, Ti: titanium, PDMS: polydimethylsiloxane,
PP: polypropylene, C_3N_4-Si: silicon-doped carbon nitride, DLC: diamond-like carbon,
PTFE: polytetrafluoroethylene, Ta: tantalum, Cr: chromium, Al_2O_3: alumina,
TiO_2: titanium dioxide

8.1 TEXTURES AND COATINGS

Textures for samples used in studies **I** (Fig. 13) and **IV** (Fig. 14) were fabricated using UV-lithography. The textures were definite and the sizes of the patterns were similar to the mask counterparts. Figure 15 represents the PP samples used in study **II**, textured using injection molding. The adhesion of coatings deposited upon the all tested samples was good without any signs of delamination. The quality of samples before and after all characterizations was made with SEM (studies **I** and **II**), AFM (studies **I-III**) and optical microscope (studies **I, III** and **IV** and **unpublished data I** and **II**). Samples demonstrated to be homogenous and remained the same after all treatments and tests. The only exception was the nano-scale structuring (Fig. 15b), which was partly destroyed in some samples because of ion beam cleaning before deposition of C_3N_4-Si coating (see study **II**, Fig. 2).

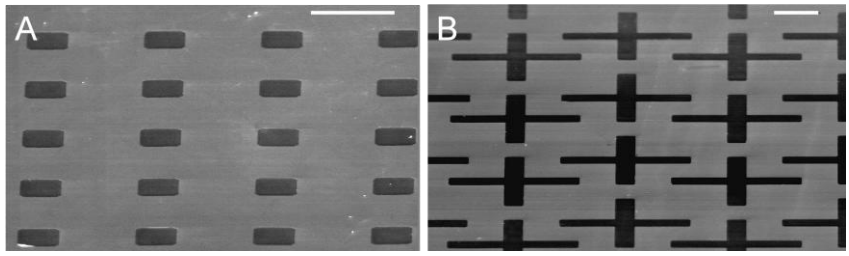

Figure 13: *A tilted SEM image of ultraviolet-lithographically patterned test samples of study **I**. The background is silicon and the features are amorphous diamond, coated using ultra-short pulsed laser deposition method. Osteoblast-like cells were cultured upon these samples for 24 or 48 hours. Scalebar is 50 μm.*

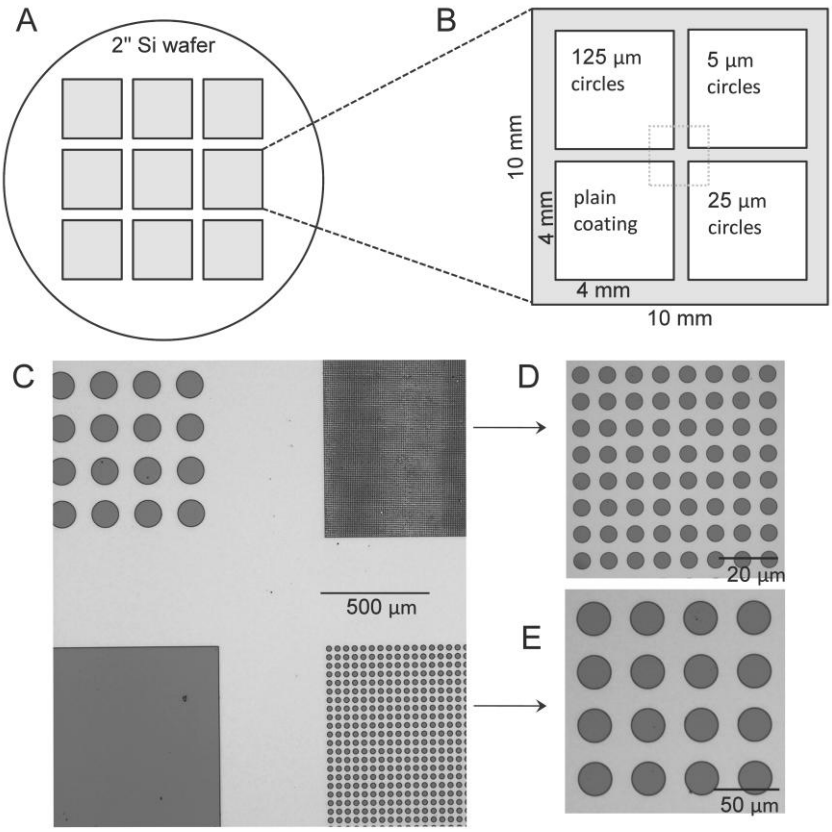

Figure 14: *The schematic representation of ultraviolet-lithographically patterned test samples of study* ***IV****. The samples were fabricated on 2 inches silicon wafers (a), facilitating the creation of nine 10 mm x 10 mm sample pieces. Each sample consists of four 4 mm x 4 mm areas (b,c), in which one contains spots of diameter of 5 µm (d), another contains spots of diameter of 25 µm (e) and third contains spots of diameter of 125 µm. One area was plain surface. In half of the samples, silicon was background and the features were coated with Ti, Ta, Cr or DLC and on another half of the samples silicon was used to create the features and the coating was the background. In every case, spots accounted for 30.6% and background for 69.4% of the total sample area. S. aureus incubation was done with these samples for 90 min to test adhesion of bacteria.*

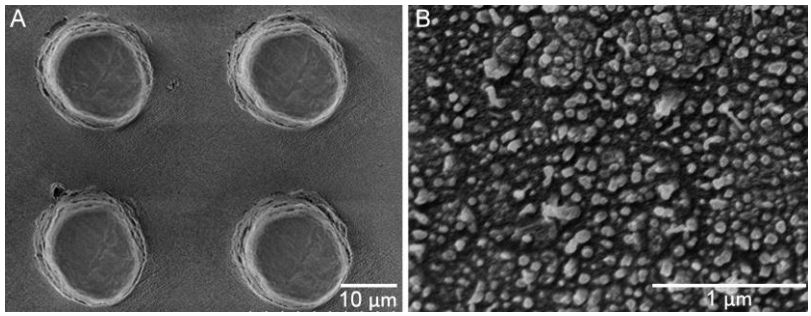

Figure 15: *SEM images of injection molded polypropylene samples used in study* ***II*** *with micropillars with diameter, spacing and height of 20 µm (a). Micro- and nano-structured samples contain a nanostructure on top of the micropillar, the sides of the pillars as well as the plateau between the pillars (b). Osteoblast-like cells were cultured upon these samples for 48 hours.*

8.2 SURFACE ROUGHNESS OF TESTED SAMPLES

Table 6 shows R_a values of tested samples (studies **I-III** and **unpublished data II)**. In study **II**, only smooth and MNST samples before and after deposition were characterized for R_a values. The values obtained for smooth surfaces demonstrated that the C_3N_4-Si coating does not change the roughness properties of PP samples. R_a values for MNST surfaces were significantly higher than for smooth surfaces demonstrating the existence of nanostructure. However, the R_a values of coated and uncoated MNST surfaces differed from each other ($p < 0.01$) probably due to the partly destroyed nanostructure during cleaning process. Surface roughness values of the samples used in study **IV** are not presented in the Table 6, because measurements were conducted randomly in only a few samples. However, also these measurements demonstrated that surfaces were quite smooth, R_a below 10 nm. The roughening of factory-polished Si wafers (Fig. 16a) into the matt (Fig. 16b) and rough (Fig. 16c) surfaces was successfully performed (**unpublished data II**). The surface roughness correlated with Saos-2 adhesion as will be described in Chapter 8.5.

Table 6: *Averaged surface roughness values (R_a) of tested materials determined using profilometer or atomic force microscope.*

Study	Material	R_a (nm)
I	AD	0.2±0.1
I	AD-Ti-h	0.2±0.1
I	AD-PDMS-h	0.2±0.1
I	Si	0.2±0.1
II	PP (smooth)	4.0±1.4*
II	C_3N_4-Si coated PP (smooth)	4.0±1.2*
II	PP (MNST)	16.0±7.7**
II	C_3N_4-Si coated PP (MNST)	7.1±5.1*
III	DLC	0.6±0.1§
III	DLC-PTFE-h	2.0±0.1#
III	DLC-PDMS-h	1.2±0.1§,#
III	Ti	1.8±0.2§,#
III	Ta	1.5±0.3§,#
III	Cr	0.8±0.1§
Unpubl. II	Si smooth	< 10
Unpubl. II	Si matt	100±10.0
Unpubl. II	Si rough	1000±100.0

AD: amorphous diamond, Ti: titanium, PDMS: polydimethylsiloxane, Si: silicon, PP: polypropylene, C_3N_4-Si: silicon-doped carbon nitride, MNST: micro-and nano-structured, DLC: diamond-like carbon, PTFE: polytetrafluoroethylene, Ta: tantalum, Cr: chromium

* $p < 0.01$, as compared to MNST uncoated sample group
** $p < 0.01$, as compared to all sample group
§ $p < 0.05$, as compared to DLC-PTFE
\# $p < 0.05$, as compared to DLC

The values are mean ± SD. Statistical analysis performed with one-way ANOVA was carried out between the materials tested in separate studies.

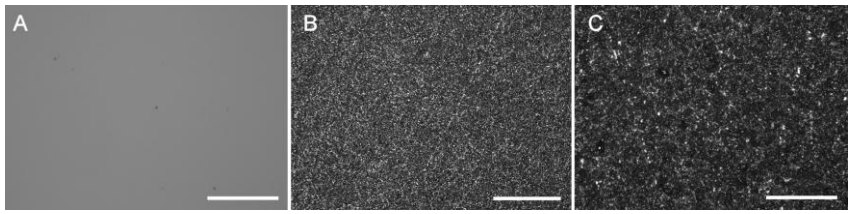

Figure 16: *Optical microscope images of smooth (a), matt (b) and rough (c) silicon surfaces used to investigate the effect of surface roughness on attachment of Saos-2 cells. Scalebar is 500 μm.*

8.3 WETTABILITY PROPERTIES

Contact angles of tested materials used in studies **I-III** are presented in Table 7. SFE components calculated with two theoretical models; van Oss (van Oss et al. 1988) and Owens-Wendt (Owens & Wendt 1969) are for one showed in Tables 8 and 9. The OW calculations were utilized to obtain the dispersive γ_S^D and polar γ_S^P component of SFE, and the VO approach defined the Lifshitz–van der Waals (apolar) γ_S^{LW} and the Lewis acid-base (polar) γ_S^{AB} components, the latter being divided into two parts, electron-acceptor (γ_S^+) and electron-donor (γ_S^-) components.

In study **I**, AD coatings were modified by PDMS and Ti dopants to modify the wettability properties. It was hypothesized that the smaller the contact angle and higher the SFE of the coating, the better would be the attachment and proliferation of Saos-2 cells. As will be described in Chapter 8.5, it is these properties that affect the cell behaviour and it was found that the Lewis acid-base polar component (γ_S^{AB}) calculated by the VO method correlated best with Saos-2 adhesion. In study **II**, highly hydrophobic PP surfaces were coated with C_3N_4-Si films to make the surface more hydrophilic. It was possible to reduce the contact angles of PP surfaces drastically and also in this study it was seen the clear correlation between the adhesion and spreading of osteoblast-like cells and

the wettability properties of the surface. In study **III**, the biofilm resistance could not be explained by the wettability properties of surface but it was noted that serum protein pre-treatment caused a significant ($p < 0.001$) drop in water contact angles of all studied materials, being greatest (38%) for DLC-PTFE-h.

Table 7: *Contact angles, θ (°) for the surfaces of different test materials.*

Study	Materials	θ^{water}	$\theta^{diiodomethe}$	$\theta^{glycerol}$
I	AD	$72.4\pm2.4^{*}$	$40.6\pm2.1^{*}$	$66.5\pm2.5^{*}$
I	AD-Ti-h	$81.9\pm2.4^{*}$	$44.7\pm2.5^{*}$	$71.7\pm3.4^{*}$
I	AD-PDMS-h	$100.0\pm4.1^{*}$	$64.1\pm3.2^{*}$	$94.0\pm1.7^{*}$
I	Si	$32.0\pm1.2^{*}$	$35.9\pm1.1^{*}$	$28.7\pm1.9^{*}$
II	Smooth PP	$97.1\pm1.7^{*}$	$54.7\pm1.1^{*}$	-
II	Smooth PP, coated	$63.0\pm1.5^{*}$	$39.6\pm2.4^{*}$	-
II	MST PP	$136.1\pm1.9^{*}$	$64.3\pm1.3^{*}$	-
II	MST PP, coated	$69.1\pm0.9^{*}$	$44.3\pm1.5^{*}$	-
II	MNST PP	$146.2\pm1.6^{*}$	$72.5\pm1.6^{*}$	-
II	MNST PP, coated	$53.5\pm1.4^{*}$	$30.6\pm1.4^{*}$	-
III	DLC	$67.4\pm2.0^{**}$ $(55.7\pm3.2)^{a,**}$	$36.1\pm1.0^{**}$	-
III	DLC-PTFE-h	$106.0\pm1.1^{\#}$ $(65.9\pm5.1)^{a,\#}$	$71.4\pm1.1^{\#}$	-
III	DLC-PDMS-h	$101.7\pm1.2^{**,\#}$ $(81.1\pm2.1)^{a,**,\#}$	$68.5\pm1.1^{**,\#}$	-
III	Ti	$67.6\pm2.0^{**}$ $(48.6\pm3.0)^{a,**,\#}$	$35.4\pm1.2^{**}$	-
III	Ta	$64.1\pm1.6^{**,\#}$ $(53.9\pm3.8)^{a,**}$	$33.4\pm1.4^{**,\#}$	-
III	Cr	$71.2\pm1.1^{**,\#}$ $(48.0\pm4.0)^{a,**,\#}$	$37.7\pm1.5^{**}$	-

AD: amorphous diamond, Ti: titanium, PDMS: polydimethylsiloxane, Si: silicon, PP: polypropylene, MST: microstructured, MNST: micro- and nano-structured, DLC: diamond-like carbon, PTFE: polytetrafluoroethylene, Ta: tantalum, Cr: chromium.
[a] after serum incubation

*p< 0.05, as compared to all other
**p < 0.05, as compared to DLC-PTFE-h
# p < 0.05, as compared to DLC

The values are mean ± SD. Statistical analysis performed with one-way ANOVA was carried out between the materials tested in separate studies.

Table 8: *Total surface free energy (γ_S) and its dispersive (γ_S^D) and polar (γ_S^P) or Lifshitz-van der Waals (γ_S^{LW}) and Lewis acid-base (γ_S^{AB}) components of tested samples expressed by mJ/m² (study **I**). Electron-acceptor (γ_S^+) and electron-donor (γ_S^-) components are calculated by dividing γ_S^{AB} into two parts.*

	OW model			**VO model**				
Material	γ_S	γ_S^D	γ_S^P	γ_S	γ_S^{LW}	γ_S^{AB}	γ_S^+	γ_S^-
AD	45.8 ±1.6*	39.3 ±1.0*	6.5 ±0.9*	40.8 ±1.2*	39.3 ±1.0*	1.5 ±1.3	0.1 ±0.1	11.8 ±3.5
AD-Ti-h	40.5 ±1.6*	37.1 ±1.3*	3.4 ±0.6*	38.2 ±1.5*	37.1 ±1.3*	1.1 ±1.1	0.2 ±0.2	5.7 ±2.2#
AD-PDMS-h	27.1 ±1.7*	26.2 ±1.9*	0.9 ±0.7*	26.2 ±1.9*	26.2 ±1.9*	0.0 ±0.0#	0.0 ±0.0	3.2 ±2.5#
Si	68.7 ±0.6*	41.6 ±0.5*	27.1 ±0.8*	58.4 ±0.9*	41.6 ±0.5*	16.8 ±0.7*	2.0 ±0.2*	35.4 ±1.7*

OW: Owens-Wedth, VO: van Oss, AD: amorphous diamond, Ti: titanium, PDMS: polydimethylsiloxane, Si: silicon

*$p < 0.01$, as compared to all other
# $p < 0.01$, as compared to AD

Values are mean ± SD. One-way ANOVA was used to determine the statistical differences.

Table 9: *Total surface free energy (γ_S) and its dispersive (γ_S^D) and polar (γ_S^P) components of tested samples expressed by mJ/m².*

OW model				
Study	Material	γ_S	γ_S^D	γ_S^P
II	Smooth PP	32.3 ±0.7*	31.6 ±0.6*	0.6 ±0.2$^{\#}$
II	Smooth PP, coated	50.6 ±1.2*	39.8 ±1.2*	10.8 ±0.8*
II	MST PP	26.1 ±0.8*	26.1 ±0.8*	0.0 ±0.0$^{\#}$
II	MST PP, coated	45.9 ±0.9*	37.4 ±0.8*	8.5 ±0.3*
II	MNST PP	21.5 ±0.9*	21.5 ±0.9*	0.0 ±0.0$^{\#}$
II	MNST PP, coated	58.3 ±0.8*	44.0 ±0.6*	14.3 ±0.8*
III	DLC	49.6 ±1.2§	41.5 ±0.5§	8.1 ±0.8§
III	DLC-PTFE-h	24.5 ±0.5**	23.7 ±0.6**	0.8 ±0.2**
III	DLC-PDMS-h	22.5 ±0.6§,**	22.1 ±0.6§,**	0.4 ±0.1**
III	Ti	49.7 ±1.1§	41.8 ±0.5§	7.9 ±0.9§
III	Ta	52.1 ±1.1§,**	42.8 ±0.6§,**	9.3 ±0.6§
III	Cr	47.3 ±0.7§,**	40.8 ±0.7§	6.6 ±0.5§,**

OW: Owens-Wendt, PP: polypropylene, MST: microstructured, MNST: micro- and nano-structured, DLC: diamond-like carbon, PTFE: polytetrafluoroethylene, PDMS: polydimethylsiloxane Ti: titanium, Ta: tantalum, Cr: chromium

*p < 0.01, as compared to all other
# p < 0.01, as compared to coated surfaces
§ p < 0.05, as compared to DLC-PTFE
** p < 0.05, as compared to DLC

Values are given as mean ± SD. Statistical analysis performed with one-way ANOVA was carried out between the materials tested in separate studies.

8.4 ZETA POTENTIAL VALUES

In study **III**, sample surfaces were also characterized for surface zeta potential to determine whether it has any effects on biofilm formation. Zeta potentials at pH 7.4 for all biomaterials were negative as seen in Fig. 17. Figure 17 also represents **unpublished results I** of the zeta potentials of three ceramic materials; Al_2O_3, titanium dioxide (TiO_2) and C_3N_4. It can be seen that the zeta potential values of these materials were all negative

and in the same range as the adhesion of osteoblast-like cells upon these ceramics (Chapter 8.5).

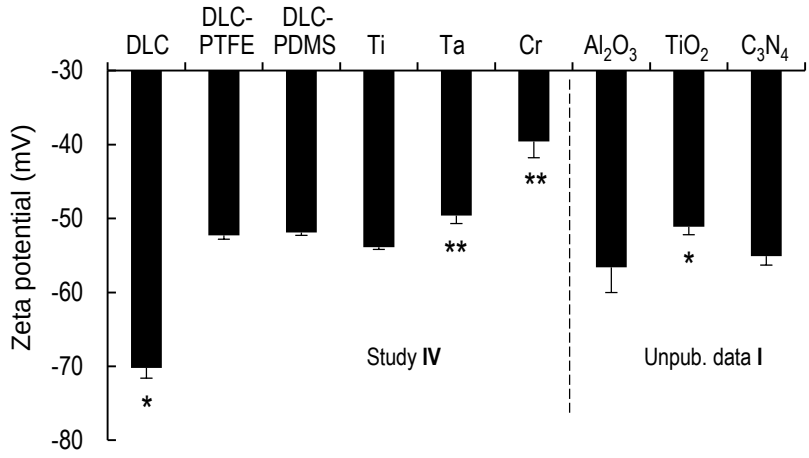

Figure 17: *Zeta potentials of DLC, DLC-PTFE-h, DLC-PDMS-h, Ti, Ta and Cr measured at pH 7.4. Highly negative zeta potential of DLC might explain its good biofilm formation resistance (Study* ***III****). This figure also shows the zeta potentials of three ceramic material:* Al_2O_3, TiO_2 *and* C_3N_4. *It can be seen that the zeta potential values of these materials were all negative and in the same range as was the adhesion of osteoblast-like cells upon these ceramics (****unpublished data I).*** *Error bars indicate the standard deviations. *p < 0.01, as compared to other materials, **p < 0.01, as compared to DLC-PTFE. Statistical analysis performed with one-way ANOVA was carried out between the materials tested in separate studies.*

8.5 SAOS-2 CELL ATTACHMENT AND SPREADING ON TEST MATERIALS

In study **I**, adhesion of Saos-2 cells was not statistically different between AD and its hybrid coatings after 24 h of cultivation (Fig. 18). Nevertheless, after 48 h, the number of attached cells on AD and AD-Ti-h coating was significantly greater (**$p < 0.01$ and *$p < 0.05$, respectively) than on Si and on AD-PDMS-h coating (Fig. 18). Pure AD had a slight but not significantly higher adhesion rate of cells than AD-Ti-h coating. It was also noted that the

number of cells did not increase at the time point 48 h on Si as was found with AD and its hybrid coatings (Fig. 18).

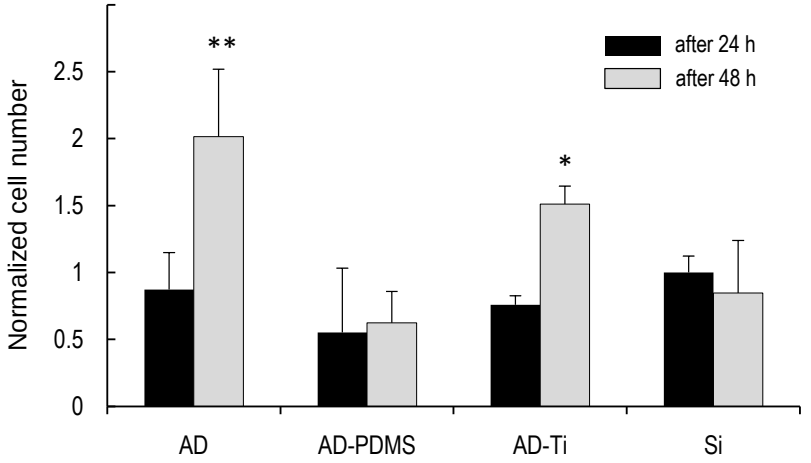

Figure 18: *The number of attached cells on AD and AD-Ti-h coating was significantly greater (**p < 0.01 and *p < 0.05, respectively) than on Si and on AD-PDMS-h coating after 48 h. The number of cells did not increase at the time point 48 h on Si as was found with AD and its hybrid coatings (Study* ***I****). The number of viable cells was determined using the MTT assay and a standard curve normalized to the number of cells. Results are normalized so that Si at the timepoint 24-hours was designated the value of one. Error bars indicate the standard deviations. One-way ANOVA was used to determine the statistical differences between materials.*

As seen in Fig. 19, SEM analysis of cultured cells after 24 h cultivation indicated that Saos-2 cells could be guided to grow inside the square (a) or cruciform (b) features of AD coating. The morphology of cells had switched to being flattened and spread out to the size of AD squares and the focal adhesions had been mainly formed on the AD structures (Fig. 19c). The adoption of cells to the square or cruciform shape demonstrated that the guiding effect of the cells could be also mediated by a physical shape of the pattern in addition to the chemical composition of the feature. Size and spreading of Saos-2 cells appeared to be similar on all AD coatings. After 48 h, cells formed a well flattened confluent layer that covered the entire surface and

individual cells could no longer be easily distinguished (Fig. 19d).

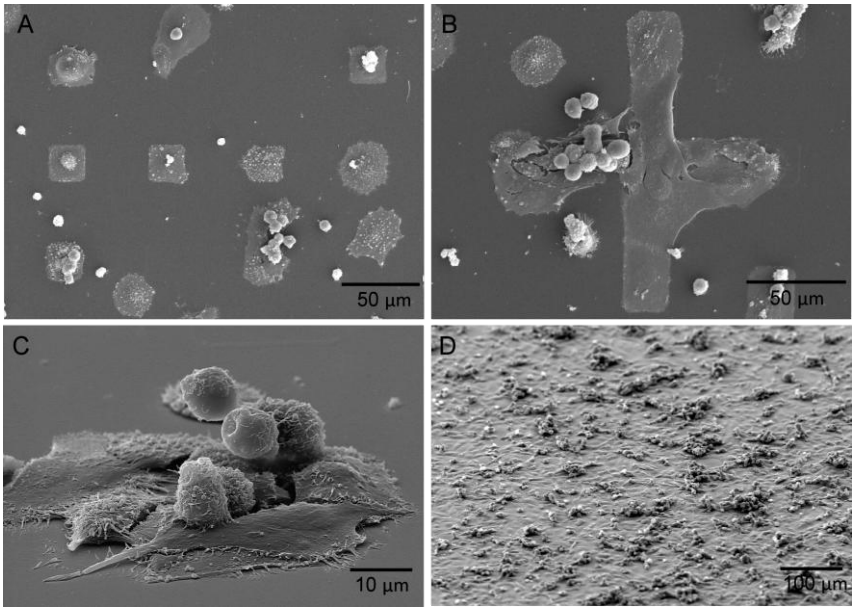

Figure 19: *Guided growth of Saos-2 cells according to the edges of the AD coated square (a) and cruciform (b) features after 24-hour cultivation. The tilted SEM image (c) shows the flattened morphology of cells with numerous focal adhesions upon the AD feature. After 48-hours in culture, the cells had formed a confluent monolayer upon the surface (d). (Study* ***I****)*

In study **II**, after 48 h cultivation, the number of attached cells on the C_3N_4-Si coated MNST samples was slightly but not significantly greater than on the C_3N_4-Si coated MST samples (Fig. 20). However, both these groups significantly differed ($p < 0.01$) from C_3N_4-Si coated smooth samples as well as from their uncoated counterparts. SEM pictures (Fig. 21) indicated that on the smooth uncoated PP surface (a), the cell growth was inhibited and thus cells assumed a round shape with diffuse or limited establishment of focal adhesions. In coated smooth PP samples, the cells were seen to adhere to each other with cellular microextensions and were connected to the substrate as well as to the neighbouring cells (Fig. 21b). The uncoated MNST surface

differed from the uncoated smooth surface so that on the former surface, Saos-2 cells tended to grow in cell clusters with an apparent three-dimensional structure (Fig. 21c). On the C_3N_4-Si coated MST surface, the cells used the plateau between the micropillars for attachment (Fig. 21d). This was the major difference from the situation with the C_3N_4-Si coated MNST surface where the cells were attached on top of the pillars and formed cellular extensions to the edges of the neighbouring nanostructured pillars (Fig. 21e,f). Therefore, C_3N_4-Si coated MNST appeared to be a very ideal surface for Saos-2 cells attachment.

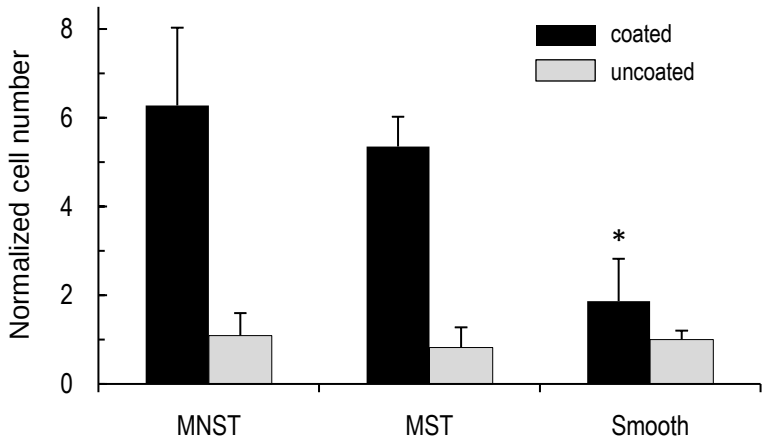

Figure 20: *Quantity of Saos-2 cells on C_3N_4-Si coated and uncoated micro- and nano-structured (MNST), microstructured (MST) and smooth polypropylene surfaces. The number of attached cells on the C_3N_4-Si coated MNST samples was slightly but not significantly greater than on the C_3N_4-Si coated MST samples. Both these groups significantly differed (*$p < 0.01$) from C_3N_4-Si coated smooth sample as well as from their uncoated counterparts (Study **II**). Results are normalized so that uncoated smooth sample was designated the value of one. Error bars indicate the standard deviations. One-way ANOVA was used to determine the statistical differences between materials.*

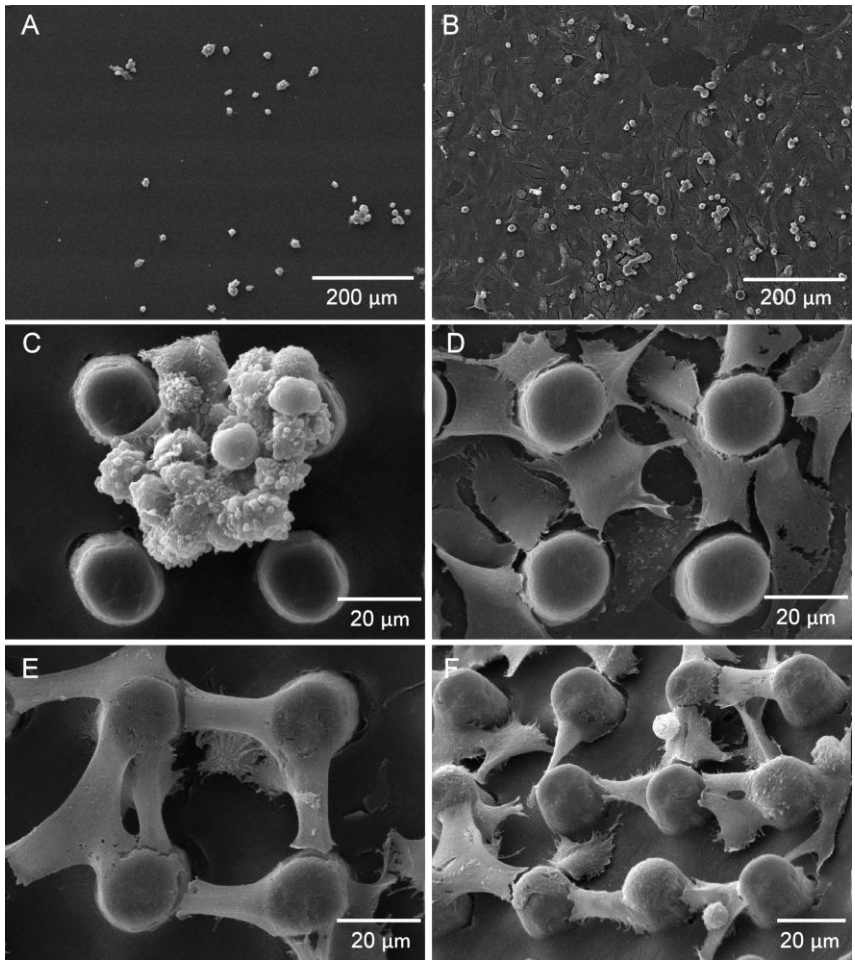

Figure 21: *Saos-2 cells on uncoated smooth (a) and on C_3N_4-Si coated smooth PP surfaces (b) after 48-hours in culture. On uncoated surface, the cells have a rounded appearance with minimal focal adhesions (a), whereas on a coated surface, the cells are spread out and flattened of their morphology with numerous focal adhesions (b). On an uncoated MNST surface, the cells are as rounded as on uncoated smooth surface, but they have accumulated together (c). The most interesting observation can be seen in figures d, e and f. On coated MST surface, the cells grow on the plateau between the micropillars (d) while on the coated MNST surfaces (e, f) cells also are attached via extensions on the top and the sides of the micropillars. (Study* ***II****)*

Figure 22 represents the **unpublished results I** of Saos-2 adhesion on different ceramic materials. In this experiment, the

main aim was to determine the correlation between the zeta potential and the adhesion of osteoblast-like cells. MTT assay revealed that there was no statistical difference between these ceramic coatings (Fig. 22) which had zeta potential values in the same range (Fig. 17).

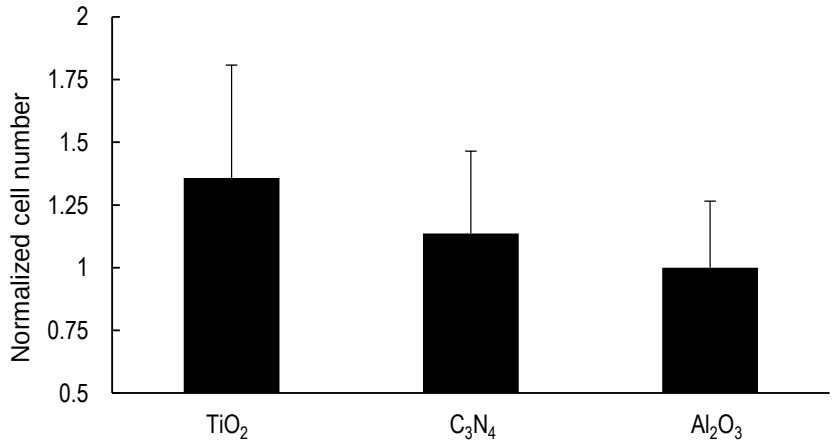

Figure 22: *The number of Saos-2 cells on TiO_2, C_3N_4 and Al_2O_3 surfaces after 48-hour incubation. Statistically significant differences between materials were not found. The presence of viable cells was spectrophotometrically assessed by the MTT assay and a standard curve normalized to the number of cells. Results are normalized so that Al_2O_3 coated sample is designated a value of one. Error bars indicate the standard deviations. One-way ANOVA was used to determine the statistical differences between materials.*

Figure 23 represents the **unpublished results II** of Saos-2 adhesion on Si wafers with smooth, matt and rough surfaces. The roughness of either matt or rough surfaces evoked the 36 % and 85 % higher Saos-2 adhesion compared to smooth surface, respectively. These differences were statistically significant ($p < 0.05$).

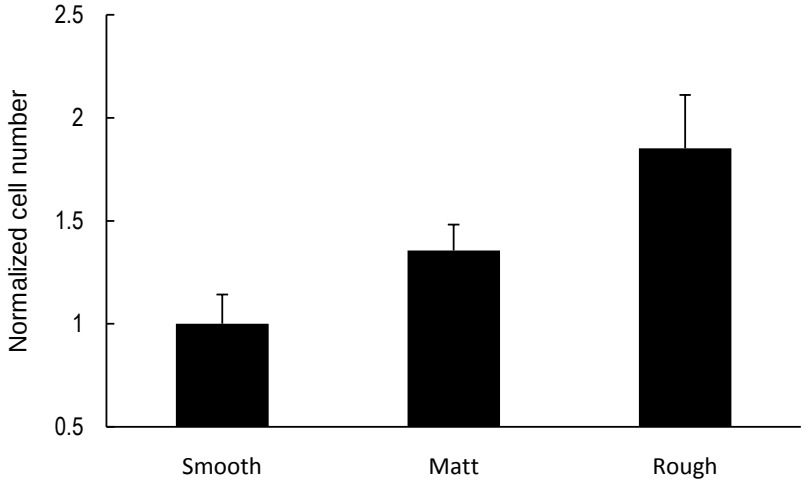

Figure 23: *The quantity of Saos-2 cells on smooth (R_a < 10 nm), matt (R_a = 100 ± 10 nm) and rough (R_a = 1000 ± 100 nm) silicon wafers. The Saos-2 adhesion rates were 36 % and 85 % higher with matt and rough surfaces compared to smooth surface, respectively. The differences were statistically significant ($p < 0.05$) between these groups (**unpublished data II**). After 48-hours' incubation, the number of viable cells was determined using the MTT assay and the standard curve normalized to the number of cells. Results are normalized so that silicon wafers with smooth surface was designated the value of one. Error bars indicate the standard deviations. One-way ANOVA was used to determine the statistical differences between materials.*

8.6 STAPHYLOCOCCAL BEHAVIOUR ON STUDIED SAMPLES

In study **III**, at 16 hours DLC-PTFE-h and DLC were clearly better able to resist biofilm formation of *S. epidermidis* than conventional biomaterial metals Ti (Fig. 24), Ta and Cr as well as DLC-PDMS-h. Biofilm formation was practically completed on Ti, Ta, Cr and DLC-PDMS-h so that they were 98.95 %, 99.60 %, 99.11 % and 99.75 %, respectively, covered by biofilm whereas coverage was only 87.71 % and 55.84 % for DLC and DLC-PTFE-h, respectively (Fig. 25). In this study, biofilm resistance did not correlate in a straightforward way with surface roughness (Table 6), wettability (Tables 7 and 9) or zeta potential (Fig. 17). However, DLC is highly negative in its surface charge which

might be an important explanation for the good biofilm formation resistance. With DLC-PTFE-h, the good anti-biofilm properties appeared to be related to the fluoride content of this hybrid.

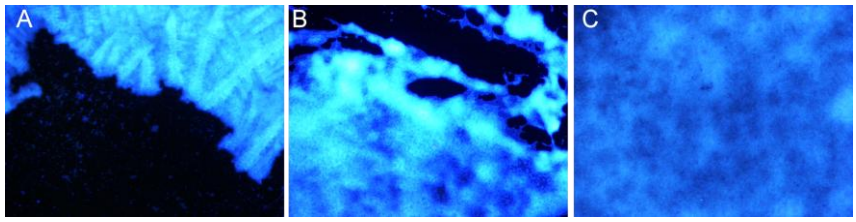

Figure 24: *Pictures of Calcofluor White stained biofilm formations visualized under epifluoresence microscope on DLC-PTFE (a), DLC (b) and Ti (c) surfaces. Biofilm is seen as light and the pure background as black. (Study* ***III****)*

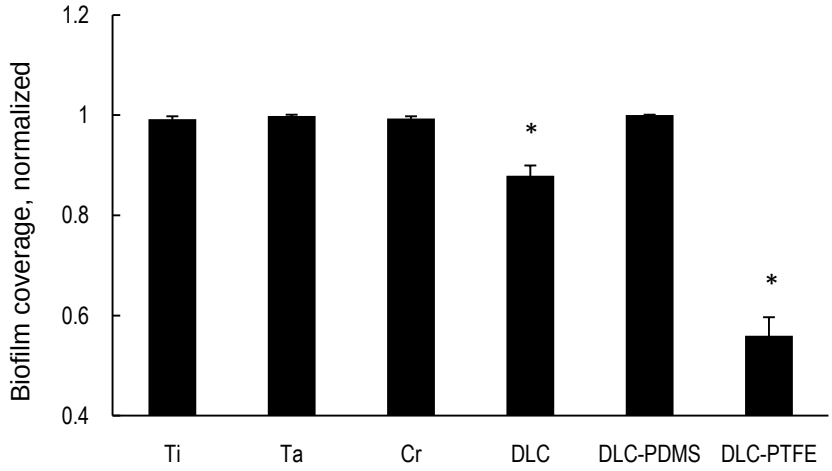

Figure 25: *Area covered by Calcofluor White stained biofilm produced by Staphylococcus epidermidis on different biomaterials after 16-hours' incubation. DLC-PTFE-h and DLC statistically differed (*p < 0.001) from other materials in their abilities to resist biofilm formation (Study* ***III****). Error bars indicate the standard errors of the mean. Results are normalized so that DLC-PDMS was designated the value of one. One-way ANOVA was used to determine the statistical differences between materials.*

In study **IV**, after cultured *S. aureus* for 90 min under static conditions and in the presence of serum it was noted that the rank order of the biomaterials was Ti, Ta, Cr, and DLC, with the DLC being clearly most resistant against colonization with *S. aureus* (Fig. 26 and 27). Adhesion of *S. aureus* was studied using different size (125 μm, 25 μm and 5 μm) microtextured circular spots of biomaterial coating and either the background being Si or the reverse situation (Fig. 14). In every size, spots formed 30.6% and background 69.4% of the total sample area. Adhesion was also studied with a homogenous plain coating surface. Calculations for bacterial adherence were conducted with samples of 125 μm biomaterial spots on a Si background (Fig. 26). The difference in adhesion of *S. aureus* for Ti and Ta over Cr and DLC was very clear when the area of the biomaterial covered by adherent bacteria was calculated (Fig. 26a). This order of adhesion and its magnitude were similarly apparent when the ratio of adherence index (bacterial binding to the tested biomaterial/bacterial binding to the silicon background) was calculated for Ti (22.69%/0.68%), Ta (14.34%/0.84%), Cr (1.41%/0.66%) and DLC (0.38%/0.40%) and compared against each other (Fig. 26b).

The adhesion of bacteria with other sizes of spots and plain surface is described in Table 10. Some other results of this study can be summarized as follows. First, micropatterned surfaces proved to be very useful for quantitative comparison of bacterial adherence on different materials. Second, when a bacterial friendly coating was uniform or when it covered 69.4% of the total surface area, the bacteria were relatively homogenously covering the available surface. However, when only 30.6% of the surface area was covered by bacteria friendly biomaterials, bacteria formed small areas of biofilm-like bacterial communities. Finally, when the diameter of the spots was only 5 μm, bacteria seemed to grow also on the background.

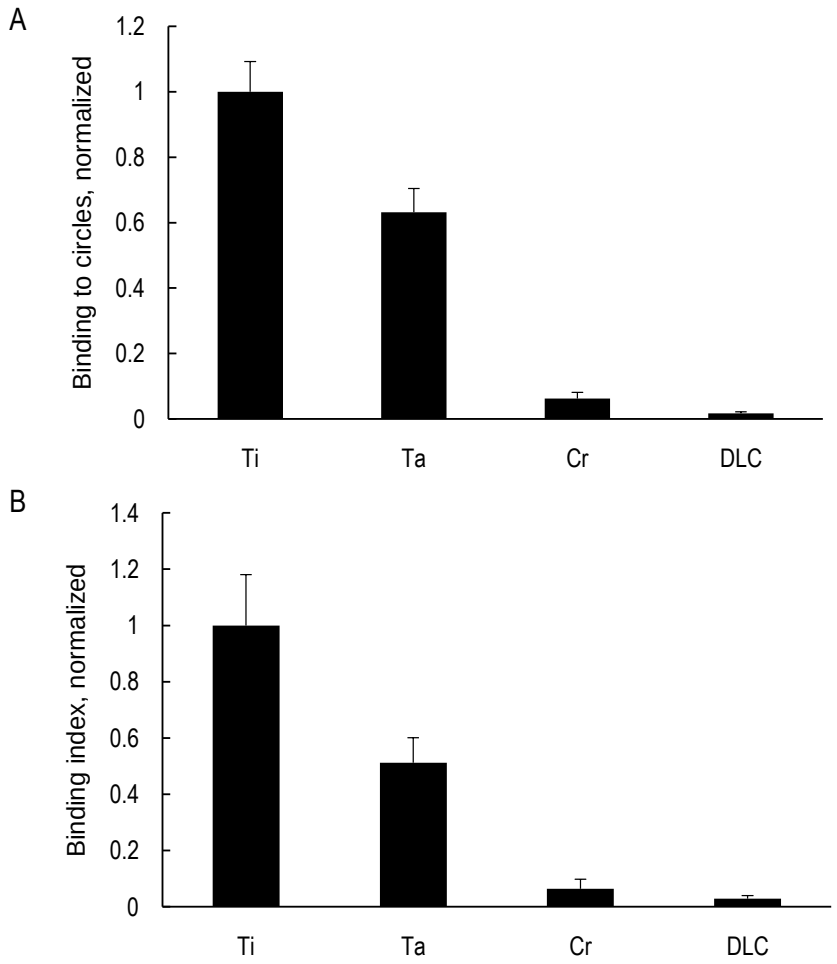

Figure 26: *Acridine Orange stained Staphylococcus Aureus adhesion on biomaterial surfaces with coatings on the 125 µm circular spots with silicon background after 90-minutes incubation (a).Spots formed 30.6 % of the total sample area and the results are expressed as the percentage of the spots covered by adherent bacteria. Results are normalized so that Ti was designated the value of one. Figure 26b completes the results of Fig. 26a by demonstrating the adherence index (bacterial binding to the tested biomaterial/bacterial binding to the silicon background). As seen in these figures, DLC proved to be superior in its ability to resist bacterial adhesion (Study* ***IV****). Error bars indicate the standard deviations of the mean.*

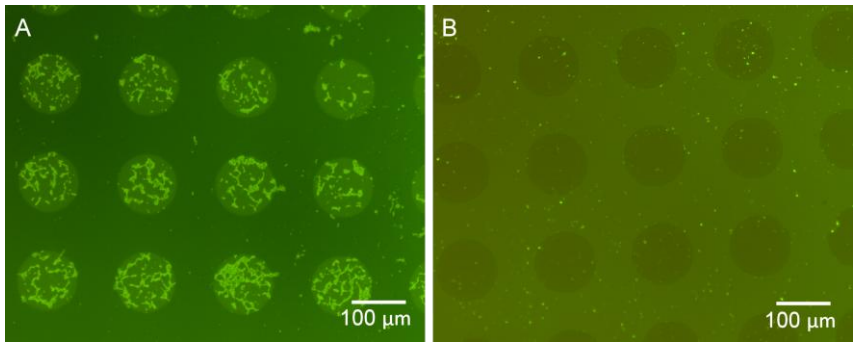

Figure 27: *Clear difference between Ti (a) and DLC (b) in their abilities to resist bacterial adhesion. In these ultraviolet-lithographically patterned samples, coatings are in the spots with diameter of 125 µm and the background is silicon. DLC spots are almost clear of bacteria (b). (Study **IV**)*

Table 10*: Summary of the adhesion of S. aureus to test samples. For each material pair (the left column) the results are expressed for patterned (e.g. titanium spots on silicon background or Ti/Si) and for reverse patterned (e.g. silicon spots on titanium background or Si/Ti) samples compared to plain unpatterned surface (right column). The results are designated so that the number of stars increases with the increased bacterial adhesion. Diamond-like carbon (DLC) resisted best the bacterial adhesion, followed by chromium (Cr), tantalum (Ta) and titanium (Ti). This rank order was demonstrated with both patterned, reverse patterned and plain samples.*

Material (spots/ background)	**Size of the spots: 125 µm**	**Size of the spots: 25 µm**	**Size of the spots: 5 µm**	**Plain unpatterned surface**
DLC/Si	¤/¤	¤/¤	¤/¤	¤¤ DLC
Si/DLC	¤/¤	¤/¤	¤/¤	-
Cr/Si	¤¤¤/¤	¤¤¤/¤	¤¤/¤¤	¤¤¤¤ Cr
Si/Cr	¤/¤¤¤	¤/¤¤¤	¤¤/¤¤	-
Ta/Si	¤¤¤¤¤/¤	¤¤¤¤¤/¤	¤¤¤/¤¤¤	¤¤¤¤¤¤ Ta
Si/Ta	¤/¤¤¤¤¤	¤/¤¤¤¤¤	¤¤¤/¤¤¤	-
Ti/Si	¤¤¤¤¤¤¤/¤	¤¤¤¤¤¤¤/¤	¤¤¤¤/¤¤¤¤	¤¤¤¤¤¤¤¤ Ti
Si/Ti	¤/¤¤¤¤¤¤¤	¤/¤¤¤¤¤¤¤	¤¤¤¤/¤¤¤¤	-

9 Discussion

In the present thesis, novel carbon-based materials were successfully used to enhance adhesion of osteoblast-like cells or to prevent biofilm formation. UV-lithography and injection molding demonstrated to be effective methods to texture surfaces for contact guidance and morphological modification of osteoblast-like cells. The USPLD technique was useful in the production of well-adherent novel hybrid coatings with different wettability properties, which may help to guide the cellular responses. DLC and DLC-PTFE were demonstrated to be superior in their ability to resist bacterial adhesion.

9.1 SAMPLE FABRICATION FOR CELL AND BACTERIA STUDIES

It is essential to conduct *in vitro* tests if one wishes to make improvements in biomaterials for use as orthopedic implant applications. First of all, sample fabrication needs to be performed in clean conditions in a reproducible way. Cells and bacteria can sense even minimal impurities or cutting dust in the samples and this may distort the cellular responses. In this thesis (studies **I** and **IV**), UV-lithography was employed to produce the desired patterns onto Si wafers. UV-lithography (Madou 2002) is a very well-controlled, rapid and inexpensive way to produce patterns with feature sizes ranging from 1.5 μm to 500 μm. Both the size and shape of the patterns produced can affect adhesion and spreading of the cells and biofilm formation by bacteria on the sample surface. In study **I**, UV-lithographically patterned samples revealed the guiding effect of Saos-2 cells seen by preferential cellular adhesion to the AD and AD hybrids patterns compared to Si background. A finding that generally rounded cells initially adopted the geometrical architecture of the square or cruciform shape was in agreement

with other studies (Kaivosoja et al. 2010, Myllymaa et al. 2010). The guiding effect may be utilized in orthopedic implant applications so that the diffuse dispersion of cells can be restricted and they can be guided to grow to critical sections not only in the desired direction but also in an intended orientation. In study **IV**, UV-lithography was used to fabricate different sized Ti, Ta, Cr and DLC patterns on Si background and to study the bacterial adherence to these textures. UV-lithography enabled to study the bacterial adherence to different sized structures with all the thin film coatings in the same array and minimized the biological alterations. Samples were also fabricated in the reverse manner (biomaterials on background and Si on patterns) which confirmed the material related effect of bacterial adherence. The size variation of the patterns and the comparison to the plain unpatterned surfaces to the patterned surfaces provided new information about bacterial colonization and biofilm formation. UV-lithography was also found to be an effective and reliable method for ranking the order of bacterial adherence on different biomaterials. However, some difficulties were also observed with this technique. The material used as the substrate, Si wafers, with a typical thickness of 0.25-1.0 mm, is very fragile and the handling of Si wafers is rather difficult. Also the cutting of these wafers produces some Si dust which may disturb the cell or bacteria interactions. Winkelmann et al. (2003) used a photoresist layer to prevent the production of Si dust to samples. This method, however, carries a risk of biomaterial contamination with photoresist residues. In this study, the presence of this dust was minimized by using a protective thin plastic film during cutting and washing the samples with mild detergent after cutting. Si can be doped with impurity atoms such as boron or phosphorous, *i.e.* changing it into n-type or p-type Si, in order to enhance the electrical conductivity. However, this conductivity may affect the behaviour of bacteria or cells seeded and growing on it. In this study, p-type Si was systematically used without encountering problems. The background material was actually SiO_2, since an oxide layer naturally forms on its surface. This happens also to the metals

used in *in vitro* tests but because similar oxide layers form also on real medical implant materials, it does not seem to be a problem. It is impossible to use UV-lithography for patterning curved surfaces. Nevertheless, real implants typically contain curved and other complicated geometrical surfaces and at present it is the best option to pattern these kinds of *in vitro* surfaces using soft lithography (Xia & Whitesides 1998). Another advantage of soft lithography compared to conventional photolithography is that the technique itself is suited to texturing of three dimensional structures (Xia & Whitesides 1998, Mata et al. 2009). When the optimized surface texture has been found, the real implant surface can be textured using *e.g.* laser processing.

In this thesis (study **II**), PP samples were textured using injection molding methods. The advantages of polymers include low cost, chemical availability and possibility to create complex three dimensional structures. Polymers like polystyrene, polymethylmethacrylate, polycarbonate and polydimethyl-siloxane and have been used in some previous studies (Flemming et al. 1999). Polypropylene was chosen for use in the study **II** due to its straightforward handling properties as well as its optimal level of stiffness required for cell adhesion (Vagaska et al. 2010). A rather new method, injection molding, was effective in controlling both micro- and nanodimensions of the structures. It is also suitable for mass production of *in vitro* samples with different hierarchical structures. The advantage of this method is that it can be used to produce a nanotexture placed deliberately on the surface. Another advantage is that the shape of the feature is rounded, since sharp edges are not common in the human body. Micro- and nano-scale dual structures combined with high surface energy achieved by proper coating significantly enhance osteoblastic cells adhesion. In the future, this method will be used to produce dual structures optimized for different purposes.

In every sub-project of this thesis, thin film deposition played an important role. Thin films refer to thin material layers ranging from the thickness of singular atomic layers to several

micrometers. In this thesis, the thicknesses of layers were about 200 nm. The coating techniques used were USPLD (studies **I** and **II** and **unpublished data I**) (Amberla et al. 2006), DC sputtering (studies **III** and **IV**) and FPAD (studies **III** and **IV**). In studies **I** and **II**, hybrid thin film coatings in a very well controlled and reproducible manner were produced and in study **II**, the wettability properties of PP surfaces were drastically changed. Cleaning of samples before deposition can be challenging. Even a gentle ion beam cleaning partly destroyed the nanostructures on PP in study **II**. In the future, it would be worthwhile to use chemical treatments at an elevated temperature or an even gentler vacuum handling for cleaning of the samples. In the future, USPLD could be used to deposit proteins like Fn or Vn, which affect the bone cell adhesion onto implant surface. Since this method can be used for deposition on large surfaces with dimensions of tens of centimetres, a real implant for implantation in animal models or human patients could be produced.

9.2 *IN VITRO* STUDIES

Direct contact testing of novel biomaterials with *in vitro* cell cultures can be used as a first stage test of acute toxicity and cytocompatibility. It avoids the unnecessary use of animals and may provide an early indicator of potential *in vivo* problems. ISO-10993-5 guidelines for "Biological Evaluation of Medical Devices" set by the International Organization for Standardization allows for the use of visual grading systems in new material cytotoxicity determinations (Bhatia & Yetter 2008). The US Food and Drug Administration guidelines for medical device evaluation are also largely in concordance with this standard (Bhatia & Yetter 2008). A visual grading method requires only microscopic inspection of cell–material interactions and provides an inexpensive and fast way for screening of large numbers of potential biomaterial candidates. In this thesis (studies **I** and **II** and **unpublished data I** and **II**)

also a quantitative MTT colorimetric assay was used to measure cell viability and was demonstrated to be more accurate than microscopic methods at detecting differences between different coating materials and surface textures. Bhatia and Yetter (2008) demonstrated a high degree of correlation between the visual cytotoxicity rating and the quantitative cell viability measurement performed using MTT colorimetric assay. To summarize the results of studies **I** and **II** and the article of Bhatia and Yetter (2008), it seems that the quantitative method of cell viability confirms the microscopic observations and in some cases provides additional information. One drawback of *in vitro* tests arises from the limited lifespan of cultured cells and the fact that cells come from the different microenvironments. Therefore, the test of material toxicity is limited to quite acute studies and one cannot extrapolate that all osteoblastic cells will behave in the same way on the substrate. However, well-characterized osteoblast-like cells do represent a successful *in vitro* model to study bone-biomaterial interactions. For instance, the Saos-2 cell line used in studies **I** and **II** of this thesis, is well characterized and known to possess several osteoblastic features *e.g.* elevated alkaline phosphatase and parathyroid hormone-sensitive adenylate cyclase, production of mineralized matrix and expression of osteonectin. (Rodan et al. 1987, Dass et al. 2007) MSCs (Mendonca et al. 2009b, Ozawa & Kasugai 1996) as well as osteogenic MC3T3-E1 (Oya et al. 2010, Sudo et al. 1983) cells may be used for evaluating the ability of the implant material to provide an environment for these cells to differentiate into osteoblasts and function as suitable for mineralized tissue formation. This *in vitro* osteogenesis may be investigated by measuring the DNA content, ALP activity and calcium content in culture, as well as the expression of osteopontin and bone sialoprotein (Ozawa & Kasugai 1996). Favourable differentiation into osteoblasts and a large amount of mineralized tissue formation on implant surfaces may be used as an indicator of rapid bone bonding of the implant *in vivo.* There is also an increasing need for techniques that enhance osteogenic differentiation of stem cells and/or identify new

progenitor cells for tissue engineering and regenerative medicine applications. The lithographic methods used in this thesis also provide potential tools for testing the cell's capacity for electrical stimulation and whether this results in enhanced osteogenesis (McCullen et al. 2010). The fabrication of 3D scaffolds with precisely engineered architecture and tailored surface topography may also be used in future to guide and selectively stimulate cells and tissues (Mata et al. 2009).

The evaluating bacteria-material interaction *in vitro* is a challenging and complicated process. Well sophisticated *in vitro* techniques take into account general culturing circumstances as well as the possible sterilization or chemical treatments of substrate before culturing. As it has been demonstrated that serum proteins have a role in biofilm formation (Patel et al. 2007), in studies **III** and **IV**, experiments were conducted using biomaterials precoated with serum proteins and in the presence of the diluted TSB to mimic the natural environment in the human body. In study **III**, biofilm formation was studied using the fluorochromic stain which interacts with polysaccharide components of biofilm. In the future, it may be also possible to study the biofilm thickness and viability when more information about material-biofilm construction is gathered (Patel et al. 2007, Saldarriaga Ferńandez et al. 2010). Other challenges will be to clarify the physical factors like hydrophobicity and the charge of the studied bacteria and investigate the influence of suspending medium on these parameters (Bayoudh et al. 2009). One recent study was found in which the "race for the surface" of osteoblastic cells and bacteria *in vitro* was studied (Subbiahdoss et al. 2009). This kind of study would be an important step forwards when the culture medium and other culture circumstances do not favour either the studied bacteria or the cell and of course under conditions similar to the environment in the human body.

9.3 THE EFFECT OF SURFACE PHYSICOCHEMICAL PROPERTIES FOR CELL AND BACTERIA RESPONSES

In this thesis, samples were textured using UV-lithography (studies **I** and **IV**) and injection molding (study **II**). In study **I**, microtextured square or cruciform features were also coated with AD, AD-Ti-h and AD-PDMS-h and the background was Si. At timepoint of 24 hours, the number of cells on plain Si did not differ from the number of cells on plain AD and its hybrid coatings. However, SEM observations with patterned samples indicated the preferential adhesion of cells to the AD and its hybrid patterns compared to Si background. The cells adopted to grow in the geometric of square or cruciform features and the focal adhesions mainly formed on the patterns of AD and its hybrids with the cells preferring the very edges of the patterns. Due to technical reasons, the confocal laser scanning microscopy used in this study did not clearly pinpoint the locations of focal adhesions compared to the feature edges. Preferential localization of vinculin containing focal adhesions was noted in a previous study from our group in which Saos-2 cells were cultured on micropatterned thin films (Kaivosoja et al. 2010). Study **I** indicated that the guiding effect of the cells could be also mediated by a physical shape of the pattern in addition to the chemical composition of the substrate. This observation was in agreement with other studies (Parker et al. 2002, Myllymaa et al. 2010).

In study **II**, PP surfaces were structured with pillars of height, diameter and spacing of 20 μm. In combined micro- and nano-structured surfaces these pillars and also the plateau between pillars was nanostructured. Pure texturing did not affect the osteoblastic cells adhesion compared to smooth surfaces, but when the surfaces were also coated with C_3N_4-Si thin films, cell adhesion became enhanced on these textured surfaces. MNST surfaces displayed slightly but not significantly better adhesion of cells than MST surfaces. An increased area of a uniform nano-rough region (Puckett et al. 2008, Okada et al. 2010) as well as inclusion of lower micropillars would be a effective way to

further enhance cell adhesion. Cell-cell contact has been demonstrated to regulate stem cell osteogenic differentiation (Tang et al. 2010) and texturing must be planned so that it does not prevent the cells from contacting each other.

An interesting issue requiring clarification is the optimal height of microstructures to promote enhanced adhesion of osteoblasts. One way to approach this problem might be to detect the size range of the filopodia produced the osteoblasts *in vitro*. Features with heights similar to the sizes of "natural filopodia" might help cells to gain a relatively stable foothold on the structure which could provide cells with long-term vitality and function (Mata et al. 2003).

Previously, the effects of surface roughness on cell adhesion have been studied using surfaces roughened mainly by etching, grinding, or sandblasting with resulting average roughness values somewhat greater than 10 μm (von Recum et al. 1996). Nowadays, nanoroughness (less than 100 nm), typically produced with different deposition methods has become the most widely studied feature in cell-material interactions. Nanoroughness has been shown to enhance osteoblastic cells adhesion and differentiation (Puckett et al. 2008, Das et al. 2009, Reising et al. 2008, Dalby et al. 2006, Pareta et al. 2009, Okada et al. 2010, Grausova et al. 2009, Yang et al. 2009) as well as to increase osteoinductive gene expression of adherent human MSCs (Mendonca et al. 2009b, 2010). Recent studies have also suggested that nanostructured materials may be used for inhibition of bacterial adhesion and biofilm formation in orthopedic implants (Montanaro et al. 2008, Weir et al. 2008). Unpublished results **II** revealed that surface roughness R_a ~ 100 nm and R_a ~ 1000 nm evoked the 36 % and 85 % higher Saos-2 adhesion compared to roughness R_a < 10 nm, respectively. The textured orthopedic implant applications currently in use frequently have configuration diameters (of pores, beads, or wires) larger than 50 μm (von Recum et al. 1996). Recent studies have demonstrated that the osteogenesis of stem cells occurred best in large pattern sizes (~ 100 μm x 100 μm) (McBeath et al. 2004) whereas osteogenesis was hindered at middle-size

features (40-70 μm x 40-70 μm) (McBeath et al. 2004, Myllymaa et al. 2010). One could speculate that a combination of following texture sizes > 100 μm, 1-3 μm and nanoroughness may enhance the integration of implants into the host bone tissue.

In study **IV,** surface texturing provided new information of bacterial behaviour in different sizes features. Bacteria were demonstrated to cover the available surface relatively homogenously when a bacteria friendly coating was uniform or when it was in the background and covered 69.4% of the total surface area. Small areas of biofilm-like bacterial communities formed when the bacteria friendly biomaterials were in the spots and formed 30.6% of the surface area. An interesting observation was made with 5 μm spots with spacing approximately 3 μm. With these textures, no division of bacteria between biomaterials or Si could be seen. One could speculate that the extracellular polymeric matrix might form bridges between bacteria friendly areas which are sufficiently close together. A few bacteria in bacteria unfriendly areas might be actually contact with the underlying bacterial slime and not with bacteria unfriendly material.

In study **I**, pure AD had a lower contact angle (72.4°) and a higher SFE with a higher polar component (γ_S^{AB}) compared to AD hybrid coatings. In that study, SFE components were calculated using two models, *i.e.* van Oss (van Oss et al. 1988) and Owens-Wendt (Owens & Wendt 1969) to compare whether there was a difference between these two models. The polar component calculated by VO method was found to be the most critical factor in determining Saos-2 adhesion. The VO model uses three liquids in determining the contact angles whereas the OW model uses only two. When accurate information of the polar component of surface is needed, the VO approach is a better choice. Also in other studies, the polar component of the surface has been demonstrated to play a dominant role in the functions of osteoblastic cells (Feng et al. 2003, Redey et al. 2000). This may be due to the fact that the constituents of cells and the culture medium are all polar and thus the cells and the coating material interact mainly through polar forces. If the polar

component of surface is high enough, this causes higher interaction energy between cells and the coating and irreversible adhesion of cells as happened on AD. Instead, weaker cell adhesion was seen in AD-PDMS which had the most non-wettable property and the smallest polar component. At a timepoint of 24 hours, the cells were quite well adhered to reference Si, but the number of cells was decreased with time. The reason for the good adhesion seen at the first timepoint is probably due to the favourable wettability properties of Si but since it is a very hydrophilic material, short-distance repulsive interactions might cause reversible adhesion of cells at later time points even though there is known to be poor cytocompatibility. Increased wettability with a higher SFE has been shown to enhance the osteoblastic cells functions (Lim et al. 2008, Khang et al. 2008, Feng et al. 2003, Liao et al. 2003, Zhao et al. 2005, Zhao 2007b). It may be also probable that cells preferentially adhere to surfaces with moderate hydrophilicity as has been demonstrated in a few studies (Van Wachem et al. 1985, Lee et al. 1997, 1998). Favourable cell adhesion may be considered not only in terms of stable polar binding between cell and material, but also for promoting the adsorption of protein molecules in an appropriate and flexible spatial conformation making possible the protein reorganization and accessibility of the specific ligands via cell adhesion receptors (Vagaska et al. 2010). On extremely hydrophilic surfaces, the cell adhesion-mediating proteins may be bound too loosely, so they do not provide firm adhesion and spreading of cells on the material surface (Bačáková et al. 2004, 2007). On the other hand, hydrophobic surfaces are thought to promote strong adsorption and subsequent denaturation of proteins, which distorts the conformation of cell adhesion receptor-binding domains. In addition, a preferential and strong adsorption to Alb which acts as non-adhesive for cells has been reported on these surfaces (Arima & Iwata 2007, Choi et al. 2008, Hao & Lawrence 2007). In recent studies, FPAD produced pure DLC coatings have displayed controversial results with respect to osseointegration (Myllymaa et al. 2010, Calzado-Martin et al. 2010). Further

studies will concentrate on identifying an even more optimal AD hybrid material with moderate hydrophilicity. This modification might be beneficial for osteogenic differentiation of progenitor cells.

In study **II**, osteocompatible C_3N_4-Si-coating drastically enhanced the wettability properties of PP samples. Furthermore, the surface micro- and nanotexturing significantly enhanced the adhesion and spreading of osteoblast-like cells compared to the situation with uncoated and untextured surfaces. The synergistic effect of favourable wettability and topography properties of materials to enhance osteoblastic cells adhesion has also been demonstrated in other studies (Khang et al. 2008, Feng et al. 2003, Misra et al. 2009).

It is often reported that hydrophilic surfaces display lower adhesion rates of bacteria compared with hydrophobic control surfaces (Bruinsma et al. 2001, Bayoudh et al. 2006, 2009, Gallardo-Moreno et al. 2009, Cerca et al. 2005, Patel et al. 2007). With hydrophilic surfaces, the hydrophilic repulsion between bacteria and surfaces cause the reversible adhesion of bacteria whereas in hydrophobic surfaces, the attractive LW and EL interactions cause the irreversible adhesion of cells (Bayoudh et al. 2009, Boks et al. 2009). However, the biological specific interactions and specific experimental conditions like the presence of serum proteins (Patel et al. 2007, MacKintosh et al. 2006) and the ionic strength of the culture medium (Bayoudh et al. 2009) both have a major influence on the adhesion properties of adhesive proteins as well as bacteria and these need to be taken into account. Also the hydrophilicity of certain bacteria strains may have an influence on the adhesion process (Bruinsma et al. 2001, Bayoudh et al. 2006, 2009). In study **III**, the biofilm resistance of DLC-PTFE-h and DLC compared to DLC-PDMS-h, Ti, Ta and Cr could not be explained as a straightforward by the surface roughness, wettability or zeta potential of these coatings. The zeta potentials of the all biomaterials studied were negative, but particularly that of the DLC (approximately -70 mV). This suggests that the important explanation for the good biofilm formation resistance of DLC

might be the considerable repulsive forces existing between this coating and the bacterial cells. Fluoride is widely used for its antibacterial properties particular in dentistry (Wiegand et al. 2007). The fluoride content of DLC-PTFE-h might explain the good antibiofilm property of this coating. In the future, testing with DLC-PTFE hybrid coatings with different corrosion rates of fluoride and the DLC coatings with different surface charge values might define the most critical factor in resistance to bacterial adhesion and biofilm formation as observed in studies **III** and **IV**.

The electric charge of a biomaterial surface is considered to be one of the material-based physicochemical factors affecting cell/protein/bacteria-biomaterial interactions. It is established that negatively charged surfaces enhance the osteoblastic cells-biomaterial interactions *in vitro* (Cheng et al. 2005, Ohgaki et al. 2001, Bodhak et al. 2010, Thian et al. 2010). It has been speculated that one reason for enhanced osteoblast-like cells adhesion on negatively charged surfaces is their ability to selectively adsorb calcium (Ca^{2+}) ions which, in turn, favour adsorption of cell adhesive proteins (*e.g.* fibronectin and osteonectin) and consequently promote adhesion and mineralization of osteoblastic cells (Bodhak et al. 2010, Cheng et al. 2005, Ohgaki et al. 2001). On positively charged surfaces, Cl^- reacts with surrounding cations, prefentially with Na^{2+} which consequently provide the formation of NaCl crystals which, in turn, together with anti-adhesive molecules (*e.g.* HCO_3^-) can be selectively attracted on a positively charged surface but this will result in poor cell adhesion (Bodhak et al. 2009, 2010, Ohgaki et al. 2001, Yamashita et al. 1996). Unpublished results (**I**) revealed that three tested ceramic materials (Al_2O_3, TiO_2 and C_3N_4) were negatively charged (ζ= -51-(-57) mV) and the cells adhered very well onto these surfaces but no difference was found on cell adhesion between these materials with apparently the same zeta potential as was predictable. In conclusion, a negative charge on the bone implant material would be favourable for bone cell adhesion as well as bacterial prevention, since stronger

repulsive forces exist between negatively charged bacterial cells and negatively charged surfaces.

New, valuable information about interactions between osteoblast-like cells and textured carbon-based surfaces was obtained in these short-term *in vitro* studies. Moreover, some indications about bacteria behaviour on textured carbon-based surfaces were obtained. In the future, also long-term studies examining *in vitro* osteogenesis as well as *in vivo* tests will be needed to investigate whether the new generation of intelligent orthopedic implants will be more biocompatible and bioactive than their current counterparts. It is a challenge to combine the properties of surface roughness, texture, wettability and charge to enhance bone cell adhesion and differentiation as well as being able to prevent biofilm formation; this thesis provides a solid foundation for this kind of research.

10 Summary and conclusions

In this thesis, novel fabrication techniques to produce carbon-based thin films and ways to modify their physicochemical properties were developed. The optimal orthopedic implant should be bioactive, *i.e.* it should induce the desired cellular responses, leading to integration of the material into the bone tissue as well preventing the formation of biofilm. *In vitro* studies were carried out to clarify the effects of surface properties such as surface chemistry, surface wettability, roughness, texture and zeta potential on the adhesion and behaviour of osteoblast-like cells and bacteria on biomaterial coatings. The most important results of the studies included in this thesis can be summarized as follows:

1. Microtexturing of bone implant surfaces can be used to regulate the contact guidance of osteoblastic cells according to the shape of microtextures as demonstrated with UV-lithographically patterned Si samples with *in vitro* cell tests (**I**). Samples with different sized microtextures appear to be effective tools to collect detailed knowledge about bacterial adhesion and colonization processes (**IV**).

2. The USPLD method is a very useful way to produce novel hybrid materials (AD-Ti, AD-PDMS, C_3N_4-Si) in order to modify the wettability properties of polymers (**II**) and ceramics (**I**).

3. Synergetic effect of injection molded surface micro- and nanotexturing with moderately wettable carbon-based coating on enhanced osteoblast-like cells adhesion was clearly demonstrated (**II**).

4. Increased surface roughness (**unpublished data II**) and texturing (**I** and **II**) of osteocompatible material enhances the adhesion of osteoblast-like cells. The Lewis acid-base component (γ_S^{AB}) of surface free energy was demonstrated to be a critical factor in the adhesion of these osteoblast-like cells (**I**).

5. Physicochemical properties of DLC and DLC-PTFE-hybrid did not explain unequivalently their ability to resist biofilm formation compared to commonly used implant metals and DLC-PDMS-h. Further studies are needed to clarify the factors beyond the antibacterial properties.

6. Overall, novel carbon-based materials proved to be promising coating candidates for bone implant applications because of their abilities to enhance adhesion of osteoblastic cells (**I, II**) and to prevent bacterial adhesion and biofilm formation (**III, IV**).

11 References

Abe, L., Nishimura, I. & Izumisawa, Y. (2008) Mechanical and histological evaluation of improved grit-blast implant in dogs: pilot study. *J.Vet.Med.Sci.,* 70, 1191-8.

Abramoff, M.D., Magelhaes, P.J. & Ram S.J. (2004) Image processing with ImageJ. *Biophotonics Int.,* 11, 36-42.

Abu-Amer, Y., Darwech, I. & Clohisy, J.C. (2007) Aseptic loosening oftotal joint replacements: mechanisms underlying osteolysis and potential therapies. *Arthritis Res.Ther.,* 9, 10.1186/ar2170.

Affatato, S., Frigo, M. & Toni, A. (2000) An *in vitro* investigation of diamond-like carbon as a femoral head coating. *J.Biomed.Mater.Res.,* 53, 221-6.

Aisenberg, S. & Chabot, R. (1971) Ion-beam deposition of thin films of diamonlike carbon. *J. Appl. Phys.,* 42, 2953-8.

Allen, M., Law, F. & Rushton, N. (1994) The effects of diamond-like carbon coatings on macrophages, fibroblasts and osteoblast-like cells in vitro. *Clin.Mater.,* 17, 1-10.

Allen, M., Myer, B. & Rushton, N. (2001) *In vitro* and *in vivo* investigations into the biocompatibility of diamond-like carbon (DLC) coatings for orthopedic applications. *J.Biomed.Mater.Res.,* 58, 319-28.

Altankov, G., Richau, K. & Groth, T. (2003) The role of surface zeta potential and substratum chemistry for regulation of dermal fibroblasts interaction. *Mat.-wiss.u.Werkstofftec.,* 34, 1120-8.

Alvarez, K., Hyun, S.-K., Nakano, T., Umakoshi, Y. & Nakajima, H. (2009) In vivo osteocompatibility of lotus-type porous nickel-free stainless steel in rats. *Mater.Sci.Eng.,C,* 29, 1182-90.

Amarante, E.S., Chambrone, L., Lotufo, R.F. & Lima, L.A. (2008) Early dental plaque formation on toothbrushed titanium implant surfaces. *Am.J.Dent.,* 21, 318-22.

Amberla, T., Rekow, M., Köngäs, J., Asonen, H., Salminen, T., Viitanen, N., Kulmala, M., Vuoristo, P., Pessa, M., Lappalainen, R. (2006) *Pulsed laser deposition with a high average power fiber laser.* In: *Proc. of the 49th Annual Technical Conference,* Washington D.C., USA, April 22-27, 2006, pp. 79-82.

An, Y.H. & Friedman, R.J. (1997) Laboratory methods for studies of bacterial adhesion. *J.Microbiol.Meth.,* 30, 141–152.

An, Y.H. & Friedman, R.J. (1998) Concise review of mechanisms of bacterial adhesion to biomaterial surfaces. *J.Biomed.Mater.Res.,* 43, 338-48.

An, Y.H. & Martin, K.L. (eds.) (2003) *Handbook of histology methods for bone and cartilage*, Humana Press, Totowa, NJ, USA.

Anselme, K. (2000) Osteoblast adhesion on biomaterials. *Biomaterials,* 21, 667-81.

Anselme, K. & Bigerelle, M. (2005) Topography effects of pure titanium substrates on human osteoblast long-term adhesion. *Acta Biomater.,* 1, 211-22.

Anttila, A., Lappalainen, R., Tiainen, V.-M. & Hakovirta, M. (1997) Superior attachment of high-quality hydrogen-free amorphous diamond films to solid materials. *Adv.Mater.,* 9, 1161-4.

Archibeck, M.J., Jacobs, J.J., Roebuck, K.A. & Glant, T.T. (2001) The basic science of periprosthetic osteolysis. *Instr.Course Lect.,* 50, 185-95.

Arciola, C.R., Campoccia, D., Gamberini, S., Donati, M.E., Pirini, V., Visai, L., Speziale, P. & Montanaro, L. (2005) Antibiotic resistance in exopolysaccharide-forming *Staphylococcus epidermidis* clinical isolates from orthopaedic implant infections. *Biomaterials,* 26, 6530-5.

Arima, Y. & Iwata, H. (2007) Effect of wettability and surface functional groups on protein adsorption and cell adhesion using well-defined mixed self-assembled monolayers. *Biomaterials,* 28, 3074-82.

Arora, A., Song, Y., Chun, L., Huie, P., Trindade, M., Smith, R.L. & Goodman, S. (2003) The role of the TH1 and TH2 immune responses in loosening and osteolysis of cemented total hip replacements. *J.Biomed.Mater.Res. Part A,* 64, 693-7.

Ashby, M.J., Neale, J.E., Knott, S.J. & Critchley, I.A. (1994) Effect of antibiotics on non-growing planktonic cells and biofilms of Escherichia coli. *J.Antimicrob.Chemother.,* 33, 443-52.

Aslam, S. (2008) Effect of antibacterials on biofilms. *Am.J.Infect.Control,* 36, 175.e9-11.

Atienza, C.,Jr & Maloney, W.J. (2008) Highly cross-linked polyethylene bearing surfaces in total hip arthroplasty. *J.Surg.Orthop.Adv.,* 17, 27-33.

Au, A., Ha, J., Hernandez, M., Polotsky, A., Hungerford, D.S. & Frondoza, C.G. (2006) Nickel and vanadium metal ions induce apoptosis of T-lymphocyte Jurkat cells. *J.Biomed.Mater.Res.Part A,* 79, 512-21.

Bacakova, L., Filova, E., Kubies, D., Machova, L., Proks, V., Malinova, V., Lisa, V. & Rypacek, F. (2007) Adhesion and growth of vascular smooth muscle cells in cultures on bioactive RGD peptide-carrying polylactides. *J.Mater.Sci.Mater.Med.,* 18, 1317-23.

Bacakova, L., Filova, E., Rypacek, F., Svorcik, V. & Stary, V. (2004) Cell adhesion on artificial materials for tissue engineering. *Physiol.Res.,* 53 , 35-45.

Baier, R.E. (1980) *Substrata influences on the adhesion of micro-organisms and their resultant new surface properties*. In: Bitton, G. & Marshall, K.S (eds.) *Adsorption of Micro-Organisms to Surface*, Wiley Interscience, NY, USA, pp. 59–104.

Baker, M.A. & Hammer, P. (1997) Study of the chemical composition and microstructure of ion beam-deposited CN_x films including an XPS C 1s peak simulation. *Surf.Interface Anal.,* 25, 301-14.

Basketter, D.A., Briatico-Vangosa, G., Kaestner, W., Lally, C. & Bontinck, W.J. (1993) Nickel, cobalt and chromium in consumer products: a role in allergic contact dermatitis? *Contact Dermatitis,* 28, 15-25.

Bayoudh, S., Othmane, A., Bettaieb, F., Bakhrouf, A., Ouada, H.B. & Ponsonnet, L. (2006) Quantification of the adhesion free energy between bacteria and hydrophobic and hydrophilic substrata. *Mater.Sci.Eng.,C,* 26, 300-5.

Bayoudh, S., Othmane, A., Mora, L. & Ouada, H.B. (2009) Assessing bacterial adhesion using DLVO and XDLVO theories and the jet impingement technique. *Colloids Surf.B,* 73, 1-9.

Bendavid, A., Martin, P.J., Comte, C., Preston, E.W., Haq, A.J., Magdon Ismail, F.S. & Singh, R.K. (2007) The mechanical and biocompatibility properties of DLC-Si films prepared by pulsed DC plasma activated chemical vapor deposition. *Diamond Relat.Mater.,* 16, 1616-22.

Betancourt, T. & Brannon-Peppas, L. (2006) Micro- and nanofabrication methods in nanotechnological medical and pharmaceutical devices. *Int.J.Nanomed.,* 1, 483-95.

Bhatia, S.K. & Yetter, A.B. (2008) Correlation of visual *in vitro* cytotoxicity ratings of biomaterials with quantitative *in vitro* cell viability measurements. *Cell Biol.Toxicol.,* 24, 315-9.

Black, J. (1994) Biological performance of tantalum. *Clin.Mater.,* 16, 167-73.

Black, J. (1999) *Biological performance of materials: Fundamentals of biocompatibility, 3rd ed.,* Marcel Dekker, NY, USA.

Block, J.E. & Stubbs, H.A. (2005) Reducing the risk of deep wound infection in primary joint arthroplasty with antibiotic bone cement. *Orthopedics,* 28, 1334-45.

Bobyn, J.D., Stackpool, G.J., Hacking, S.A., Tanzer, M. & Krygier, J.J. (1999) Characteristics of bone ingrowth and interface mechanics of a new porous tantalum biomaterial. *J.Bone Joint Surg.Br.,* 81, 907-14.

Bodhak, S., Bose, S. & Bandyopadhyay, A. (2009) Role of surface charge and wettability on early stage mineralization and bone cell-materials interactions of polarized hydroxyapatite. *Acta Biomater.,* 5, 2178-88.

Bodhak, S., Bose, S. & Bandyopadhyay, A. (2010) Electrically polarized HAp-coated Ti: in vitro bone cell-material interactions. *Acta Biomater.,* 6, 641-51.

Boks, N.P., Kaper, H.J., Norde, W., van der Mei, H.C. & Busscher, H.J. (2009) Mobile and immobile adhesion of staphylococcal strains to hydrophilic and hydrophobic surfaces. *J.Colloid Interface Sci.,* 331, 60-4.

Bougherara, H., Bureau, M.N. & Yahia, L. (2010) Bone remodeling in a new biomimetic polymer-composite hip stem. *J.Biomed.Mater.Res.Part A,* 92, 167-74.

Boyd, K.J., Marton, D., Todorov, S.S., Al-Bayati, A.H., Kulik, J., Zuhr, R.A. & Rabalais, J.W. (1995) Formation of C-N thin films by ion beam deposition. *J.Vac.Sci.Technol.A,* 13, 2110-22.

Brach Del Prever, E.M., Bistolfi, A., Bracco, P. & Costa, L. (2009) UHMWPE for arthroplasty: past or future? *J.Orthop.Traumatol.,* 10, 1-8.

Breme, J. & Biehl, V. (1998) *Metallic biomaterials*. In: Black ,J. & Hasting G. (eds.) *Handbook of Biomaterial Properties,* Chapman & Hall, London, UK, pp. 135-214.

Brett, P.M., Harle, J., Salih, V., Mihoc, R., Olsen, I., Jones, F.H. & Tonetti, M. (2004) Roughness response genes in osteoblasts. *Bone,* 35, 124-33.

Bruinink, A. & Wintermantel, E. (2001) Grooves affect primary bone marrow but not osteoblastic MC3T3-E1 cell cultures. *Biomaterials,* 22, 2465-73.

Bruinsma, G.M., van der Mei, H.C. & Busscher, H.J. (2001) Bacterial adhesion to surface hydrophilic and hydrophobic contact lenses. *Biomaterials,* 22, 3217-24.

Bucci-Sabattini, V., Cassinelli, C., Coelho, P.G., Minnici, A., Trani, A. & Ehrenfest, D.M.D. (2010) Effect of titanium implant surface nanoroughness and calcium phosphate low impregnation on bone cell activity in vitro. *Oral Surg.,Oral Med.,Oral Pathol.,Oral Radiol.,Endod.,* 109, 217-24.

Burke, M. & Goodman, S. (2008) *Failure mechanisms in joint replacement*. In: Revell, P.A. (ed.) *Joint replacement technology*, CRC Press, Boca Raton, FL, USA, pp. 264-285.

Cai, K., Frant, M., Bossert, J., Hildebrand, G., Liefeith, K. & Jandt, K.D. (2006) Surface functionalized titanium thin films: zeta-potential, protein adsorption and cell proliferation. *Colloids Surf.,B,* 50, 1-8.

Calzado-Martín, A., Saldaña, L., Korhonen, H., Soininen, A., Kinnari, T.J., Gómez-Barrena, E., Tiainen, V.-M., Lappalainen, R., Munuera, L., Konttinen, Y.T. & Vilaboa, N. (2010) Interactions of human bone cells with diamond-like carbon polymer hybrid coatings. *Acta Biomater.,* 6, 3325-38.

Carlson, R.P., Taffs, R., Davison, W.M. & Stewart, P.S. (2008) Anti-biofilm properties of chitosan-coated surfaces. *J.Biomater.Sci.Polym.Ed.,* 19, 1035-46.

Cerca, N., Pier, G.B., Vilanova, M., Oliveira, R. & Azeredo, J. (2005) Quantitative analysis of adhesion and biofilm formation on hydrophilic and hydrophobic surfaces of clinical isolates of *Staphylococcus epidermidis*. *Res.Microbiol.,* 156, 506-14.

Chai, F., Mathis, N., Blanchemain, N., Meunier, C. & Hildebrand, H.F. (2008) Osteoblast interaction with DLC-coated Si substrates. *Acta Biomater.,* 4, 1369-81.

Chapin, K.C. & Lauerdale, T. (2007) *Reagents, stains, and media: Bacteriology*. In: Murray, R., Baron, E.J. & Jorgensen, J. (eds.) *Manual of clinical microbiology 1, 9th ed.,* ASM Press, WA, USA, pp. 334-364.

Charest, J.L., Bryant, L.E., Garcia, A.J. & King, W.P. (2004) Hot embossing for micropatterned cell substrates. *Biomaterials,* 25, 4767-75.

Chen, J.S., Lau, S.P., Sun, Z., Chen, G.Y., Li, Y.J., Tay, B.K. & Chai, J.W. (2001) Metal-containing amorphous carbon films for hydrophobic application. *Thin Solid Films,* 398-399, 110-5.

Chen, W., Liu, Y., Courtney, H.S., Bettenga, M., Agrawal, C.M., Bumgardner, J.D. & Ong, J.L. (2006) In vitro anti-bacterial and biological properties of magnetron co-sputtered silver-containing hydroxyapatite coating. *Biomaterials,* 27, 5512-7.

Cheng, K., Weng, W., Wang, H. & Zhang, S. (2005) In vitro behavior of osteoblast-like cells on fluoridated hydroxyapatite coatings. *Biomaterials,* 26, 6288-95.

Chin, M.Y., Sandham, A., de Vries, J., van der Mei, H.C. & Busscher, H.J. (2007) Biofilm formation on surface characterized micro-implants for skeletal anchorage in orthodontics. *Biomaterials,* 28, 2032-40.

Choi, H.W., Dauskardt, R.H., Lee, S.-C., Lee, K.-R. & Oh, K.H. (2008) Characteristic of silver doped DLC films on surface properties and protein adsorption. *Diamond Relat.Mater.,* 17, 252-7.

Chua, P.-H., Neoh, K.-G., Kang, E.-T. & Wang, W. (2008) Surface functionalization of titanium with hyaluronic acid/chitosan polyelectrolyte multilayers and RGD for promoting osteoblast functions and inhibiting bacterial adhesion. *Biomaterials,* 29, 1412-21.

Clover, J., Dodds, R.A. & Gowen, M. (1992) Integrin subunit expression by human osteoblasts and osteoclasts in situ and in culture. *J.Cell.Sci.,* 103, 267-71.

Cochran, D.L., Nummikoski, P.V., Higginbottom, F.L., Hermann, J.S., Makins, S.R. & Buser, D. (1996) Evaluation of an endosseous titanium implant with a sandblasted and acid-etched surface in the canine mandible: radiographic results. *Clin.Oral Implants Res.,* 7, 240-52.

Cogan, N.G. (2006) Effects of persister formation on bacterial response to dosing. *J.Theor.Biol.,* 238, 694-703.

Cohn, R.M., Gonzalez Della Valle, A., Peterson, M. & Cornell, C.N. (2008) Similar wear in total hip arthroplasties with metallic or zirconia femoral heads. *HSS J.,* 4, 107-11.

Cooper, L.F., Masuda, T., Yliheikkila, P.K. & Felton, D.A. (1998) Generalizations regarding the process and phenomenon of osseointegration. Part II. In vitro studies. *Int.J.Oral Maxillofac.Implants,* 13, 163-74.

Costerton, J.W., Montanaro, L. & Arciola, C.R. (2005) Biofilm in implant infections: its production and regulation. *Int.J.Artif.Organs,* 28, 1062-8.

Costerton, W., Veeh, R., Shirtliff, M., Pasmore, M., Post, C. & Ehrlich, G. (2003) The application of biofilm science to the study and control of chronic bacterial infections. *J.Clin.Invest.,* 112, 1466-77.

Cui, F.Z. & Li, D.J. (2000) A review of investigations on biocompatibility of diamond-like carbon and carbon nitride films. *Surf.Coat.Technol.,* 131, 481-7.

Cui, F.Z., Qing, X.L., Li, D.J. & Zhao, J. (2005) Biomedical investigations on CNx coating. *Surf.Coat.Technol.,* 200, 1009-13.

Curtis, A. & Wilkinson, C. (1997) Topographical control of cells. *Biomaterials,* 18, 1573-83.

Dalby, M.J., McCloy, D., Robertson, M., Agheli, H., Sutherland, D., Affrossman, S. & Oreffo, R.O.C. (2006) Osteoprogenitor response to semi-ordered and random nanotopographies. *Biomaterials,* 27, 2980-7.

Darouiche, R. (2001) Device-associated infections: A macroproblem that starts with microadherence. *Clin.Infect.Dis.,* 33, 1567-72.

Das, K., Bose, S. & Bandyopadhyay, A. (2009) TiO2 nanotubes on Ti: Influence of nanoscale morphology on bone cell-materials interaction. *J.Biomed.Mater.Res.Part A*, 90, 225-37.

Dass, C.R., Ek, E.T.H. & Choong, P.F.M. (2007) Human xenograft osteosarcoma models with spontaneous metastasis in mice: clinical relevance and applicability for drug testing. *J.Cancer Res.Clin.Oncol.*, 133, 193-8.

Davies, J.E. (1996) *In vitro* modeling of the bone/implant interface. *Anat.Rec.*, 245, 426-45.

Davies, D.G. (2000) *Physiological events in biofilm formation*. In: Allison, D., Gilbert, P., Lappin-Scott, M. & Wilson, M (eds.) *Community structure and co-operation in biofilms*, Cambridge University Press, Cambridge, UK, pp. 37–51.

Dawei, W., Dejun, F., Huaixi, G., Zhihong, Z., Xianquan, M. & Xiangjun, F. (1997) Structure and characteristics of C_3N_4 thin films prepared by rf plasma-enhanced chemical vapor deposition. *Phys.Rev.B*, 56, 4949-54.

Dearnaley, G. & Arps, J.H. (2005) Biomedical applications of diamond-like carbon (DLC) coatings: A review. *Surf.Coat.Technol.*, 200, 2518-24.

Degasne, I., Basle, M.F., Demais, V., Hure, G., Lesourd, M., Grolleau, B., Mercier, L. & Chappard, D. (1999) Effects of roughness, fibronectin and vitronectin on attachment, spreading, and proliferation of human osteoblast-like cells (Saos-2) on titanium surfaces. *Calcif.Tissue Int.*, 64, 499-507.

den Braber, E.T., de Ruijter, J.E., Smits, H.T.J., Ginsel, L.A., von Recum, A.F. & Jansen, J.A. (1996) Quantitative analysis of cell proliferation and orientation on substrata with uniform parallel surface micro-grooves. *Biomaterials*, 17, 1093-9.

Derjaguin, B.V. & Landau, L. (1941) Theory of the stability of strongly charged lyophobic sols and of the adhesion on strongly charged particles in solution of electrolytes. *Acta Physicochim.*, 14, 633-62.

Disegi, J.A. & Eschbach, L. (2000) Stainless steel in bone surgery. *Injury*, 31, 2-6.

Donlan, R.M. (2001) Biofilm formation: a clinically relevant microbiological process. *Clin.Infect.Dis.*, 33, 1387-92.

Du, C., Su, X.W., Cui, F.Z. & Zhu, X.D. (1998) Morphological behaviour of osteoblasts on diamond-like carbon coating and amorphous C-N film in organ culture. *Biomaterials,* 19, 651-8.

Dunne, N.J., Hill, J., McAfee, P., Kirkpatrick, R., Patrick, S. & Tunney, M. (2008) Incorporation of large amounts of gentamicin sulphate into acrylic bone cement: effect on handling and mechanical properties, antibiotic release, and biofilm formation. *Proc.Inst.Mech.Eng.H.,* 222, 355-65.

Dunne, W.M.,Jr (2002) Bacterial adhesion: seen any good biofilms lately? *Clin.Microbiol.Rev.,* 15, 155-66.

El-Ghannam, A., Hamazawy, E. & Yehia, A. (2001) Effect of thermal treatment on bioactive glass microstructure, corrosion behavior, zeta potential, and protein adsorption. *J.Biomed.Mater.Res.,* 55, 387-95.

Eriksson, C., Nygren, H. & Ohlson, K. (2004) Implantation of hydrophilic and hydrophobic titanium discs in rat tibia: cellular reactions on the surfaces during the first 3 weeks in bone. *Biomaterials,* 25, 4759-66.

Evans, A.C., Franks, J. & Revell, P.J. (1991) Diamond-like carbon applied to bioengineering materials. *Surf. Coat. Technol*., 47, 662– 7.

FAR (2007) The 2007 implant yearbook on orthopeadic endoprosthesis. Finnish Arthoplasty Register. *Publications of the National Agency for Medicines* 1/2009.

Feighan, J.E., Goldberg, V.M., Davy, D., Parr, J.A. & Stevenson, S. (1995) The influence of surface-blasting on the incorporation of titanium-alloy implants in a rabbit intramedullary model. *J.Bone Joint Surg.Am.,* 77, 1380-95.

Feng, B., Weng, J., Yang, B.C., Qu, S.X. & Zhang, X.D. (2003) Characterization of surface oxide films on titanium and adhesion of osteoblast. *Biomaterials,* 24, 4663-70.

Fitzpatrick, F., Humphreys, H. & O'Gara, J.P. (2005) The genetics of staphylococcal biofilm formation--will a greater understanding of pathogenesis lead to better management of device-related infection? *Clin.Microbiol.Infect.,* 11, 967-73.

Flemming, R.G., Murphy, C.J., Abrams, G.A., Goodman, S.L. & Nealey, P.F. (1999) Effects of synthetic micro- and nano-structured surfaces on cell behavior. *Biomaterials,* 20, 573-88.

Fogh, J., Fogh, J.M. & Orfeo, T. (1977) One hundred and twenty-seven cultured human tumor cell lines producing tumors in nude mice. *J.Natl.Cancer Inst.,* 59, 221-6.

Franco, L.M., Pérez, J.A. & Riascos, H. (2008) Chemical analysis of CNx thin films produced by pulsed laser ablation. *Microelectron.J.,* 39, 1363-5.

Francz, G., Schroeder, A. & Hauert, R. (1999) Surface analysis and bioreactions of Ti- and V-containing a-C : H. *Surf.Interface Anal.,* 28, 3-7.

Friedmann, T.A., Sullivan, J.P., Knapp, J.A., Tallant, D.R., Follstaedt, D.M., Medlin, D.L. & Mirkarimi, P.B. (1997) Thick stress-free amorphous-tetrahedral carbon films with hardness near that of diamond. *Appl.Phys.Lett.,* 71, 3820-2.

Frisardi, V., Solfrizzi, V., Capurso, C., Kehoe, P.G., Imbimbo, B.P., Santamato, A., Dellegrazie, F., Seripa, D., Pilotto, A., Capurso, A. & Panza, F. (2010) Aluminum in the diet and alzheimer's disease: From current epidemiology to possible disease-modifying treatment. *J.Alzheimers Dis.,* 20, 17-30.

Frost, H.M. (1986) *Intermediary Organization of the Skeleton*, CRC Press, Boca Raton, FL, USA.

Fujimoto, F. & Ogata, K. (1993) Formation of Carbon Nitride Films by Means of Ion Assisted Dynamic Mixing (IVD) Method. *J.Appl.Phys.,* 32, 420-3.

Furno, F., Morley, K.S., Wong, B., Sharp, B.L., Arnold, P.L., Howdle, S.M., Bayston, R., Brown, P.D., Winship, P.D. & Reid, H.J. (2004) Silver nanoparticles and polymeric medical devices: a new approach to prevention of infection? *J.Antimicrob.Chemother.,* 54, 1019-24.

Fux, C.A., Costerton, J.W., Stewart, P.S. & Stoodley, P. (2005) Survival strategies of infectious biofilms. *Trends Microbiol.,* 13, 34-40.

Gallardo-Moreno, A.M., Pacha-Olivenza, M.A., Saldana, L., Perez-Giraldo, C., Bruque, J.M., Vilaboa, N. & Gonzalez-Martin, M.L. (2009) In vitro biocompatibility and bacterial adhesion of physico-chemically modified Ti6Al4V surface by means of UV irradiation. *Acta Biomater.,* 5, 181-92.

Geetha, M., Singh, A.K., Asokamani, R. & Gogia, A.K. (2009) Ti based biomaterials, the ultimate choice for orthopaedic implants – A review. *Prog.Mater.Sci.,* 54, 397-425.

Gessner, A., Waicz, R., Lieske, A., Paulke, B., Mäder, K. & Muller, R.H. (2000) Nanoparticles with decreasing surface hydrophobicities: influence on plasma protein adsorption. *Int.J.Pharm.,* 196, 245-9.

Giavaresi, G., Branda, F., Causa, F., Luciani, G., Fini, M., Nicoli Aldini, N., Rimondini, L., Ambrosio, L. & Giardino, R. (2004) Poly(2-hydroxyethyl methacrylate) biomimetic coating to improve osseointegration of a PMMA/HA/glass composite implant: in vivo mechanical and histomorphometric assessments. *Int.J.Artif.Organs,* 27, 674-80.

Gilbert, P., Das, J. & Foley, I. (1997) Biofilm susceptibility to antimicrobials. *Adv.Dent.Res.,* 11, 160-7.

Gonzalez, O., Smith, R.L. & Goodman, S.B. (1996) Effect of size, concentration, surface area, and volume of polymethylmethacrylate particles on human macrophages in vitro. *J.Biomed.Mater.Res.,* 30, 463-73.

Götz, F. (2004) Staphylococci in colonization and disease: prospective targets for drugs and vaccines. *Curr.Opin.Microbiol.,* 7, 477-87.

Gouzman, I., Brener, R. & Hoffman, A. (1995) Nitridation of diamond and graphite surfaces by low energy N+2 ion irradiation. *Surf.Sci.,* 331-333, 283-8.

Granchi, D., Cenni, E., Tigani, D., Trisolino, G., Baldini, N. & Giunti, A. (2008) Sensitivity to implant materials in patients with total knee arthroplasties. *Biomaterials,* 29, 1494-500.

Granchi, D., Cenni, E., Trisolino, G., Giunti, A. & Baldini, N. (2006) Sensitivity to implant materials in patients undergoing total hip replacement. *J.Biomed.Mater.Res.Part B,* 77, 257-64.

Grausova, L., Bacakova, L., Kromka, A., Potocky, S., Vanecek, M., Nesladek, M. & Lisa, V. (2009) Nanodiamond as promising material for bone tissue engineering. *J.Nanosci.Nanotechnol,* 9, 3524-34.

Green, A.M., Jansen, J.A., van der Waerden, J.P.C.M. & von Recum, A.F. (1994) Fibroblast response to microtextured silicone surfaces: Texture orientation into or out of the surface. *J.Biomed.Mater.Res.,* 28, 647-53.

Greenfield, E.M., Bi, Y., Ragab, A.A., Goldberg, V.M., Nalepka, J.L. & Seabold, J.M. (2005) Does endotoxin contribute to aseptic loosening of orthopedic implants? *J.Biomed.Mater.Res.Part B,* 72, 179-85.

Grill, A. (2003) Diamond-like carbon coatings as biocompatible materials—an overview. *Diamond Relat.Mater.,* 12, 166-70.

Gristina, A.G. (1987) Biomaterial-centered infection: microbial adhesion versus tissue integration. *Science,* 237, 1588-95.

Gronthos, S., Stewart, K., Graves, S.E., Hay, S. & Simmons, P.J. (1997) Integrin expression and function on human osteoblast-like cells. *J.Bone Miner.Res.,* 12, 1189-97.

Guglielmotti, M.B., Renou, S. & Cabrini, R.L. (1999) A histomorphometric study of tissue interface by laminar implant test in rats. *Int.J.Oral Maxillofac.Implants,* 14, 565-70.

Hacking, S.A., Bobyn, J.D., Toh, K.-K., Tanzer, M. & Krygier, J.J. (2000) Fibrous tissue ingrowth and attachment to porous tantalum. *J.Biomed.Mater.Res.,* 52, 631-8.

Hallab, N.J., Bundy, K.J., O'Connor, K., Moses, R.L. & Jacobs, J.J. (2001b) Evaluation of metallic and polymeric biomaterial surface energy and surface roughness characteristics for directed cell adhesion. *Tissue Eng.,* 7, 55-71.

Hallab, N., Merritt, K. & Jacobs, J.J. (2001a) Metal sensitivity in patients with orthopaedic implants. *J.Bone Joint Surg.Am.,* 83, 428-36.

Hamdan, M., Blanco, L., Khraisat, A. & Tresguerres, I.F. (2006) Influence of titanium surface charge on fibroblast adhesion. *Clin.Implant Dent.Relat.Res.,* 8, 32-8.

Hamilton, D.W. & Brunette, D.M. (2005) "Gap guidance" of fibroblasts and epithelial cells by discontinuous edged surfaces. *Exp.Cell Res.,* 309, 429-37.

Hamilton, D.W., Wong, K.S. & Brunette, D.M. (2006) Microfabricated discontinuous-edge surface topographies influence osteoblast adhesion, migration, cytoskeletal organization, and proliferation and enhance matrix and mineral deposition in vitro. *Calcif.Tissue Int.,* 78, 314-25.

Hao, L. & Lawrence, J. (2007) Wettability modification and the subsequent manipulation of protein adsorption on a Ti6Al4V

alloy by means of CO_2 laser surface treatment. *J.Mater.Sci.Mater.Med.,* 18, 807-17.

Harle, J., Salih, V., Olsen, I., Brett, P., Jones, F. & Tonetti, M. (2004) Gene expression profiling of bone cells on smooth and rough titanium surfaces. *J.Mater.Sci.Mater.Med.,* 15, 1255-8.

Harris, L.G., Meredith, D.O., Eschbach, L. & Richards, R.G. (2007) *Staphylococcus aureus* adhesion to standard micro-rough and electropolished implant materials. *J.Mater.Sci.Mater.Med.,* 18, 1151-6.

Harrison, R.G. (1912) The cultivation of tissues in extraneous media as a method of morpho-genetic study. *Anat.Rec.,* 6, 181-93.

Hasebe, T., Shimada, A., Suzuki, T., Matsuoka, Y., Saito, T., Yohena, S., Kamijo, A., Shiraga, N., Higuchi, M., Kimura, K., Yoshimura, H. & Kuribayashi, S. (2006) Fluorinated diamond-like carbon as antithrombogenic coating for blood-contacting devices. *J.Biomed.Mater.Res.Part A,* 76, 86-94.

Hasirci, V. & Hasirci, N. (2005) *Control of polymeric material surfaces*. In: Vadgama, P. (ed.) *Surfaces and interfaces for biomaterials*, Woodhead Publishing Limited, Cambridge, UK, pp. 29-59.

Hauert, R. (2003) A review of modified DLC coatings for biological applications. *Diamond Relat.Mater.,* 12, 583-9.

Hauert, R., Müller, U., Francz, G., Birchler, F., Schroeder, A., Mayer, J. & Wintermantel, E. (1997) Surface analysis and bioreactions of F and Si containing a-C:H. *Thin Solid Films,* 308-309, 191-4.

Heilmann, C., Hussain, M., Peters, G. & Götz, F. (1997) Evidence for autolysin-mediated primary attachment of Staphylococcus epidermidis to a polystyrene surface. *Mol.Microbiol.,* 24, 1013-24.

Hersel, U., Dahmen, C. & Kessler, H. (2003) RGD modified polymers: biomaterials for stimulated cell adhesion and beyond. *Biomaterials,* 24, 4385-415.

Hughes, D.E., Salter, D.M., Dedhar, S. & Simpson, R. (1993) Integrin expression in human bone. *J.Bone Miner.Res.,* 8, 527-33.

Hynes, R.O. (1992) Integrins: versatility, modulation, and signaling in cell adhesion. *Cell,* 69, 11-25.

Ignatius, A., Peraus, M., Schorlemmer, S., Augat, P., Burger, W., Leyen, S. & Claes, L. (2005) Osseointegration of alumina with a bioactive

coating under load-bearing and unloaded conditions. *Biomaterials,* 26, 2325-32.

Ishihara, M., Kosaka, T., Nakamura, T., Tsugawa, K., Hasegawa, M., Kokai, F. & Koga, Y. (2006) Antibacterial activity of fluorine incorporated DLC films. *Diamond Relat.Mater.,* 15, 1011-4.

Ismail, F.S., Rohanizadeh, R., Atwa, S., Mason, R.S., Ruys, A.J., Martin, P.J. & Bendavid, A. (2007) The influence of surface chemistry and topography on the contact guidance of MG63 osteoblast cells. *J.Mater.Sci.Mater.Med.,* 18, 705-14.

Itoh, S., Nakamura, S., Kobayashi, T., Shinomiya, K., Yamashita, K. & Itoh, S. (2006) Effect of electrical polarization of hydroxyapatite ceramics on new bone formation. *Calcif.Tissue Int.,* 78, 133-42.

Iwaya, Y., Machigashira, M., Kanbara, K., Miyamoto, M., Noguchi, K., Izumi, Y. & Ban, S. (2008) Surface properties and biocompatibility of acid-etched titanium. *Dent.Mater.J.,* 27, 415-21.

Jäger, M., Zilkens, C., Zanger, K. & Krauspe, R. (2007) Significance of nano- and microtopography for cell-surface interactions in orthopaedic implants. *J.Biomed.Biotechnol.,* 2007, 10.1155/2007/69036.

Jing, F.J., Huang, N., Wang, L., Fu, R.K.Y., Mei, Y.F., Leng, Y.X., Chen, J.Y., Liu, X.Y. & Chu, P.K. (2007) Behavior of human umbilical vein endothelial cells on micro-patterned amorphous hydrogenated carbon films produced by plasma immersion ion implantation & deposition and plasma etching. *Diamond Relat.Mater.,* 16, 550-7.

Jinno, T., Goldberg, V.M., Davy, D. & Stevenson, S. (1998) Osseointegration of surface-blasted implants made of titanium alloy and cobalt-chromium alloy in a rabbit intramedullary model. *J.Biomed.Mater.Res.,* 42, 20-9.

Jiranek, W.A., Hanssen, A.D. & Greenwald, A.S. (2006) Antibiotic-loaded bone cement for infection prophylaxis in total joint replacement. *J.Bone Joint Surg.Am.,* 88, 2487-500.

Jones, D.S., Garvin, C.P., Dowling, D., Donnelly, K. & Gorman, S.P. (2006) Examination of surface properties and *in vitro* biological performance of amorphous diamond-like carbon-coated polyurethane. *J.Biomed.Mater.Res.Part B,* 78, 230-6.

Kaivosoja, E., Myllymaa, S., Kouri, V.-P., Myllymaa, K., Lappalainen, R. & Konttinen, Y.T. (2010) Enhancement of silicon using micro-patterned surfaces of thin films. *Eur.Cell.Mater.,* 19, 147-57.

Kantawong, F., Burgess, K.E.V., Jayawardena, K., Hart, A., Burchmore, R.J., Gadegaard, N., Oreffo, R.O.C. & Dalby, M.J. (2009) Whole proteome analysis of osteoprogenitor differentiation induced by disordered nanotopography and mediated by ERK signalling. *Biomaterials,* 30, 4723-31.

Kaplan, F.S., Hayes, W.C., Keaveny, T.M., Boskey, A., Einhorn, T.A. & Iannotti, J.P. (1994) *Biomaterials*. In: Simon, S.P. (ed.) *Orthopedic basic science*, American Academy of Orthopedic Surgeons, Columbus, OH, USA, pp. 460-78.

Kasemo, B. (1998) Biological surface science. *Curr.Opin.Solid State Mater.Sci.,* 3, 451-9.

Katsikogianni, M. & Missirlis, Y.F. (2004) Concise review of mechanisms of bacterial adhesion to biomaterials and of techniques used in estimating bacteria-material interactions. *Eur.Cell.Mater.,* 8, 37-57.

Katsikogianni, M., Spiliopoulou, I., Dowling, D.P. & Missirlis, Y.F. (2006) Adhesion of slime producing Staphylococcus epidermidis strains to PVC and diamond-like carbon/silver/fluorinated coatings. *J.Mater.Sci.Mater.Med.,* 17, 679-89.

Katti, K.S., Katti, D.R. & Dash, R. (2008b) Synthesis and characterization of a novel chitosan/ montmorillonite/ hydroxyapatite nanocomposite for bone tissue engineering. *Biomed.Mater.,* 3, 10.1088/1748-6041/3/3/034122.

Katti, K.S., Verma, T. & Katti, D.R. (2008a) *Materials for joint replacement*. In: Revell, P.A. (ed.) *Joint replacement technology*, CRC Press, Boca Raton, FL, USA, pp. 81-104.

Kelly, S., Regan, E.M., Uney, J.B., Dick, A.D., McGeehan, J.P., The Bristol Biochip Group, Mayer, E.J. & Claeyssens, F. (2008) Patterned growth of neuronal cells on modified diamond-like carbon substrates. *Biomaterials,* 29, 2573-80.

Kennedy, S.B., Washburn, N.R., Simon, C.G.Jr. & Amis, E.J. (2006) Combinatorial screen of the effect of surface energy on fibronectin-mediated osteoblast adhesion, spreading and proliferation. *Biomaterials,* 27, 3817-24.

Keurentjes, J.C., Kuipers, R.M., Wever, D.J. & Schreurs, B.W. (2008) High incidence of squeaking in THAs with alumina ceramic-on-ceramic bearings. *Clin.Orthop.Relat.Res.,* 466, 1438-43.

Khang, D., Lu, J., Yao, C., Haberstroh, K.M. & Webster, T.J. (2008) The role of nanometer and sub-micron surface features on vascular and bone cell adhesion on titanium. *Biomaterials,* 29, 970-83.

Khorasani, M.T. & Mirzadeh, H. (2007) Effect of oxygen plasma treatment on surface charge and wettability of PVC blood bag—In vitro assay. *Radiat.Phys.Chem.,* 76, 1011-6.

Khorasani, M.T., Moemenbellah, S., Mirzadeh, H. & Sadatnia, B. (2006) Effect of surface charge and hydrophobicity of polyurethanes and silicone rubbers on L929 cells response. *Colloids Surf.,B,* 51, 112-9.

Kieswetter, K., Schwartz, Z., Hummert, T.W., Cochran, D.L., Simpson, J., Dean, D.D. & Boyan, B.D. (1996) Surface roughness modulates the local production of growth factors and cytokines by osteoblast-like MG-63 cells. *J.Biomed.Mater.Res.,* 32, 55-63.

Kim, H.J., Kim, S.H., Kim, M.S., Lee, E.J., Oh, H.G., Oh, W.M., Park, S.W., Kim, W.J., Lee, G.J., Choi, N.G., Koh, J.T., Dinh, D.B., Hardin, R.R., Johnson, K., Sylvia, V.L., Schmitz, J.P. & Dean, D.D. (2005) Varying Ti-6Al-4V surface roughness induces different early morphologic and molecular responses in MG63 osteoblast-like cells. *J.Biomed.Mater.Res.Part A,* 74, 366-73.

Kim, Y.H., Lee, D.K., Cha, H.G., Kim, C.W., Kang, Y.C. & Kang, Y.S. (2006) Preparation and characterization of the antibacterial Cu nanoparticle formed on the surface of SiO_2 nanoparticles. *J.Phys.Chem.B,* 110, 24923-8.

Kinnari, T.J., Soininen, A., Esteban, J., Zamora, N., Alakoski, E., Kouri, V.P., Lappalainen, R., Konttinen, Y.T., Gomez-Barrena, E. & Tiainen, V.M. (2007) Adhesion of staphylococcal and Caco-2 cells on diamond-like carbon polymer hybrid coating. *J.Biomed.Mater.Res.Part A,* 86, 760-8.

Kluess, D., Mittelmeier, W. & Bader, R. (2008) *Ceramics for joint replacement*. In: Revell P.A. (ed.) *Joint replacement technology*, CRC Press, Boca Raton, FL, USA, pp. 163-75.

Kodjikian, L., Burillon, C., Roques, C., Pellon, G., Freney, J. & Renaud, F.N.R. (2003) Bacterial adherence of *Staphylococcus epidermidis* to intraocular lenses: a bioluminescence and scanning electron microscopy study. *Invest.Ophthalmol.Vis.Sci.,* 44, 4388-94.

Kohal, R.J., Wolkewitz, M., Hinze, M., Han, J.-S., Bächle, M. & Butz, F. (2009) Biomechanical and histological behavior of zirconia implants: an experiment in the rat. *Clin.Oral Implants Res.,* 20, 333-9.

Konttinen, Y.T., Milośev, I., Trebśe, R., Rantanen ,P., Linden, R., Tiainen, V.-M. & Virtanen, S. (2008) *Metals for joint replacement*. In: Revell P.A. (ed.) *Joint replacement technology*, CRC Press, Boca Raton, FL, USA, pp. 115-62.

Koponen, H.-K., Saarikoski, I., Korhonen, T., Pääkkö, M., Kuisma, R., Pakkanen, T.T., Suvanto, M. & Pakkanen, T.A. (2007) Modification of cycloolefin copolymer and poly(vinyl chloride) surfaces by superimposition of nano- and microstructures. *Appl.Surf.Sci.,* 253, 5208-13.

Krajewski, A., Malavolti, R. & Piancastelli, A. (1996) Albumin adhesion on some biological and non-biological glasses and connection with their Z-potentials. *Biomaterials,* 17, 53-60.

Krajewski, A., Piancastelli, A. & Malavolti, R. (1998) Albumin adhesion on ceramics and correlation with their Z-potential. *Biomaterials,* 19, 637-41.

Ku, C.-H., Pioletti, D.P., Browne, M. & Gregson, P.J. (2002) Effect of different Ti-6Al-4V surface treatments on osteoblasts behaviour. *Biomaterials,* 23, 1447-54.

Kunzler, T.P., Drobek, T., Schuler, M. & Spencer, N.D. (2007) Systematic study of osteoblast and fibroblast response to roughness by means of surface-morphology gradients. *Biomaterials,* 28, 2175-82.

Kurtz, S., Ong, K., Lau, E., Mowat, F. & Halpern, M. (2007a) Projections of primary and revision hip and knee arthroplasty in the United States from 2005 to 2030. *J.Bone Joint Surg.Am.,* 89, 780-5.

Kurtz, S.M., Ong, K.L., Schmier, J., Mowat, F., Saleh, K., Dybvik, E., Kärrholm, J., Garellick, G., Havelin, L.I., Furnes, O., Malchau, H. & Lau, E. (2007b) Future clinical and economic impact of revision total hip and knee arthroplasty. *J.Bone Joint Surg.Am.,* 89, 144-51.

Kwok, S.C.H., Yang, P., Wang, J., Liu, X. & Chu, P.K. (2004) Hemocompatibility of nitrogen-doped, hydrogen-free diamond-like carbon prepared by nitrogen plasma immersion ion implantation–deposition.*J.Biomed.Mater.Res.Part A*, 70, 107–14.

Kwok, S.C.H., Zhang, W., Wan, G.J., McKenzie, D.R., Bilek, M.M.M. & Chu, P.K. (2007) Hemocompatibility and anti-bacterial properties of silver doped diamond-like carbon prepared by pulsed filtered cathodic vacuum arc deposition. *Diamond Relat.Mater.,* 16, 1353-60.

Lampin, M., Warocquier-Clerout, R., Legris, C., Degrange, M. & Sigot-Luizard, M.F. (1997) Correlation between substratum roughness and wettability, cell adhesion, and cell migration. *J.Biomed.Mater.Res.,* 36, 99-108.

Landsberg, J.P., McDonald, B. & Watt, F. (1992) Absence of aluminium in neuritic plaque cores in Alzheimer's disease. *Nature,* 360, 65-8.

Lappalainen, R., Heinonen, H., Anttila, A. & Santavirta, S. (1998) Some relevant issues related to the use of amorphous diamond coatings for medical applications. *Diamond Relat.Mater.,* 7, 482-5.

Lappalainen, R., Selenius, M., Anttila, A., Konttinen, Y.T. & Santavirta, S.S. (2003) Reduction of wear in total hip replacement prostheses by amorphous diamond coatings. *J.Biomed.Mater.Res.Part B,* 66, 410-3.

Laube, N., Kleinen, L., Bradenahl, J. & Meissner, A. (2007) Diamond-Like Carbon Coatings on Ureteral Stents—A New Strategy for Decreasing the Formation of Crystalline Bacterial Biofilms? *The J.Urol.,* 177, 1923-7.

LaVan, D.A., Padera, R.F., Friedmann, T.A., Sullivan, J.P., Langer, R. & Kohane, D.S. (2005) In vivo evaluation of tetrahedral amorphous carbon. *Biomaterials,* 26, 465-73.

LeBaron, R.G. & Athanasiou, K.A. (2000) Extracellular matrix cell adhesion peptides: functional applications in orthopedic materials. *Tissue Eng.,* 6, 85-103.

Lee, J.H., Khang, G., Lee, J.W. & Lee, H.B. (1998) Interaction of different types of cells on polymer surfaces with wettability gradient. *J.Colloid Interface Sci.,* 205, 323-30.

Lee, J.H., Lee, J.W., Khang, G. & Lee, H.B. (1997) Interaction of cells on chargeable functional group gradient surfaces. *Biomaterials,* 18, 351-8.

Lewis, K. (2005) Persister cells and the riddle of biofilm survival. *Biochemistry (Mosc.),* 70, 267-74.

Lewis, P.M., Moore, C.A., Olsen, M., Schemitsch, E.H. & Waddell, J.P. (2008) Comparison of mid-term clinical outcomes after primary total hip arthroplasty with Oxinium vs cobalt chrome femoral heads. *Orthopedics,* 31, 37183.

Li, D. & Niu, L. (2003) Influence of N atomic percentages on cell attachment for CN_x coatings. *Bull.Mater.Sci.,* 26, 371-5.

Li, D.J., Zhang, S.J. & Niu, L.F. (2001) Influence of NH^{n+} beam bombarding energy on structural characterization and cell attachment of CN_x coating. *Appl.Surf.Sci.,* 180, 270-9.

Liao, H., Andersson, A.-S., Sutherland, D., Petronis, S., Kasemo, B. & Thomsen, P. (2003) Response of rat osteoblast-like cells to microstructured model surfaces in vitro. *Biomaterials,* 24, 649-54.

Lichter, J.A., Thompson, M.T., Delgadillo, M., Nishikawa, T., Rubner, M.F. & Van Vliet, K.J. (2008) Substrata mechanical stiffness can regulate adhesion of viable bacteria. *Biomacromolecules,* 9, 1571-8.

Lim, J.Y., Shaughnessy, M.C., Zhou, Z., Noh, H., Vogler, E.A. & Donahue, H.J. (2008) Surface energy effects on osteoblast spatial growth and mineralization. *Biomaterials,* 29, 1776-84.

Lincks, J., Boyan, B.D., Blanchard, C.R., Lohmann, C.H., Liu, Y., Cochran, D.L., Dean, D.D. & Schwartz, Z. (1998) Response of MG63 osteoblast-like cells to titanium and titanium alloy is dependent on surface roughness and composition. *Biomaterials,* 19, 2219-32.

Linder, S., Pinkowski, W. & Aepfelbacher, M. (2002) Adhesion, cytoskeletal architecture and activation status of primary human macrophages on a diamond-like carbon coated surface. *Biomaterials,* 23, 767-73.

Litzler, P.-Y., Benard, L., Barbier-Frebourg, N., Vilain, S., Jouenne, T., Beucher, E., Bunel, C., Lemeland, J. & Bessou, J. (2007) Biofilm formation on pyrolytic carbon heart valves: Influence of surface free energy, roughness, and bacterial species. *J.Thorac.Cardiovasc.Surg.,* 134, 1025-32.

Liu, A.Y. & Cohen, M.L. (1989) Prediction of New Low Compressibility Solids. *Science,* 245, 841-2.

Liu, C., Zhao, Q., Liu, Y., Wang, S. & Abel, E.W. (2008) Reduction of bacterial adhesion on modified DLC coatings. *Colloids Surf.,B,* 15, 182-7.

Long, M. & Rack, H.J. (1998) Titanium alloys in total joint replacement—a materials science perspective. *Biomaterials,* 19, 1621-39.

Lopez, S., Dunlop, H.M., Benmalek, M., Tourillon, G., Wong, M.-S. & Sproul, W.D. (1997) XPS, XANES and ToF-SIMS characterization of reactively magnetron-sputtered carbon nitride films. *Surf. Interface Anal.,* 25, 315-23.

Lu, X. & Leng, Y. (2003) Quantitative analysis of osteoblast behavior on microgrooved hydroxyapatite and titanium substrata. *J.Biomed.Mater.Res.Part A,* 66, 677-87.

Lyklema, J. (1995) *Fundamentals of interface and colloid science, vol. II, Solid–liquid interface*, Academic Press, London, UK.

MacKintosh, E.E., Patel, J.D., Marchant, R.E. & Anderson, J.M. (2006) Effects of biomaterial surface chemistry on the adhesion and biofilm formation of *Staphylococcus epidermidis in vitro*. *J.Biomed.Mater.Res.Part A,* 78, 836-42.

Madou, M.J. (2002) *Fundamentals of microfabrication: The Science of Miniaturization, 2nd ed.,* CRC Press, Boca Raton, FL, USA.

Majewski, P.J. & Allidi, G. (2006) Synthesis of hydroxyapatite on titanium coated with organic self-assembled monolayers. *Mater.Sci.Eng.,A,* 420, 13-20.

Marra, A. (2004) Can virulence factors be viable antibacterial targets? *Expert Rev.Anti-Infect.Ther.,* 2, 61-72.

Marshall, K. C., Stout, R. & Mitchell R. (1971) Mechanism of the initial events in the sorption of marine bacteria to surfaces. *J. Gen. Microbiol.,* 68, 337-48.

Marti, A. (2000) Cobalt-base alloys used in bone surgery. *Injury,* 31, 18-21.

Martin, R.B., Burr, D.B. & Sharkey N.A. (1998) *Skeletal tissue mechanics*, Springer-Verlag, NY, USA.

Martínez, E., Engel, E., Planell, J.A. & Samitier, J. (2009) Effects of artificial micro- and nano-structured surfaces on cell behaviour. *Ann.Anat.,* 191, 126-35.

Mata, A., Boehm, C., Fleischman, A.J., Muschler, G. & Roy, S. (2002) Growth of connective tissue progenitor cells on microtextured polydimethylsiloxane surfaces. *J.Biomed.Mater.Res.,* 62, 499-506.

Mata, A., Kim, E.J., Boehm, C.A., Fleischman, A.J., Muschler, G.F. & Roy, S. (2009) A three-dimensional scaffold with precise micro-architecture and surface micro-textures. *Biomaterials,* 30, 4610-7.

Mata, A., Su, X., Fleischman, A.J., Roy, S., Banks, B.A., Miller, S.K. & Midura, R.J. (2003) Osteoblast attachment to a textured surface in the absence of exogenous adhesion proteins. *IEEE Trans. Nanobioscience,* 2, 287-94.

McBeath, R., Pirone, D.M., Nelson, C.M., Bhadriraju, K. & Chen, C.S. (2004) Cell shape, cytoskeletal tension, and RhoA regulate stem cell lineage commitment. *Dev.Cell,* 6, 483-95.

McCann, M.T., Gilmore, B.F. & Gorman, S.P. (2008) Staphylococcus epidermidis device-related infections: pathogenesis and clinical management. *J.Pharm.Pharmacol.,* 60, 1551-71.

McCullen, S.D., McQuilling, J.P., Grossfeld, R.M., Lubischer, J.L., Clarke, L.I. & Loboa, E.G. (2010) Application of low frequency AC electric fields via interdigitated electrodes: effects on cellular viability, cytoplasmic calcium, and osteogenic differentiation of human adipose-derived stem cells. *Tissue Eng.Part C,* in press.

McKenzie, D.R. (1996) Tetrahedral bonding in amorphous carbon. *Rep. Prog .Phys.,* 59, 1611-64.

Mehmood, S., Jinnah, R.H. & Pandit, H. (2008) Review on ceramic-on-ceramic total hip arthroplasty. *J.Surg.Orthop.Adv.,* 17, 45-50.

Mendonca, G., Mendonca, D.B., Simoes, L.G., Araujo, A.L., Leite, E.R., Duarte, W.R., Cooper, L.F. & Aragao, F.J. (2009a) Nanostructured alumina-coated implant surface: effect on osteoblast-related gene expression and bone-to-implant contact in vivo. *Int.J.Oral Maxillofac.Implants,* 24, 205-15.

Mendonça, G., Mendonça, D.B.S., Aragão, F.J.L. & Cooper, L.F. (2010) The combination of micron and nanotopography by H_2SO_4/H_2O_2 treatment and its effects on osteoblast-specific gene expression of hMSCs. *J.Biomed.Mat.Res.Part A,* 94, 169-79.

Mendonça, G., Mendonça, D.B.S., Simões, L.G.P., Araújo, A.L., Leite, E.R., Duarte, W.R., Aragão, F.J.L. & Cooper, L.F. (2009b) The effects of implant surface nanoscale features on osteoblast-specific gene expression. *Biomaterials,* 30, 4053-62.

Michiardi, A., Aparicio, C., Ratner, B.D., Planell, J.A. & Gil, J. (2007) The influence of surface energy on competitive protein adsorption on oxidized NiTi surfaces. *Biomaterials,* 28, 586-94.

Millar, M. (2005) *Microbial biofilms and clinical implants*. In: Vadgama, P. (ed.) *Surfaces and interfaces for biomaterials*, Woodhead Publishing Limited, Cambridge, UK, pp. 619-636.

Miikkulainen, V., Rasilainen, T., Puukilainen, E., Suvanto, M. & Pakkanen, T.A. (2008) Atomic layer deposition as pore diameter adjustment tool for nanoporous aluminum oxide injection molding masks. *Langmuir,* 24, 4473-7.

Misra, R.D.K., Thein-Han, W.W., Pesacreta, T.C., Hasenstein, K.H., Somani, M.C. & Karjalainen, L.P. (2009) Cellular response of preosteoblasts to nanograined/ultrafine-grained structures. *Acta Biomatater.,* 5, 1455-67.

Mitura, E., Mitura, S., Niedzielski, P., Has, Z., Wolowiec, R., Jakubowski, A., Szmidt, J., Sokolowska, A., Louda, P., Marciniak, J. & Koczy, B. (1994) Diamond-like carbon coatings for biomedical applications. *Diamond Relat.Mater.,* 3, 896-8.

Mitura, K., Niedzielski, P., Bartosz, G., Moll, J., Walkowiak, B., Pawlowska, Z., Louda, P., Kiec-Swierczynska, M. & Mitura, S. (2006) Interactions between carbon coatings and tissue. *Surf.Coat. Technol.,* 201, 2117-23.

Mohanty, M., Anilkumar, T.V., Mohanan, P.V., Muraleedharan, C.V., Bhuvaneshwar, G.S., Derangere, F., Sampeur, Y. & Suryanarayanan, R. (2002) Long term tissue response to titanium coated with diamond like carbon. *Biomol.Eng.,* 19, 125-8.

Montanaro, L., Campoccia, D. & Arciola, C.R. (2008) Nanostructured materials for inhibition of bacterial adhesion in orthopedic implants: a minireview. *Int.J.Artif.Organs,* 31, 771-6.

Morrison, M.L., Buchanan, R.A., Liaw, P.K., Berry, C.J., Brigmon, R.L., Riester, L., Abernathy, H., Jin, C. & Narayan, R.J. (2006) Electrochemical and antimicrobial properties of diamondlike carbon-metal composite films. *Diamond Relat.Mater.,* 15, 138-46.

Muhonen, V., Heikkinen, R., Danilov, A., Jämsä, T. & Tuukkanen J. (2007) The effect of oxide thickness on osteoblast attachment and survival on NiTi alloy. *J.Mater.Sci.Mater.Med.,* 18, 959-67.

Mwenifumbo, S., Li, M., Chen, J., Beye, A. & Soboyejo, W. (2007) Cell/surface interactions on laser micro-textured titanium-coated silicon surfaces. *J.Mater.Sci.Mater.Med.*, 18, 9-23.

Myllymaa, S., Kaivosoja, E., Myllymaa, K., Sillat, T., Korhonen, H., Lappalainen, R. & Konttinen, Y.T. (2010) Adhesion, spreading and osteogenic differentiation of mesenchymal stem cells cultured on micropatterned amorphous diamond, titanium, tantalum and chromium coatings on silicon. *J.Mater.Sci.Mater.Med.*, 21, 329-41.

Myllymaa, S., Myllymaa, K. & Lappalainen, R. (2009) *Flexible implantable thin film electrodes*. In: Naik, G.R. (ed.) *Recent Advances in Biomedical Enginering*, Intech, Vukovar, Groatia, pp. 165-89.

Nakamura, S., Kobayashi, T., Nakamura, M. & Yamashita, K. (2009) Enhanced in vivo responses of osteoblasts in electrostatically activated zones by hydroxyapatite electrets. *J.Mater.Sci.Mater.Med.*, 20, 99-103.

Narayan, R.J. (2007) *Diamond-Like Carbon - Medical and Mechanical applications*. In: Eason, R. (ed.) *Pulsed laser deposition of thin films – Applications-led growth of functional materials*, John Wiley & Sons Inc., Hoboken, NJ, USA, pp. 333-62.

Nebe, J.G., Luethen, F., Lange, R., Beck, U. (2007) Interface interactions of osteoblasts with structured titanium and the correlation between physicochemical characteristics and cell biological parameters. *Macromol.Biosci.*, 7, 567-78.

Neumann, A.W. & Godd, R.J. (1979) *Techniques of measuring contact angles*. In: Good, R.J. & Stromberg, R.R. (eds.) *Surface and colloid sciene - Experimental methods*, Plenum Publishing, NY, USA, pp. 31-61.

Neut, D., van der Mei, H.C., Bulstra, S.K. & Busscher, H.J. (2007) The role of small-colony variants in failure to diagnose and treat biofilm infections in orthopedics. *Acta Orthop.*, 78, 299-308.

Oga, M., Arizono, T. & Sugioka, Y. (1992) Inhibition of bacterial adhesion by tobramycin-impregnated PMMA bone cement. *Acta Orthop.Scand.*, 63, 301-4.

O'Gara, J.P. (2007) *ica* and beyond: biofilm mechanisms and regulation in *Staphylococcus epidermidis* and *Staphylococcus aureus*. *FEMS Microbiol.Lett.*, 270, 179-88.

O'Gara, J.P. & Humphreys, H. (2001) *Staphylococcus epidermidis* biofilms: importance and implications. *J.Med.Microbiol.,* 50, 582-7.

Ohgaki, M., Kizuki, T., Katsura, M. & Yamashita, K. (2001) Manipulation of selective cell adhesion and growth by surface charges of electrically polarized hydroxyapatite. *J.Biomed.Mater.Res.,* 57, 366-73.

Okada, S., Ito, H., Nagai, A., Komotori, J. & Imai, H. (2010) Adhesion of osteoblast-like cells on nanostructured hydroxyapatite. *Acta Biomater.,* 6, 591-7.

Okazaki, Y., Rao, S., Ito, Y. & Tateishi, T. (1998) Corrosion resistance, mechanical properties, corrosion fatigue strength and cytocompatibility of new Ti alloys without Al and V. *Biomaterials,* 19, 1197-215.

Okpalugo, T.I.T., Murphy, H., Ogwu, A.A., Abbas, G., Ray, S.C., Maguire, P.D., McLaughlin, J. & McCullough, R.W. (2006) Human microvascular endothelial cellular interaction with atomic N-doped DLC compared with Si-doped DLC thin films. *J.Biomed.Mater.Part B,* 78, 222-9.

Okumura, A., Goto, M., Goto, T., Yoshinari, M., Masuko, S., Katsuki, T. & Tanaka, T. (2001) Substrate affects the initial attachment and subsequent behavior of human osteoblastic cells (Saos-2). *Biomaterials,* 22, 2263-71.

Olivares, R., Rodil, S.E. & Arzate, H. (2004) In vitro studies of the biomineralization in amorphous carbon films. *Surf.Coat.Technol.,* 177-8, 758-64.

Orsini, G., Assenza, B., Scarano, A., Piattelli, M. & Piattelli, A. (2000) Surface analysis of machined versus sandblasted and acid-etched titanium implants. *Int.J.Oral Maxillofac.Implants,* 15, 779-84.

Ortner, D.J & Putschar, W.G.J. (1981) *Identification of Pathological Conditions in Human Skeletal Remains. Smithsonian Contributions to Anthropology*, *No 28*, Smithsonian Institution Press, WA, USA.

Osathanon, T., Bespinyowong, K., Arksornnukit, M., Takahashi, H. & Pavasant, P. (2006) Ti-6Al-7Nb promotes cell spreading and fibronectin and osteopontin synthesis in osteoblast-like cells. *J.Mater.Sci.Mater.Med.,* 17, 619-25.

Otto, M. (2004) Quorum-sensing control in Staphylococci -- a target for antimicrobial drug therapy? *FEMS Microbiol.Lett.,* 241, 135-41.

Otto, M. (2008) Staphylococcal biofilms. *Curr.Top.Microbiol.Immunol.,* 322, 207-28.

Owens, D.K. & Wendt, R.C. (1969) Estimation of the surface free energy of polymers. *J.Appl.Polym.Sci.,* 13, 1741-7.

Oya, K., Tanaka, Y., Moriyama, Y., Yoshioka, Y., Kimura, T., Tsutsumi, Y., Doi, H., Nomura, N., Noda, K., Kishida, A. & Hanawa, T. (2010) Differences in the bone differentiation properties of MC3T3-E1 cells on polished bulk and sputter-deposited titanium specimens. *J.Biomed.Mater.Res.Part A,* 94, 611-8.

Ozawa, S. & Kasugai, S. (1996) Evaluation of implant materials (hydroxyapatite, glass-ceramics, titanium) in rat bone marrow stromal cell culture. *Biomaterials,* 17, 23-9.

Palmer, J., Flint, S. & Brooks, J. (2007) Bacterial cell attachment, the beginning of a biofilm. *J.Ind.Microbiol.Biotechnol.,* 34, 577-88.

Pareta, R.A., Reising, A.B., Miller, T., Storey, D. & Webster, T.J. (2009) An understanding of enhanced osteoblast adhesion on various nanostructured polymeric and metallic materials prepared by ionic plasma deposition. *J.Biomed.Mater.Res.Part A*, 92, 1190-210.

Parker, K.K., Brock, A.L., Brangwynne, C., Mannix, R.J., Wang, N., Ostuni, E., Geisse, N.A., Adams, J.C., Whitesides, G.M. & Ingber, D.E. (2002) Directional control of lamellipodia extension by constraining cell shape and orienting cell tractional forces. *FASEB J.,* 16, 1195-204.

Patel, J.D., Ebert, M., Ward, R. & Anderson, J.M. (2007) *S. epidermidis* biofilm formation: effects of biomaterial surface chemistry and serum proteins. *J.Biomed.Mater.Res.Part A,* 80, 742-51.

Pearce, A.I., Richards, R.G., Milz, S., Schneider, E. & Pearce, S.G. (2007) Animal models for implant biomaterial research in bone: a review. *Eur.Cell.Mater.,* 13, 1-10.

Pereni, C.I., Zhao, Q., Liu, Y. & Abel, E. (2006) Surface free energy effect on bacterial retention. *Colloids Surf.,B,* 48, 143-7.

Petrie, T.A., Raynor, J.E., Reyes, C.D., Burns, K.L., Collard, D.M. & Garcia, A.J. (2008) The effect of integrin-specific bioactive coatings on tissue healing and implant osseointegration. *Biomaterials,* 29, 2849-57.

Pizzoferrato, A., Ciapetti, G., Stea, S., Cenni, E., Arciola, C.R., Granchi, D. & Savarino, L. (1994) Cell culture methods for testing biocompatibility. *Clin.Mater.,* 15, 173-90.

Ponsonnet, L., Reybier, K., Jaffrezic, N., Comte, V., Lagneau, C., Lissac, M. & Martelet, C. (2003) Relationship between surface properties (roughness, wettability) of titanium and titanium alloys and cell behaviour. *Mater.Sci.Eng.,C,* 23, 551-60.

Popov, C., Kulisch, W., Reithmaier, J.P., Dostalova, T., Jelinek, M., Anspach, N. & Hammann, C. (2007) Bioproperties of nanocrystalline diamond/amorphous carbon composite films. *Diamond Relat.Mater.,* 16, 735-9.

Puckett, S., Pareta, R. & Webster, T.J. (2008) Nano rough micron patterned titanium for directing osteoblast morphology and adhesion. *Int.J.Nanomed.,* 3, 229-41.

Puleo, D.A. & Nanci, A. (1999) Understanding and controlling the bone–implant interface. *Biomaterials,* 20, 2311-21.

Puukilainen, E., Koponen, H.-K., Xiao, Z., Suvanto, S. & Pakkanen, T.A. (2006) Nanostructured and chemically modified hydrophobic polyolefin surfaces. *Colloid.Surf.,A,* 287, 175-81.

Puukilainen, E., Rasilainen, T., Suvanto, M. & Pakkanen, T.A. (2007) Superhydrophobic polyolefin surfaces: controlled micro- and nanostructures. *Langmuir,* 23, 7263-8.

Quigley, F.P., Buggy, M. & Birkinshaw, C. (2002) Selection of elastomeric materials for compliant-layered total hip arthroplasty. *Proc.Inst.Mech.Eng.H.,* 216, 77-83.

Quirós, C., Núñez, R., Prieto, P., Elizalde, E., Fernández, A., Schubert, C., Donnet, C. & Sanz, J.M. (1999) Tribological and chemical characterization of ion beam-deposited CN_x films. *Vacuum,* 52, 199-202.

Ratner, B.D., Hoffman, A.S., Schoen, F.J. & Lemons, J.E. (eds.) (1996) *Biomaterial science: an introduction to materials in medicine*, Academic Press, San Diego, CA, USA.

Rea, S.M., Brooks, R.A., Schneider, A., Best, S.M. & Bonfield, W. (2004) Osteoblast-like cell response to bioactive composites-surface-topography and composition effects. *J.Biomed.Mater.Res.Part B,* 70, 250-61.

Redey, S.A., Nardin, M., Bernache-Assolant, D., Rey, C., Delannoy, P., Sedel, L. & Marie, P.J. (2000) Behavior of human osteoblastic cells on stoichiometric hydroxyapatite and type A carbonate apatite: role of surface energy. *J.Biomed.Mater.Res.,* 50, 353-64.

Reising, A., Yao, C., Storey, D. & Webster, T.J. (2008) Greater osteoblast long-term functions on ionic plasma deposited nanostructured orthopedic implant coatings. *J.Biomed.Mater.Res.Part A,* 87, 78-83.

Revell, P.A. (2008) *Biological causes of prosthetic joint failure*. In: Revell, P.A. (ed.) *Joint replacement technology*, CRC Press, Boca Raton, FL, USA, pp. 349-96.

Reyes, C.D., Petrie, T.A., Burns, K.L., Schwartz, Z. & Garcia, A.J. (2007) Biomolecular surface coating to enhance orthopaedic tissue healing and integration. *Biomaterials,* 28, 3228-35.

Richards, R.G., Stiffanic, M., Owen, G.R.H., Riehle, M., Gwynn, I.A.P. & Curtis, A.S.G. (2001) Immunogold labelling of fibroblast focal adhesion sites visualised in fixed material using scanning electron microscopy, and living, using internal reflection microscopy. *Cell Biol.Int.*, 25, 1237-49.

Ries, M.D. (2005) Highly cross-linked polyethylene: the debate is over--in opposition. *J.Arthroplasty,* 20, 59-62.

Roach, P., Eglin, D., Rohde, K. & Perry, C.C. (2007) Modern biomaterials: a review - bulk properties and implications of surface modifications. *J.Mater.Sci.Mater.Med.,* 18, 1263-77.

Robertson, J. (2002) Diamond-like amorphous carbon. *Mater.Sci.Eng.,R,* 37, 129-281.

Robling, A.G., Castillo, A.B. & Turner C.H. (2006) Biomechanical and molecular regulation of bone remodeling. *Annu.Rev.Biomed.Eng.*, 8, 455-98.

Rodan, S.B., Imai, Y., Thiede, M.A., Wesolowski, G., Thompson, D., Bar-Shavit, Z., Shull, S., Mann, K. & Rodan, G.A. (1987) Characterization of a human osteosarcoma cell line (Saos-2) with osteoblastic properties. *Cancer Res.,* 47, 4961-6.

Rodil, S.E., Olivares, R. & Arzate, H. (2005) In vitro cytotoxicity of amorphous carbon films. *Biomed.Mater.Eng.,* 15, 101-12.

Rodil, S.E., Olivares, R., Arzate, H. & Muhl, S. (2003) Properties of carbon films and their biocompatibility using in-vitro tests. *Diamond Relat.Mater.*, 12, 931-7.

Rohde, H., Burandt, E.C., Siemssen, N., Frommelt, L., Burdelski, C., Wurster, S., Scherpe, S., Davies, A.P., Harris, L.G., Horstkotte, M.A., Knobloch, J.K.-M., Ragunath, C., Kaplan, J.B. & Mack, D. (2007) Polysaccharide intercellular adhesin or protein factors in biofilm accumulation of Staphylococcus epidermidis and Staphylococcus aureus isolated from prosthetic hip and knee joint infections. *Biomaterials,* 28, 1711-20.

Roy, R.K., Choi, H.W., Yi, J.W., Moon, M.-W., Lee, K.-R., Han, D.K., Shin, J.H., Kamijo, A. & Hasebe, T. (2009) Hemocompatibility of surface-modified, silicon-incorporated, diamond-like carbon films. *Acta Biomater.,* 5, 249-56.

Roy, R.K. & Lee, K.-R. (2007) Biomedical applications of diamond-like carbon coatings: a review. *J.Biomed.Mater.Res.Part B,* 83, 72-84.

Sabokbar, A., Pandey, R. & Athanasou, N.A. (2003) The effect of particle size and electrical charge on macrophage-osteoclast differentiation and bone resorption. *J.Mater.Sci.Mater.Med.,* 14, 731-8.

Saldana, L., Gonzalez-Carrasco, J.L., Rodriguez, M., Munuera, L. & Vilaboa, N. (2006) Osteoblast response to plasma-spray porous Ti6Al4V coating on substrates of identical alloy. *J.Biomed.Mater.Res.Part A,* 77, 608-17.

Saldarriaga Fernandez, I.C., Mei, H.C., Metzger, S., Grainger, D.W., Engelsman, A.F., Nejadnik, M.R. & Busscher, H.J. (2010) In vitro and in vivo comparisons of staphylococcal biofilm formation on a cross-linked poly(ethylene glycol)-based polymer coating. *Acta Biomater.,* 6, 1119-24.

Santavirta, S., Bohler, M., Harris, W.H., Konttinen, Y.T., Lappalainen, R., Muratoglu, O., Rieker, C. & Salzer, M. (2003) Alternative materials to improve total hip replacement tribology. *Acta Orthop.Scand.,* 74, 380-8.

Santavirta, S.S., Lappalainen, R., Pekko, P., Anttila, A. & Konttinen, Y.T. (1999) The counterface, surface smoothness, tolerances, and coatings in total joint prostheses. *Clin.Orthop.Relat.Res.,* 369, 92-102.

Sarró, M.I., Moreno, D.A., Ranninger, C., King, E. & Ruiz, J. (2006) Influence of gas nitriding of Ti6Al4V alloy at high temperature on the adhesion of Staphylococcus aureus. *Surf.Coat.Technol.,* 201, 2807-12.

Scholes, S.C., Burgess, I.C., Marsden, H.R., Unsworth, A., Jones, E. & Smith, N. (2006) Compliant layer acetabular cups: friction testing of a range of materials and designs for a new generation of prosthesis that mimics the natural joint. *Proc.Inst.Mech.Eng.H.,* 220, 583-96.

Schroeder, A., Francz, G., Bruinink, A., Hauert, R., Mayer, J. & Wintermantel, E. (2000) Titanium containing amorphous hydrogenated carbon films (a-C: H/Ti): surface analysis and evaluation of cellular reactions using bone marrow cell cultures in vitro. *Biomaterials,* 21, 449-56.

Schulz, H., Leonhardt, M., Scheibe, H.-J. & Schultrich, B. (2005) Ultra hydrophobic wetting behaviour of amorphous carbon films. *Surf.Coat.Technol.,* 200, 1123-6.

Schwartz, Z., Raz, P., Zhao, G., Barak, Y., Tauber, M., Yao, H. & Boyan, B.D. (2008) Effect of micrometer-scale roughness of the surface of Ti6Al4V pedicle screws in vitro and in vivo. *J.Bone Joint Surg.Am.,* 90, 2485-98.

Scotchford, C.A., Ball, M., Winkelmann, M., Vörös, J., Csucs, C., Brunette, D.M., Danuser, G. & Textor, M. (2003) Chemically patterned, metal-oxide-based surfaces produced by photolithographic techniques for studying protein- and cell-interactions. II: Protein adsorption and early cell interactions. *Biomaterials,* 24, 1147-58.

Secinti, K.D., Ayten, M., Kahilogullari, G., Kaygusuz, G., Ugur, H.C. & Attar, A. (2008) Antibacterial effects of electrically activated vertebral implants. *J.Clin.Neurosci.,* 15, 434-9.

Sethuraman, A., Han, M., Kane, R.S. & Belfort, G. (2004) Effect of surface wettability on the adhesion of proteins. *Langmuir,* 20, 7779-88.

Shao, W., Zhao, Q., Abel, E.W. & Bendavid, A. (2010) Influence of interaction energy between Si-doped diamond-like carbon films and bacteria on bacterial adhesion under flow conditions. *J.Biomed.Mater.Res.Part A.,* 93, 133-9.

Sheeja, D., Tay, B.K. & Nung, L.N. (2004) Feasibility of diamond-like carbon coatings for orthopaedic applications. *Diamond Relat.Mater.,* 13, 184-90.

Sheeja, D., Tay, B.K., Yu, L. & Lau, S.P. (2002) Low stress thick diamond-like carbon films prepared by filtered arc deposition for tribological applications. *Surf.Coat. Technol.,* 154, 289-93.

Shi, Z., Neoh, K.G., Kang, E.T., Poh, C. & Wang, W. (2008) Bacterial adhesion and osteoblast function on titanium with surface-grafted chitosan and immobilized RGD peptide. *J.Biomed.Mater.Res.Part A,* 86, 865-72.

Shier, D., Butler, J. & Lewis, R. (2009) *Hole's essentials of human anatomy and physiology, 10th ed.*, McGraw-Hill Companies, Boston, MA, USA.

Silver, S. (2003) Bacterial silver resistance: molecular biology and uses and misuses of silver compounds. *FEMS Microbiol.Rev.,* 27, 341-53.

Singh, A., Ehteshami, G., Massia, S., He, J., Storer, R.G. & Raupp, G. (2003) Glial cell and fibroblast cytotoxicity study on plasma-deposited diamond-like carbon coatings. *Biomaterials,* 24, 5083-9.

Smeets, R., Kolk, A., Gerressen, M., Driemel, O., Maciejewski, O., Hermanns-Sachweh, B., Riediger, D. & Stein, J.M. (2009) A new biphasic osteoinductive calcium composite material with a negative zeta potential for bone augmentation. *Head.Face Med.,* 13, 10.1186/1746-160X-5-13.

Smith, T.J., Galm, A., Chatterjee, S., Wells, R., Pedersen, S., Parizi, A.M., Goodship, A.E. & Blunn, G.W. (2006) Modulation of the soft tissue reactions to percutaneous orthopaedic implants. *J.Orthop.Res.,* 24, 1377-83.

Soininen, A., Tiainen, V.-M., Konttinen, Y.T., van der Mei, H.C., Busscher, H.J. & Sharma, P.K. (2009) Bacterial adhesion to diamond-like carbon as compared to stainless steel. *J.Biomed.Mater.Res.Part B,* 90, 882-5.

Sousa, C., Teixeira, P. & Oliveira, R. (2009) Influence of surface properties on the adhesion of *Staphylococcus epidermidis* to acrylic and silicone. *Int.J.Biomater.,* 2009, 718017.

Steele, D.G. & Bramblett, C.A. (1988) *The Anatomy and Biology of the Human Skeleton*, *8th ed*., Texas A&M University Press, College Station, TX, USA.

Stobie, N., Duffy, B., McCormack, D.E., Colreavy, J., Hidalgo, M., McHale, P. & Hinder, S.J. (2008) Prevention of *Staphylococcus*

epidermidis biofilm formation using a low-temperature processed silver-doped phenyltriethoxysilane sol–gel coating. *Biomaterials,* 29, 963-9.

Subbiahdoss, G., Kuijer, R., Grijpma, D.W., van der Mei, H.C. & Busscher, H.J. (2009) Microbial biofilm growth vs. tissue integration: "the race for the surface" experimentally studied. *Acta Biomater.,* 5, 1399-404.

Sudo, H., Kodama, H.A., Amagai, Y., Yamamoto, S. & Kasai, S. (1983) In vitro differentiation and calcification in a new clonal osteogenic cell line derived from newborn mouse calvaria. *J.Cell Biol.,* 96, 191-8.

Sumita, M., Hanawa, T. & Teoh, S.H. (2004) Development of nitrogen-containing nickel-free austenitic stainless steels for metallic biomaterials—review. *Materil.Sci.Eng.,C,* 24, 753-60.

Tanaka, K., Tamura, J., Kawanabe, K., Nawa, M., Uchida, M., Kokubo, T. & Nakamura, T. (2003) Phase stability after aging and its influence on pin-on-disk wear properties of Ce-TZP/Al_2O_3 nanocomposite and conventional Y-TZP. *J.Biomed.Mater.Res.Part A,* 67, 200-7.

Tang, H., Cao, T., Liang, X., Wang, A., Salley, S.O., McAllister, J.II. & Ng, K.Y. (2009) Influence of silicone surface roughness and hydrophobicity on adhesion and colonization of *Staphylococcus epidermidis*. *J.Biomed.Mater.Res.Part A,* 88, 454-63.

Tang, J., Peng, R. & Ding, J. (2010) The regulation of stem cell differentiation by cell-cell contact on micropatterned material surfaces. *Biomaterials,* 31, 2470-6.

Tanimoto, Y., Shibata, Y., Kataoka, Y., Miyazaki, T. & Nishiyama, N. (2008) Osteoblast-like cell proliferation on tape-cast and sintered tricalcium phosphate sheets. *Acta Biomater.,* 4, 397-402.

Tay, B.K., Cheng, Y.H., Ding, X.Z., Lau, S.P., Shi, X., You, G.F. & Sheeja, D. (2001) Hard carbon nanocomposite films with low stress. *Diamond Relat.Mater.,* 10, 1082-7.

Taylor, R.L., Verran, J., Lees, G.C. & Ward, A.J. (1998) The influence of substratum topography on bacterial adhesion to polymethyl methacrylate. *J.Mater.Sci.Mater.Med.,* 9, 17-22.

Teixeira, S., Monteiro, F.J., Ferraz, M.P., Vilar, R. & Eugenio, S. (2007) Laser surface treatment of hydroxyapatite for enhanced tissue integration: surface characterization and osteoblastic interaction studies. *J.Biomed.Mater.Res.Part A,* 81, 920-9.

Tessier, P.Y., Pichon, L., Villechaise, P., Linez, P., Angleraud, B., Mubumbila, N., Fouquet, V., Straboni, A., Milhet, X. & Hildebrand, H.F. (2003) Carbon nitride thin films as protective coatings for biomaterials: synthesis, mechanical and biocompatibility characterizations. *Diamond Relat.Mater.,* 12, 1066-9.

Thian, E.S., Ahmad, Z., Huang, J., Edirisinghe, M.J., Jayasinghe, S.N., Ireland, D.C., Brooks, R.A., Rushton, N., Bonfield, W. & Best, S.M. (2010) The role of surface wettability and surface charge of electrosprayed nanoapatites on the behaviour of osteoblasts. *Acta Biomater.,* 6, 750-5.

Tomlins, P.E., Leach, R., Vagdama, P., Mikhalovsky, S. & James, S. (2005) *On the topographical characterization of biomaterial surfaces*. In: Vadgama, P. (ed.) *Surfaces and interfaces for biomaterials*, Woodhead Publishing Limited, Cambridge, UK, pp. 693-718.

Turner, A.M.P., Dowell, N., Turner, S.W.P., Kam, L., Isaacson, M., Turner, J.N., Craighead, H.G. & Shain, W. (2000) Attachment of astroglial cells to microfabricated pillar arrays of different geometries. *J.Biomed.Mater.Res.,* 51, 430-41.

Uo, M., Watari, F., Yokoyama, A., Matsuno, H. & Kawasaki, T. (2001) Tissue reaction around metal implants observed by X-ray scanning analytical microscopy. *Biomaterials,* 22, 677-85.

Uzumaki, E.T., Lambert, C.S., Belangero, W.D., Freire, C.M.A. & Zavaglia, C.A.C. (2006) Evaluation of diamond-like carbon coatings produced by plasma immersion for orthopaedic applications. *Diamond Relat.Mater.,* 15, 982-8.

Vagaska, B., Bacakova, L., Filova, E. & Balik, K. (2010) Osteogenic cells on bio-inspired materials for bone tissue engineering. *Physiol.Res.,* 59, 309-22.

Valle, J., Toledo-Arana, A., Berasain, C., Ghigo, J.-M., Amorena, B., Penades, J.R. & Lasa, I. (2003) SarA and not sigmaB is essential for biofilm development by Staphylococcus aureus. *Mol.Microbiol.,* 48, 1075-87.

van de Belt, H., Neut, D., Schenk, W., van Horn, J.R., van der Mei, H.C. & Busscher, H.J. (2000) Gentamicin release from polymethylmethacrylate bone cements and *Staphylococcus aureus* biofilm formation. *Acta Orthop.Scand.,* 71, 625-9.

van de Belt, H., Neut, D., Schenk, W., van Horn, J.R., van Der Mei, H.C. & Busscher, H.J. (2001) *Staphylococcus aureus* biofilm formation on different gentamicin-loaded polymethylmethacrylate bone cements. *Biomaterials,* 22, 1607-11.

van Oss, C.J. (1995) Hydrophobicity of biosurfaces – origin, quantitative determination and interaction energies. *Colloids Surf.,B,* 5, 91-110.

van Oss, C.J., Good, R.J. & Chaudhury, M.K. (1986) The role of van der Waals forces and hydrogen bonds in "hydrophobic interactions" between biopolymers and low energy surfaces. *J. Colloid Interface Sci.*, 111, 378-90.

van Oss, C.J., Good, R.J. & Chaudhury, M.K. (1988) Additive and nonadditive surface tension components and the interpretation of contact angles. *Langmuir,* 4, 884-91.

van Oss, C.J., Chaudhury, M.K. & Good, R.J. (1989) The mechanism of phase separations of polymers in organic media-apolar and polar systems. *Sep. Sci. Technol*., 24, 15-30.

van Wachem, P.B., Beugeling, T., Feijen, J., Bantjes, A., Detmers, J.P. & van Aken, W.G. (1985) Interaction of cultured human endothelial cells with polymeric surfaces of different wettabilities. *Biomaterials,* 6, 403-8.

Veenstra, G.J.C., Cremers, F.F.M., van Dijk, H. & Fleer, A. (1996) Ultrastructural organization and regulation of a biomaterial adhesin of *Staphylococcus epidermidis*. *J.Bacteriol.,* 178, 537-41.

Verne, E., Miola, M., Vitale Brovarone, C., Cannas, M., Gatti, S., Fucale, G., Maina, G., Masse, A. & Di Nunzio, S. (2009) Surface silver-doping of biocompatible glass to induce antibacterial properties. Part I: Massive glass. *J.Mater.Sci.Mater.Med.,* 20, 733-40.

Veronesi, B., de Haar, C., Lee, L. & Oortgiesen, M. (2002) The surface charge of visible particulate matter predicts biological activation in human bronchial epithelial cells. *Toxicol.Appl.Pharmacol.,* 178, 144-54.

Verwey, E.J.W. (1947) Theory of the Stability of Lyophobic Colloids. *J. Phys.Chem.*, 51, 631-6.

Viceconti, M., Muccini, R., Bernakiewicz, M., Baleani, M. & Cristofolini, L. (2000) Large-sliding contact elements accurately predict levels of bone-implant micromotion relevant to osseointegration. *J.Biomech.*, 33, 1611-8.

Vitte, J., Benoliel, A.M., Pierres, A. & Bongrand, P. (2004) Is there a predictable relationship between surface physical-chemical properties and cell behaviour at the interface? *Eur.Cell.Mater.*, 7, 52-63.

Voevodin, A.A. & Donley, M.S. (1996) Preparation of amorphous diamond-like carbon by pulsed laser deposition: a critical review. *Surf.Coat.Technol.*, 82, 199-213.

Vogler, E.A. (1998) Structure and reactivity of water at biomaterial surfaces. *Adv.Colloid Interface Sci.*, 74, 69-117.

Voisin, M., Ball, M., O'Connell, C. & Sherlock, R. (2010) Osteoblasts response to microstructured and nanostructured polyimide film, processed by the use of silica bead microlenses. *Nanomed.Nanotechnol.Biol.Med.*, 6, 35-43.

von Eiff, C., Peters, G. & Heilmann, C. (2002) Pathogenesis of infections due to coagulase-negative staphylococci. *Lancet Infect.Dis.*, 2, 677-85.

von Recum, A.F., Shannon, C.E., Cannon, C.E., Long, K.J., Van Kooten, T.G. & Meyle, J. (1996) Surface Roughness, Porosity, and Texture as Modifiers of Cellular Adhesion. *Tissue Eng.*, 2, 241-53.

Vroman, L. & Adams, A.L. (1969) Identification of rapid changes at plasma-solid interfaces. *J.Biomed.Mater.Res.*, 3, 43-67.

Vuong, C., Kocianova, S., Yao, Y., Carmody, A.B. & Otto, M. (2004) Increased colonization of indwelling medical devices by quorum-sensing mutants of *Staphylococcus epidermidis* in vivo. *J.Infect.Dis.*, 190, 1498-505.

Wadstrom, T. (1989) Molecular aspects of bacterial adhesion, colonization, and development of infections associated with biomaterials. *J.Invest.Surg.*, 2, 353-60.

Wan, G.J., Yang, P., Fu, R.K.Y., Mei, Y.F., Qiu, T., Kwok, S.C.H., Ho, J.P.Y., Huang, N., Wu, X.L. & Chu, P.K. (2006) Characteristics and surface energy of silicon-doped diamond-like carbon films fabricated by plasma immersion ion implantation and deposition. *Diamond Relat.Mater.,* 15, 1276-81.

Wan, Y., Wang, Y., Liu, Z., Qu, X., Han, B., Bei, J. & Wang, S. (2005) Adhesion and proliferation of OCT-1 osteoblast-like cells on micro- and nano-scale topography structured poly(l-lactide). *Biomaterials,* 26, 4453-9.

Wang, X., Ohlin, C.A., Lu, Q. & Hu, J. (2006) Influence of physicochemical properties of laser-modified polystyrene on bovine serum albumin adsorption and rat C6 glioma cell behavior. *J.Biomed.Mater.Res.Part A,* 78, 746-54.

Wei, J., Igarashi, T., Okumori, N., Igarashi, T., Maetani, T., Liu, B. & Yoshinari, M. (2009) Influence of surface wettability on competitive protein adsorption and initial attachment of osteoblasts. *Biomed.Mater.,* 4, 10.1088/1748-6041/4/4/045002.

Weir, E., Lawlor, A., Whelan, A. & Regan, F. (2008) The use of nanoparticles in anti-microbial materials and their characterization. *Analyst,* 133, 835-45.

Welldon, K.J., Atkins, G.J., Howie, D.W. & Findlay, D.M. (2008) Primary human osteoblasts grow into porous tantalum and maintain an osteoblastic phenotype. *J.Biomed.Mater.Res.Part A,* 84, 691-701.

Wenz, H.J., Bartsch, J., Wolfart, S. & Kern, M. (2008) Osseointegration and clinical success of zirconia dental implants: a systematic review. *Int.J.Prosthodont.,* 21, 27-36.

Wiegand, A., Buchalla, W. & Attin, T. (2007) Review on fluoride-releasing restorative materials—Fluoride release and uptake characteristics, antibacterial activity and influence on caries formation. *Dent.Mater.,* 23, 343-62.

Williams, D.F. (1987) *Definitions in Biomaterials*, Elsevier Publishing Company, Amsterdam, The Netherlands.

Williams, D.F. (1999) *The Williams dictionary of biomaterials*, Liverpool University Press, Liverpool, UK.

Williams, D.F. (2008) On the mechanisms of biocompatibility. *Biomaterials,* 29, 2941-53.

Wilson, C.J., Clegg, R.E., Leavesley, D.I. & Pearcy, M.J. (2005) Mediation of biomaterial-cell interactions by adsorbed proteins: a review. *Tissue Eng.,* 11, 1-18.

Winkelmann, M., Gold, J., Hauert, R., Kasemo, B., Spencer, N.D., Brunette, D.M. & Textor, M. (2003) Chemically patterned, metal oxide based surfaces produced by photolithographic techniques for studying protein– and cell–surface interactions I: Microfabrication and surface characterization. *Biomaterials,* 24, 1133-45.

Wirth, C., Comte, V., Lagneau, C., Exbrayat, P., Lissac, M., Jaffrezic-Renault, N. & Ponsonnet, L. (2005) Nitinol surface roughness modulates in vitro cell response: a comparison between fibroblasts and osteoblasts. *Mater.Sci.Eng.,C,* 25, 51-60.

Wolff, J. (1892) *Das gesetz der transformation der knochen*, Hirschwald, Berlin.

Xia, Y. & Whitesides, G.M. (1998) Soft Lithography. *Annu.Rev.Mater. Sci.,* 28, 153-84.

Xie, H.G., Li, X.X., Lv, G.J., Xie, W.Y., Zhu, J., Luxbacher, T., Ma, R. & Ma, X.J. (2010) Effect of surface wettability and charge on protein adsorption onto implantable alginate-chitosan-alginate microcapsule surfaces. *J.Biomed.Mater.Res.Part A,* 92, 1357-65.

Xu, L., Li, H., Vuong, C., Vadyvaloo, V., Wang, J., Yao, Y., Otto, M. & Gao, Q. (2006) Role of the *luxS* quorum-sensing system in biofilm formation and virulence of *Staphylococcus epidermidis*. *Infect.Immun.,* 74, 488-96.

Yamashita, K., Oikawa, N. & Umegaki, T. (1996) Acceleration and Deceleration of Bone-Like Crystal Growth on Ceramic Hydroxyapatite by Electric Poling. *Chem.Mater.,* 8, 2697-700.

Yang, L., Sheldon, B.W. & Webster, T.J. (2009) Orthopedic nano diamond coatings: Control of surface properties and their impact on osteoblast adhesion and proliferation. *J.Biomed.Mater.Res.Part A,* 91, 548-56.

Yarwood, J.M. & Schlievert, P.M. (2003) Quorum sensing in *Staphylococcus* infections. *J.Clin.Invest.,* 112, 1620-5.

Young, T. (1805) An Essay on the Cohesion of Fluids. *Philosophical Transactions of the Royal Society of London*, 95, 65-87.

Zamir, E. & Geiger, B. (2001) Molecular complexity and dynamics of cell-matrix adhesions. *J.Cell.Sci.,* 114, 3583-90.

Zhang, W., Luo, Y., Wang, H., Jiang, J., Pu, S. & Chu, P.K. (2008b) Ag and Ag/N2 plasma modification of polyethylene for the enhancement of antibacterial properties and cell growth/proliferation. *Acta Biomater.,* 4, 2028-36.

Zhang, Y., Venugopal, J.R., El-Turki, A., Ramakrishna, S., Su, B. & Lim, C.T. (2008a) Electrospun biomimetic nanocomposite nanofibers of hydroxyapatite/chitosan for bone tissue engineering. *Biomaterials,* 29, 4314-22.

Zhang, W., Zhang, Y., Ji, J., Yan, Q., Huang, A. & Chu, P.K. (2007) Antimicrobial polyethylene with controlled copper release. *J.Biomed.Mater.Res.Part A,* 83, 838-44.

Zhao, Q., Liu, Y., Wang, C. & Wang, S. (2007a) Bacterial adhesion on silicon-doped diamond-like carbon films. *Diamond Relat.Mater.,* 16, 1682-7.

Zhao, Q., Liu, Y., Wang, C., Wang, S., Peng, N. & Jeynes, C. (2008) Reduction of bacterial adhesion on ion-implanted stainless steel surfaces. *Med.Eng.Phys.,* 30, 341-9.

Zhao, G., Raines, A.L., Wieland, M., Schwartz, Z. & Boyan, B.D. (2007b) Requirement for both micron- and submicron scale structure for synergistic responses of osteoblasts to substrate surface energy and topography. *Biomaterials,* 28, 2821-9.

Zhao, G., Schwartz, Z., Wieland, M., Rupp, F., Geis-Gerstorfer, J., Cochran, D.L. & Boyan, B.D. (2005) High surface energy enhances cell response to titanium substrate microstructure. *J.Biomed.Mater.Res.Part A,* 74, 49-58.

Zhao, Q., Su, X., Wang, S., Zhang, X., Navabpour, P. & Teer, D. (2009) Bacterial attachment and removal properties of silicon- and nitrogen-doped diamond-like carbon coatings. *Biofouling,* 25, 377-85.

Zolynski, K., Witkowski, P., Kaluzny, A., Has, Z., Niedzielski, P. & Mitura S. (1996) Implants with hard carbon layers for application in, pseudoarthrosis femoris sin. Ostisis post fracturam apertam olim factam. *J.Chem.Vapor Deposit*., 4, 232-9.

Appendix table

Feature type	Fabrication technique	Material	Feature dimensions	Cell type	Cellular effect	Reference
Random	Sandblasting, acid-etching, plasma spraying and polishing	Smooth and roughened Ti disks	Polished: R_a = 0.6 µm, sandblasted+acid-etched: R_a = 4.0 µm and plasma-sprayed: R_a = 5.2 µm	Alveolar bone cells	The lowest number of cells and less well-attached cells with R_a of 4.0 µm. Largest cell number and gene expression with R_a of 5.2 µm	Brett et al. 2004
Microgrooves	Manually carving with a scalpel	Tissue culture treated polystyrene, pure polystyrene	Grooves height ~ 70 µm, width ~ 100 µm. The ridge had a width and height around 45 µm and the intra-groove distance varied between 2.5-1.2 mm	MC3T3-E1 and rat bone marrow cells	Grooves influenced to rat bone marrow cells morphology, proliferation and ALP production besides of surface chemistry. MC3T3-E1 not influenced	Bruinink & Winter-mantel 2001
Random	Al blasting, dual acid-etching and impregnation	Commercial implants; control implant: an Al blasted and dual acid- etched surface, test implant: calcium phosphate low impregnated surface	Control: R_a = 1.11 µm and $R_{(\text{average interpeak distance})}$ = 49.66 µm, test: R_a= 0.84 µm and $R_{(\text{average interpeak distance})}$ = 25.27 µm	Saos-2 and MSCs	Favourable osteoblast adhesion and growth with both implants. Higher amounts of pseudopodes, vesicles and differentiation levels of cells with test implant with homogeneous nanoroughness and low impregnation of CaP	Bucci-Sabattini et al. 2010
Microgrooves	Hot embossing imprint lithography	Polyimide	Groove width ~ 4 µm, height ~5 µm, spacing 34 µm	MC3T3-E1	Alignment of cell nucleus, focal adhesions and the cell body with the microgrooves. Change in the shape only with cell bodies	Charest et al. 2004
Random	Polymer demixing and colloidal lithography	Poly(methyl methacrylate)	Nanotopography down to 10 nm	Human bone marrow cells	Cell differentiation towards an osteoblastic phenotype with nanotopographies	Dalby et al. 2006

Feature type	Fabrication technique	Material	Feature dimensions	Cell type	Cellular effect	Reference
Nanotubes	Electrochemical anodization	TiO_2 nanotubes on Ti	Diameter of nanotubes 50 nm and length 300-600 nm	Osteoblastic precursor cell	Enhanced osteoblast-material interactions on nanotube surface compared to smooth Ti	Das et al. 2009
Random	Roughening with different methods	Ti disks	R_a ~ 0.3-1.0 μm	Saos-2	Improvement of cell adhesion, spreading and proliferation with higher surface roughness	Degasne et al. 1999
Random	Microwave plasma enhanced chemical vapour deposition and oxygen plasma treatment	Nanocrystalline diamond (NCD) films on smooth and microroughened Si	Si+NCD: R_{rms} = 8.2 nm, micro-roughened Si: R_{rms} = 301 nm, after NCD coating (hierarchical micro- and nanotexture: R_{rms} = 7.6 nm)	MG-63	Higher number and metabolic activity of cells on the both NCD coated films compared to control polystyrene culture dish. Larger cells on hierarchically micro- and nano-structured diamond substrates	Grausova et al. 2009
Gap-cornered boxes and micron scale pillars	Cast molding	Epoxy	Open square boxes with gaps at each corner ranging in size from 34 x 34 μm to 65 x 65 μm in width and 4 and 10 μm in depth. Pillars with 4 or 10 μm height with spacing of 10 μm from ridge to ridge, width of the ridges 2 or 5 μm	Rat calvarian osteoblasts	Enhanced osteoblast adhesion and differentiation with discontinuous surface topographies. Stronger diagonal alignment and higher cell number at 7 days on the gap-cornered boxes than pillars whereas higher number of focal adhesions with pillars	Hamilton et al. 2006
Microgrooves	UV-lithography, reactive ion etching and plasma enhanced chemical vapor deposition	Ti and DLC coated Si	Groove width = 2-10 μm, height = 1.5-2 μm	MG-63	Cell contact guidance with all grooved samples, greatest on 2 and 4 μm grooves. Greater cell number for 2 μm grooves	Ismail et al. 2007
Nanopits	Electron beam lithography, nickel die fabrication and hot embossing	Polycaprolactone	Diameter of nanopits 120 nm, depth 100 nm, spacing 300 nm	Human bone marrow osteo-progenitor cells	Modulation of osteogenesis with controlled nanopit topography	Kantawong et al. 2009

Feature type	Fabrication technique	Material	Feature dimensions	Cell type	Cellular effect	Reference
Two type of roughness in micropatterned ridges	Electron beam deposition	Ti	Roughness < 100 nm or 100 nm-1 μm, micropatterned ridges and flat grooves 20 μm	Human osteoblasts	Enhanced adhesion on surfaces with roughness between 100 nm-1 μm compared to smoother surfaces	Khang et al. 2008
Random	Roughening with different methods	Ti disks	Not determined	MG-63	Inverse relationship between cell number and surface roughness. Enhanced cytokine and growth factor production on rougher surface	Kieswetter et al. 1996
Random	Sandblasting and polishing	$TiAl_6V_4$	R_a ~ 0.18-2.95 μm	MG-63	Decreased cell number and proliferation but increased differentiation on rough surface compared to smooth surface	Kim et al. 2005
Random	Sandblasting and lapping	Roughened or polished Ti and $TiAl_6V_4$ disks	Smooth surfaces: R_a ~ 0.2 μm, rough ones: R_a ~ 3.2-4.2 μm	MG-63	Enhanced differentiation and decreased proliferation of cells grown on rough surfaces versus smooth surfaces for both materials	Lincks et al. 1998
Microgrooves	Wet etching and magnetron sputtering	HA and Ti coated Si	Groove width = 4-38 μm, height = 2-10 μm	Saos-2	Stronger effects on the cell guidance and shape regulation with grooves with dimensions around the cell. Difference in cell shape regulation but not in contact guidance on HA and Ti	Lu & Leng 2003
Random	Atomic oxygen bombardment	Chlorotrifluoro-ethylene coated with BSA	Three texture groups with maximum feature size 0.5, 2 or 4 μm and untextured one	Osteoblastic cell line	Adherence of cells to all textured surfaces with optimum adherence to a texture having a maximum depth of 0.5–2 μm. No binding of cells to untextured BSA-coated surfaces. A time-dependent increase in cell adhesion from 1 to 4 h on BSA-coated surfaces, which was not observed for the Fn- and type I collagen-coated control surfaces	Mata et al. 2003

Feature type	Fabrication technique	Material	Feature dimensions	Cell type	Cellular effect	Reference
3D smooth and microtextured scaffold	Photolithography, molding and precise motion fixation	PDMS	Microposts with diameter and height of 10 μm	Connective tissue progenitor cells	Increased cell number and higher alkaline phosphatase mRNA expression with 3D texture scaffold compared to 3D smooth scaffold. Comparable osteocalcin mRNA expression for both types of scaffolds	Mata et al. 2009
Random	Sol-gel-derived coatings, acid-etching	Al_2O_3, TiO_2 (rutile Ru and anatse An) and ZrO_2 coatings on Ti	20-30 nm nanoscale features on all four nanostructured surfaces (An, Ru, Al and Zr). R_a (machined) ~ 95 nm and R_a (acid-etched) ~378 nm	Human MSCs	Bone-specific mRNAs were increased on four surfaces with nanoscale features compared to machined and acid-etched surfaces	Mendonca et al. 2009b
Random	Polishing, grit-blasting and acid-etching	Ti	Microscale features: R_a = 160 nm, micro-and nanoscale features: R_a = 260 nm including discrete 20-30 nm features	Human MSCs	Osteoinductive gene expression of adherent human MSCs was increased with surfaces of nanoscale features (<100 nm)	Mendonca et al. 2010
Horizontal and vertical microgrooves and -grids	Laser ablation and electron beam evaporation	Ti coated Si	Groove width = 10.5-12 μm, height = 7-14 μm, spacing 20 μm and R_{RMS} ~ 1.46-4.46 μm	Human osteoblasts	Best combination of contact guidance and cell integration with grooves with depths of ~ 9-11 μm. Spreading and proliferation rates decreased with increasing R_{RMS}. Within the microgrid patterns, cells were less mobile with no alignment effects	Mwenifumbo et al. 2007
Microsquares	UV-lithography, magnetron sputtering, FPAD	Ti, Ta, Cr and AD on silicon wafers	75 μm squares with 100 μm spacing between squares in two orthogonal directions	Human MSCs	Cells assumed geometric square shapes. Patterns allowed induced osteogenesis but less effectively than plain surfaces, except for AD	Myllymaa et al. 2010

Feature type	Fabrication technique	Material	Feature dimensions	Cell type	Cellular effect	Reference
Nanocrystals	Chemical treatments (hydrolysis)	Various types of HA nanocrystals: nanofibers, nanoneedles and nanosheets	Diameter of submicron fibers 150-200 nm, nanofibers 40-50 nm, nanoneedles 20-40 nm. Thickness of nanoflakes 10 nm and nanosheets 10 nm	Rat bone-marrow-derived MSCs	Restricted cellular activities with fine nanoneedles and nanofibers. Enhanced cell proliferation with surfaces of large grains and on a substrate consisting of wide nanosheets.	Okada et al. 2010
Random	Ionic plasma deposition and nitrogen ion immersion plasma deposition	Al or Ti coating on typical polymer and metal implant materials	Nanoroughness below 100 nm	Human osteoblasts	Increased adhesion on nanoroughened surfaces compared to untreated one. Surface treating changed not only surface roughness but also the surface chemistry and energy	Pareta et al. 2009
Nanoroughness in micropatterned regions	Electron beam evaporation	Ti	Nanoroughness ~20 nm, micropatterned regions between 22 -80 μm in width	Human osteoblasts	Greater osteoblast adhesion on the nanorough regions. Increased number of cells with wider nanorough regions	Puckett et al. 2008
Microgrooves, -pillars and -wells	Extrusion molding, LIGA (lithography, electroplating, molding) diamond wire sawing and embossing	Bioactive composites (HAPEX^{TM}, AWPEX)	Arrays of grooves, pillars and wells with lateral dimensions of 5-50 μm and large scale parallel grooves of 100-150 μm with spacing of 0.3 or 1 mm	Saos-2 and MG-63	Strong cell alignment along all feature types for both composites with features below 50 μm but not with large scale features. Enhanced cell differentiation but no effects on cell proliferation with smaller-scale features	Rea et al. 2004
Random	Ionic plasma deposition	Nanostructured Ti on UHMWPE and PTFE	Nanoroughness usually below 100 nm	Human osteoblasts	Increased osteoblast proliferation and calcium deposition on nanostructured surfaces	Reising et al. 2008
Random	Grit-blasting and machining	Roughened or polished $TiAl_6V_4$ disks	Smooth surfaces: R_a ~ 0.2 μm, rough ones: R_a ~ 2.0-3.3 μm	Human osteoblast-like cells	Reduced number and increased differentiation and local factor production of cells on rougher $TiAl_6V_4$ disks compared to smooth surface	Schwartz et al. 2008

Feature type	Fabrication technique	Material	Feature dimensions	Cell type	Cellular effect	Reference
Microdots and -stripes	Electron beam evaporation and photolithography	Ti, Al, Nb or V coated Si	Dots or stripes with diameter of 50, 100 and 150 µm	Primary human osteoblasts	No significant difference in cell number and activity between patterned and non-patterned single materials. In bimetallic surfaces cells avoided Al surfaces and aligned relative to pattern geometry of other metals	Scotchford et al. 2003
Columnar spot-like microtopo-graphy	Sintering and laser ablation	HA	Diameter of spots 5-10 µm	MG-63	Fibroblast appearance of cells on smooth surfaces whereas in the surfaces with microtopography, strong bonding of cells filopodia to spaces between the columnar structures of the surface implying resistant adherence	Teixeira et al. 2007
Micro- and nanopits	Laser ablation	Polyimide	Micropit; diameter ~ 982 µm, depth ~ 114 µm, nanopit; diameter ~ 426 nm, depth ~ 56 nm	Saos-2	Increased number and size of cells on micropits. Similar metabolic activity between treated and untreated surfaces. Diffuse actin network and less mature adhesions of cells on nanopits	Voisin et al. 2010
Micro- and nanoislands and -pits	Chemical treatment and molding	Polystyrene and polylactic acid	The diameter of larger polylactic acid islands/ polystyrene pits about 2.2 µm and that of smaller islands/pits 0.45 µm	Osteoblast-like cells	Enhanced cell adhesion on surface with nanoscale and microscale roughness compared to smooth surfaces. Effective spreading of cells on rough surfaces. No differences in proliferation	Wan et al. 2005
Random	Microwave plasma enhanced chemical vapour deposition	Nanocryst. diamond (ND), nanostruct. diamond (NDp), ND with H_2 treatment (NDH) and microcryst. diamond (MD)	R_{rms}(ND, NDp, NDH) = 20-30 nm, R_{rms}(MD) = 60-70 nm	Human osteoblasts	Enhanced cell adhesion on ND and NDH with grain sizes less than 100 nm whereas NDp and MD inhibited cell adhesion. Enhanced proliferation of cells on ND and NDH compared with MD and uncoated silicon controls	Yang et al. 2009

Katja Myllymaa

Novel Carbon Coatings and Surface Texturing for Improving Biological Response of Orthopedic Implant Materials

The interface phenomena occurring between host tissue and the surface of biomedical implant play an important role in implant survival. In addition to possessing appropriate mechanical properties, an ideal orthopedic implant material should induce the desired cellular responses, leading to integration of the implant into the bone tissue. This dissertation is focusing on the development of novel carbon-based coatings and their surface modifications, which are hypothesized to improve osteoblastic cells attachment and spreading as well as to inhibit biofilm formation. The effect of different implant surface properties, such as roughness, wettability and zeta potential on biocompatibility is also discussed.

UNIVERSITY OF
EASTERN FINLAND

Publications of the University of Eastern Finland
Dissertations in Forestry and Natural Sciences

ISBN 978-952-61-0218-4